UNIVERSITY OF NAPLES FEDERICO II

Doctorate School in Molecular Medicine

Doctorate Program in
Genetics and Molecular Medicine
Coordinator: Prof. Lucio Nitsch
XXIV Cycle

"Molecular mechanisms for plasma membrane localization of human transmembrane receptors"

Massimo D'Agostino

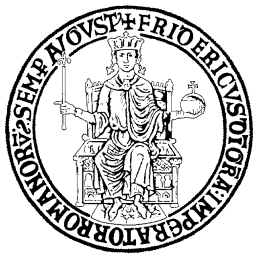

Napoli 2011

CONTENTS

CHAPTER II:

Alpha B-Crystallin over-expression reverts the dominant negative effect of mutant Frizzled4 L501fsX533 associated to the dominant form of familial exudative vitreoretinopathy.

Synopsis of Secretory Pathway.

The movement of newly synthesized proteins from the site of synthesis to their final cellular or extracellular destinations involves transport through a distinct series of vesicular compartments. Vesicle biogenesis is regulated by specific proteins and co-factors that control distinct steps including budding, transport, docking, and fusion with target membranes.
Budding requires assembly of a coat protein complex on the membrane, membrane deformation and the subsequent cleavage of the nascent vesicle from donor membrane.
Three main classes of coats have been identified:
1) **Clathrin** participates in endocytosis, lysosome biogenesis and in vesicular transport processes, yet uncharacterized, that arise from the trans-Golgi network (TGN).
2) **COPI** coatomer is involved in retrograde traffic within the Golgi and from the *cis*-Golgi region or the intermediate compartment (ERGIC) to the endoplasmic reticulum (ER).
3) **COPII** coats is required for budding from the ER.

In order to understand the role of the cytoplasmic coats for the intracellular transport of soluble or transmembrane proteins, it is important to characterize in more details their contribution along the secretory pathway from the site of proteins sinthesis. COPII proteins participate in cargo selection and concentrate some proteins in the budding vesicle at specific sites, called ER exit sites (ERESs). In mammalian cells ERESs are organized and defined by Sec-16 ***(Watson P. et al. 2006)***. Vesicle budding is followed by formation of vesicular–tubular transport carriers (VTC) ***(Aridor M. et al. 1995).*** The central role of COPII in these processes is underlined by studies showing that several human disease may result from mutations that affect proteins in COPII vesicles ***(Fred S. et al. 2001, Fath S. et al. 2007).*** The first step in the assembly of the COPII coat is the activation of the small GTPase Sar1 through its guanine exchange factor Sec12. The GDP/GTP exchange leads to the exposure of an N-terminal amphipathic helix of Sar1with consequent insertion into the ER membrane ***(Bi X. Et al. 2002, Bielli A. et al. 2005).*** This insertion causes membrane deformation and is ultimately required for membrane fission ***(Bielli A. et al. 2005, Lee M.C. et al. 2005).*** Through direct interaction with Sec23, Sar1 recruits the heterodimer Sec23–Sec24. The majority of cargoes are captured through interaction with Sec24, which exhibits multiple independent cargo binding sites ***(Mossessova E. et al. 2003, Miller E.A. et al. 2003).*** After the incorporation of cargo and the formation of a stable pre-budding complex, the outer layer of the coat is recruited to the ER membrane. This outer layer is composed of the heterotetramer Sec13–Sec31, which consists of two Sec13 and two Sec31 subunits ***(Lederkremer G.Z. et al. 2001, Stagg M.S. et al. 2006).***
Soon after budding, COPII vesicles uncoat due to the GTP hydrolysis by Sar1

(Oka T. et al. 1994). The intrinsic slow rate of Sar1 GTP hydrolysis is accelerated in two steps: i. interaction with Sec23 acting as GTPase-activating protein for Sar1; ii. binding of Sec13–Sec31 to the pre-budding complex, which increases Sec23-mediated GAP activity by an order of magnitude, presumably by optimising the interaction of Sec23 with Sar1 ***(Bielli A. et al. 2005).*** Sar1, Sec23–Sec24, and Sec13–Sec31 are the minimal machinery required to reconstitute COPII-dependent budding in vitro that is increased by the addition of Sec12. In vivo, several other factors are likely to play key roles ***(Fred S. et al. 2003, Yan S.O. et al 2010).*** For example p125A, originally identified as a Sec23A-interacting protein, interacts with the C-terminal region of Sec31A and is part of the Sec13/ Sec31A sub-complex and facilitates ER export in mammalian cells ***(Yan S.O. et al 2010).*** Incorporation of some cargo proteins in COPII vesicles is regulated by specific factors. Collagene VII, that is too big to fit into normal COPII vesicles (70nm diameter), requires the interaction with TANGO1 protein that delays vesicle budding in order to allow the entry of the protein into the much larger vesicular carrier ***(Saito K. Et al. 2009).*** In addition, it has been demonstrated that cTAGE5, an integral membrane protein containing two coiled-coil motifs and a proline-rich domain, is specifically located at the ER exit sites and acts as TANGO1 co-receptor important for the ER export of Collagene VII ***(Kota S. et al. 2011).***

The first station for soluble and transmembrane proteins exiting from the ER is the ERGIC. The principal marker for this compartment is the type I transmembrane protein ERGIC-53, a mannose-binding lectin required for the export of several cargoes from the ER ***(Appenzeller C. et al. 1999, Nichols W.C. et al. 1998)*** as well as for maintaining the structural integrity of ERGIC **(*Nichols W.C. et al. 1998*)**. Mutations in the ERGIC-53 gene cause autosomal recessive bleeding disorders resulting from the inability to package the blood clotting factors V and VIII **(*Nichols W.C. et al. 1998*)**. ERGIC-53 interacts directly with Sec23 leading to the recruitment of ERGIC-53/cargo complexes into COPII vesicles. After reaching the ERGIC, the cargo dissociates from the complex and ERGIC-53 is recycled back to the ER ***(Kappler F. et al. 1997)***. Retrograde transport is mediated by COPI vesicles. COPI was originally discovered through an in vitro reconstitution system that sought to study vesicular transport among the Golgi stacks. The initial structure identified was a seven-subunit (α, β, β', γ, δ, ε, ζ) complex named coatomer ***(Beck R. et al. 2009).*** The process of COPI vesicle biogenesis is controlled by Arf1, a small GTPase of the Ras superfamily. A guanine nucleotide exchange factor (GEF) containing a Sec7 domain induces the exchange of bound GDP to GTP in Arf1. GBF1, a large Sec7 domain-containing GEF is the major exchange factor involved in COPI vesicle biogenesis. Following nucleotide exchange, Arf1 undergoes a conformational change, leading to the exposure of a myristoylated N-terminal amphipathic helix that provides stable membrane anchorage and leads to the membrane deformation and recruits the others proteins of the COPI machinery ***(Beck R. et al. 2009).***

The next compartment along the secretory pathway is the Golgi complex. This

apparatus is a labyrinth of cisternal membranes constituting the main transport pathway for secretory proteins between the ER and the plasma membrane. It is well established that glycoproteins, glycolipids and proteoglycans in transit through the Golgi system encounter modification by a large number of glycosyltransferases, sulfotransferases, proteases and other classes of enzymes ***(Kristian Prydz et al. 2008).***

Two main models have been preposed to describe the movement of cargo proteins and lipids through the golgi-*cisternae* are principally two: *"The anterograde vesicular trafficking model"* and *"The cisternal-maturation model"*. In the first model, it was postulated that coatomer-coated vesicles carried cargo forwards from one compartment to the next. This simple and straightforward model has received considerable support for the first trafficking step of the secretory pathway, from the ER to the first post-ER compartment, which is mediated by the COPII coat.

In the second model, cargo that entry in the *cis*-Golgi will remain there for a fixed amount of time while glycosylation enzymes are delivered sequentially via retrograde trafficking to the compartment in which the cargo molecules are located.

Recently, it has been proposed an other model, "*The rapid-partitioning model*", that is principally based on three key elements: sorting of lipids into different domains at each level of the Golgi; bidirectional trafficking of cargo and processing enzymes within the Golgi; and association of proteins with their preferred lipid environment. In addition to the standard trafficking pathways of cargo and glycosylation enzymes between ER and Golgi, the model postulates the trafficking of resident Golgi enzymes and cargo in both directions through the Golgi. This bidirectional trafficking is at variance from the cisternal-maturation model, which assumes retrograde trafficking of only glycosylation enzymes ***(Catherine L. Jackson et al. 2009).***

Finally, macromolecules traversing the Golgi complex exit from this organelle in vesicular or tubular structures, rising from the **t**rans **G**olgi **N**etwork (TGN), destined for different cellular target membranes. This process is principally based on the recognition of specific sorting motifs in the cytosolic tail of transmembrane cargo and cargo receptors by cytosolic adaptors and coat proteins. The key components of these machineries include small GTPases of the ARF and Rab family adaptors, GRIP-golgins and lipids, such as phosphoinositides, sphingolipids and cholesterol. Once activated by specific nucleotide exchange factors, ARF1 promotes the recruitment of cytosolic protein complexes that recognize the cargo sorting motifs and bind to clathrin, thus functioning as adaptors between cargo proteins and clathrin coat. These coat adaptors include the AP1A and AP3 complexes and the GGAs, which mediate endosomal sorting ***(Robinson M. S. et al. 2004).***

CHAPTER I

Publications:

The ligand of Numb protein LNX1p80 and LNX2 interact with the human glycoprotein CD8a and promote its ubiquitylation and endocytosis.

Massimo D'Agostino[1], Giusy Tornillo[1], Maria Gabriella Caporaso[1], Maria Vittoria Barone[2], Eric Ghigo[3], Stefano Bonatti[1],* and Giovanna Mottola[1],*

[1]Dipartimento di Biochimica e Biotecnologie Mediche, University of Naples 'Federico II', Via S. Pansini 5, 80131 Naples, Italy

[2]Dipartimento di Pediatria, European Laboratory For the Investigation of Food Induced Disease, University of Naples 'Federico II', Via S. Pansini 5, 80131 Naples, Italy.

[3]URMITE, CNRS UMR6236-IRD 3R198, Universite´ de la Me´ diterrane´e, 27 Bd Jean Moulin 13358 Marseille CEDEX 05, France.

*Authors for correspondence (mottola@dbbm.unina.it; bonatti@dbbm.unina.it)

1.1.1 Abstract.

E3 ubiquitin ligases give specificity to the ubiquitylation process by selectively binding substrates. Recently, their function has emerged as a crucial modulator of T-cell tolerance and immunity. However, substrates, partners and mechanism of action for most E3 ligases remain largely unknown.

In this study, we identified the human T-cell co-receptor CD8 a-chain as binding partner of the ligand of Numb proteins X1 (LNX1p80 isoform) and X2 (LNX2). Both LNX mRNAs were found expressed in T cells purified from human blood, and both proteins interacted with CD8a in human HPB-ALL T cells. By using an in vitro assay and a heterologous expression system we showed that the interaction is mediated by the PDZ (PSD95-DlgA-ZO-1) domains of LNX proteins and the cytosolic C-terminal valine motif of CD8a.

Moreover, CD8a redistributed LNX1 or LNX2 from the cytosol to the plasma membrane, whereas, remarkably, LNX1 or LNX2 promoted CD8a ubiquitylation, downregulation from the plasma membrane, transport to the lysosomes, and degradation.

Our findings highlight the function of LNX proteins as E3 ligases and suggest a mechanism of regulation for CD8a localization at the plasma membrane by ubiquitylation and endocytosis.

1.1.2 Regulation of receptor level on plasma membrane.

Endocytosis is the process by which an intracellular vesicle is formed by membrane invagination, engulfing extracellular and membrane-bound components. Endocytosis and the opposite process of exocytosis are required for a large number of essential cell functions, including nutrient uptake, cell-cell communication, and the turn-over of the plasma membrane composition. The central role of these transport mechanisms is well appreciated in receptor regulation, neurotransmission, and drug delivery ***(Oved S. et al. 2002; Schmidt AA. 2002).*** In addition, it has been demostrated that endocytosis plays an important role in the signaling: several receptors signal mostly in the intracellular membrane, after activation by the ligand and internalization, or signal differently from intracellular membrane and from the cell surface ***(Amandio V. Vieira et al. 1996; Harald W Platta and Harald Stenmark 2011; Fumiko Itoh et al. 2002; Di Guglielmo M.G. et al. 2003).*** Endocytosis exists in different forms: phagocytosis, pinocytosis, receptor-mediated endocytosis. Other mechanisms include caveolae-mediated endocytosis and transient poration induced by the cellular microenvironment ***(Parton RG. et al. 2003)***. The uptake of material inside the cell was first visualized following the introduction of glutaraldehyde fixation in the 1960s; this generated electron microscopy images of vesicles with proteinaceous coats in many different tissues ***(Rosenbluth J. et al. 1964; Roth T.F. et al. 1964).*** Clathrin was then identified as being the major protein making the lattice-like coat around vesicles, which were described as "vesicles in a basket".

Clathrin-mediated endocytosis is the uptake of material into the cell from the surface using clathrin-coated vesicles. Although clathrin-coated vesicles can also be formed from other membranous compartments, the term clathrin-mediated endocytosis is used to refer only to intake through vesicles formed from the plasma membrane. The pathway is versatile, as many different cargoes can be packaged using a range of accessory adaptor proteins. Clathrin-mediated endocytosis is used by all known eukaryotic cells. Other clathrin-independent entry portals (such as caveolin-dependent pathways) have been described, although their molecular details and cargo specificity are not as well defined ***(Harvey T.M. et al. 2011).***

Clathrin-coated vesicle (CCV) formation proceeds through five stages that correspond to ultrastructural and cell biological observations: initiation, cargo selection, coat assembly, scission and uncoating. Following cargo selection and initiation of pit formation, soluble clathrin polymerize into hexagons and pentagons, the relative ratio of which accommodates a wide range of membrane curvatures. Clathrin does not bind directly to the membrane or to cargo receptors and thus relies on adaptor proteins and complexes (such as adaptor protein 2 - AP2) and accessory proteins (such as AP180 and epsin) to be recruited to the plasma membrane ***(Harvey T.M. et al. 2011).*** Although the endocytosis of cargo receptors can be stimulated by ligand binding (for example, epidermal growth factor receptor - EGFR), other receptors (for

example, transferrin receptor - TfR) are constitutively internalized. When a receptor has been taken up, it is sorted in endosomes and either sent back to the surface or targeted to more mature endosomes and later compartments (such as multivesicular bodies and lysosomes) ***(Hopkins C.R. et al. 1985).*** Receptor internalization results in the desensitization of the cell toward ligand induced signaling.

Signals for the incorporation of cargo receptors into plasma membrane-derived CCV have been defined based on examination of protein sequences. The best characterized signal sequence is the YXXØ motif, in which Ø represents a bulky hydrophobic amino acid. Such signals are found in both constitutively endocytosed receptors (i.e. transferrin receptor) and receptors which are endocytosed only after ligand binding (Epidermal Growth Factor - EGF). In the latter case, ligand binding causes phosphorylation of the receptor and a conformational change that results in the exposure of the internalization signal ***(Madshus I.H., Stang E. 2009)***. The μ2 adaptin subunit has been shown to interact with these tyrosine-based internalization signals ***(Boll W. et al. 2003).*** An alternative internalization signal, dileucine, does not interact with the μ2 chain *in-vitro*, although there is evidence indicating an interaction with AP-2 ***(Rahel Byland et al. 2007).*** An exception to the model of AP-2-mediated recruitment of receptors to CCV is provided by G-protein coupled receptors where other adaptor proteins, called β-arrestins, are critical for mediating endocytosis ***(Fadi F. Hamdan et al. 2007).*** Following endocytosis, individual receptors can be sorted between recycling and degradative pathways ***(Tsao P et al. 2001; Whistler JL et al. 2002).*** For a recycling receptor, endocytosis can serve as a mechanism for receptor resensitization by delivering internalized receptors back to the plasma membrane in a fully active state. Alternatively, for receptors that have to be degraded, rapid endocytosis can serve as a first step towards receptor down-regulation by delivering the receptors to late endosomes and lysosomes. The cascade of events for each receptor, globally referred to as 'receptor trafficking', is thought to be initiated already at the plasma membrane, where receptors are 'tagged', e.g. phosphorylated or ubiquitinated, to determine their endocytic and postendocytic fates. Receptor phosphorylation can occur in response to activation by an agonist and is necessary for receptor endocytosis ***(Premont RT, Gainetdinov RR 2007; Ferguson SS et al. 1998).*** However, it has been suggested that receptor tag not only influences endocytosis, but also influences its postendocytic fate, regulating interactions with sorting proteins or by inducing other post-translational modifications ***(Cao T.T. et al. 1999; Marchese A, Benovic J.L. 2001).*** One of the sorting signals for proteins along the exo- and endocytic pathways is the ubiquitynation, a post-translational modification by which ubiquitin, a polypeptide of 76 amino acid residues, is covalently attached to lysine (Lys) residues of a substrate protein ***(Hershko and Ciechanover, 1992).*** Once thought to only mediate proteasomal degradation in the cytosol ***(Pickart and Fushman, 2004)***, ubiquitynation might also occur at the plasma membrane where it regulates protein internalization, at the trans-Golgi

complex where it directs proteins to the late endosomes, and in endosomes to sort proteins to the multivesicular bodies ***(Mukhopadhyay and Riezman 2007; Piper and Luzio, 2007).*** In all these cases, it results in protein degradation into the lysosomes. The fate and the transport of the tagged substrate will depend on the Lys residue involved in the formation of ubiquitynation chains, as well as on the number of residues added. Single ubiquitin monomers can be attached to one or several Lys of a protein (mono- or multimonoubiquitylation, respectively). Ubiquitin itself possesses several Lys residues that can be used for the attachment of another ubiquitin molecule, allowing substrates to be modified with different types of ubiquitin chains (polyubiquitynation). Ubiquitynation occurs in a stepwise manner involving three enzymes: an ubiquitin-activating enzyme E1 is responsible for the attachment of free ubiquitin; a second ubiquitin-conjugating enzyme E2 receives it from E1; and a third ubiquitin ligase E3 catalyzes the final transfer of the ubiquitin from the E2 enzyme to the substrate. The specificity of the ubiquitynation process is determined by the E3 ligases, which are suggested to function as an adaptor to bind substrates selectively. More than 600 E3 ligases were found in the human proteome and were classified into two major groups, defined by the presence of either a HECT (homologous to the E6 associated protein C terminus) or a RING (really interesting new gene) domain as catalytic domain. Recently, it has been emerging that E3 ligases play an important function in regulating T-cell tolerance and immunity ***(Bhoj and Chen, 2009; Deshaies and Joazeiro, 2009; Gomez-Martin et al., 2008).*** For instance, the E3 ligase c-Cbl regulates T-cell receptor (TCR) activation by both degrading key signalling molecules such as PLCc-1 ***(Jeon et al., 2004)*** and controlling TCR internalization and transport to the lysosomes ***(Naramura et al., 2002).*** Interestingly, the defective expression of some E3 ligases has been related to the development of autoimmune diseases, such as encephalomyelitis, arthritis and autoimmune diabetes ***(Chiang et al., 2000; Gronski et al., 2004; Jeon et al., 2004).***

1.1.3 Human glycoprotein CD8α.

The T-cell coreceptor CD8 is a type I transmembrane protein expressed as αα homodimer on the surface of intestinal T cells, γδ T cells, thymic T-cell precursors and NK cells, and as αβ heterodimer on thymocytes and peripheral T-cells ***(Gangadharan and Cheroutre 2004, Irie et al. 1995).*** The surface expression of CD8 αβ heterodimer depends on the α chain ***(Goldrath et al. 1997),*** while efficient surface expression of the α chain requires its cytosolic C-terminal valine motif (C-TVM), a ligand of PDZ domains that modulates its delivery to the plasma membrane (PM) by sequentially interacting with GRASP65 and GRASP55 proteins ***(Iodice et al. 2001; D'Angelo et al. 2009).*** Required for the activation of cytotoxic T lymphocytes, CD8 stabilizes the interaction between the TCR on the surface of the lymphocytes and the class I major histocompatibility complex on antigen-presenting cells. Furthermore, it recruits the p56lck protein tyrosine kinase, bound to the cytosolic tail of its α-chain, to the vicinity of the TCR. CD8 functions as co-activator because Lck is a major proximal effector of the T cell activation cascade ***(Salmond et al. 2009 Weiss and Littman 1994).*** Development of cytotoxic T lymphocytes was greatly reduced in CD8α-/- mice ***(Fung-Leung et al. 1991)*** and defects in CD8α and β expression were shown to correlate with pathological conditions such as immunodeficiencies and Wiskott-Aldrich syndrome ***(de la Calle-Martin et al. 2001, Kawabata et al. 1996, Schmitz et al. 1998).*** How CD8 function is regulated at the PM and whether its impairment leads to immune diseases is still largely unknown.

1.2 Aim of the study.

As it has been mentioned above, the C-TVM of CD8α is important to obtain efficient intracellular transport to the plasma membrane (PM) thanks to the sequential interaction with GRASP65 and GRASP55 proteins. This binding occurs after the incorporation of the receptor into COPII vesicles and it is important for the best traffic rate to and through the Golgi complex but not for the delivery to the PM. However, is well known the important of PDZ domain containing proteins for the stability and dinamics for the receptor at the PM. For this reason, the aim of this study was to identify and characterize proteins that could modulate CD8α localization at the PM, in C-TVM dependent manner. To do this, drs G. D'Angelo and L. Iodice in the lab performed a yeast two-hybrid screening using a human liver cDNA library and the CD8α cytosolic C-terminal tail as bait (Fig.1A). Among positive clones, one contained a cDNA fragment encoding amino acids 56-451 of the LNX2 protein (Fig.1B). LNX2 protein was initially identified as ligand of the endocytic protein Numb (**L**igand of **N**umb protein **X**) ***(Dho et al. 1998; Rice et al. 2001).*** It was classified as RING type E3 ligases, since it contains an N-terminal RING finger domain (Fig.1C). However, it has been poorly characterized and its function as E3 ligase has never been addressed. In addition, it also contains four PDZ domains, presumably mediating protein-protein interaction. The cDNA fragment identified by the two-hybrid assay corresponded to the LNX2 N-terminal region including RING finger domain, the NPAY motif for the interaction with Numb and the first two PDZ domains (Fig.1C). Interestingly, the interaction was disrupted when the PDZ ligand signal was removed from the bait by deletion of the Tyr and Val residues from the C-TVM (CD8-ΔYV) (Fig.1B), indicating that the binding between CD8α and LNX2 is strongly dependent on this signal.
My work started to characterize LNX2-CD8α interaction in order to investigate the role of LNX2 on the plasma membrane localization of CD8α.

1.3 Materials and methods.

All of the culture reagents were obtained from Sigma-Aldrich (Milan, Italy). The solid chemical and liquid reagents were obtained from E. Merck (Darmstadt, Germany), Farmitalia Carlo Erba (Milan, Italy), Serva Feinbiochemica (Heidelberg, Germany), Delchimica (Naples, Italy) and BDH (Poole, United Kingdom). The radiochemicals were obtained from Perkin Elmer (Bruxelles, Belgium). Protein A-Sepharose CL-4B and the ECL reagents were from Amersham Biosciences (Milan, Italy).

Antibodies
The following antibodies were used: the OKT8 mouse anti-CD8α monoclonal antibody from Ortho (Raritan, NJ, USA); the N1 mouse anti-CD8α monoclonal antibody and rabbit anti-CD8α polyclonal antibody from M. Jackson (Martire et al., 1996); rabbit anti-LNX1 antibody (Kansaku et al., 2006); rabbit and mouse anti-GFP and anti-HA antibodies (Santa Cruz Biotechnology Inc.); mouse anti-EEA1 monoclonal antibody (BD Transduction Laboratories, Lexington, KY); mouse anti-CD7107a **(**LAMP1) monoclonal antibody (Biolegend); Peroxidase-conjugated anti-mouse and anti-rabbit IgG (Sigma-Aldrich, Milan, Italy). Texas-Red-conjugated anti-mouse or rabbit IgG, FITC-conjugated anti-mouse or rabbit IgG and Cy5-conjugated anti-mouse IgG (Jackson Immunoresearch Laboratories, West Grove, PA, USA).

cDNA cloning and plasmid construction
The expression vector FLTRβT8 for wild type CD8α and CD8α-ΔYV (Iodice et al., 2001; Mottola et al., 2000) and HA-Ubiquitin (Mauro et al., 2006) have been previously described. LNX1p80 (ID 4995278) and LNX2 (ID 5541168) cDNAs were obtained from I.M.A.G.E. Consortium. GFP-LNX1p80 and GFP-LNX2 expression vectors were generated by PCR and subcloning of LNX1p80 and LNX2 cDNAs in the pEGFP-N1 vector (Clontech).
For *in vitro* binding assays, GST fused to wild type or ΔYV-mutant CD8α were expressed using pGEX-6P-1 (Pharmacia Biotech.). LNX1p80, LNX2 and all their truncated forms were subcloned in the expression vector pcDNA3 (Clontech). The following LNX1p80 cDNA fragments were expressed for the *in vitro* binding assay in Fig.S1: RING-NPAF (1-760bp); RING (1-309bp); NPAF (309-760bp); PDZ(1-4) (760-2187bp); PDZ(1-2) (760-1415bp); PDZ(3-4) (1480-2187bp); PDZ(1) (760-1074bp), PDZ(2) (1114-1415bp).
The following LNX2 cDNA fragments were expressed for the *in vitro* binding assay in Fig.S1: RING-NPAY (1-666bp); RING (1-340bp); NPAY (510-666bp); PDZ(1-4) (637-2073bp); PDZ(1-2) (682-1386bp); PDZ(3-4) (1378-2073bp); PDZ(1) (682-983bp), PDZ(2) (961-1386bp).

In vitro binding assay

LNX1p80 or LNX2 proteins were *in vitro* translated and labelled by 35S-methionine using the TnTR coupled reticulocyte lysate system (Promega). 1/2 of the full-length LNX proteins or fragments producted *in vitro* were incubated with 30 μg of glutathione-Sepharose beads loaded with GST or GST fused to wild type or ΔYV-mutant CD8α. Bound proteins were eluted from the beads and analysed by SDS-PAGE and autoradiography. In all the GST-pull down experiments the loading control (L) represents 20% of the whole amount of *in vitro* translated proteins used for incubation.

Cell culture, transfection and immunofluorescence

Human embryonal kidney HEK293 and human hepatoma Huh-7 cells were routinely grown at 37ºC in Dulbecco's Modified Essential Medium (DMEM), containing 10% fetal bovine serum (FBS). HPB-ALL T cells were cultured in RPMI 1640, containing 15 % FBS.

HEK293 and Huh-7 cells were transfected by using FuGene 6.0 according to the manifacturer instruction (Roche). The effect of CD8α expression on LNX protein localization was obtained by simultaneous cotransfection of CD8α and LNX proteins expression vectors and, 40 hrs later, cell fixation or lysis. To observe the effect of LNX proteins expression on CD8α localization and protein level, cells were initially transfected with LNX proteins expression vectors in order to allow LNX proteins accumulation and, 24 hrs later, transfected a second time with CD8α expression vectors. Then, after further 24 hrs, they were either lysed or fixed.

Indirect immunofluorescence was performed as previously described (Mottola et al., 2000). Single confocal images were acquired at 63x and 100x magnification on a Meta Zeiss Confocal Microscope (Carl Zeiss, Jena, Germany).

To separately stain CD8α protein on either cell surface (extra) or intracellular membranes (intra), after fixation cells were incubated with the rabbit anti-CD8α polyclonal antibody, then permeabilized and incubated with the mouse anti-CD8α monoclonal antibody (Mottola G., et al. 2000). Two distinct secondary antibodies allow separately visualizing the two fractions. Then, in order to measure the ratio between the plasma membrane and intracellular CD8α in cell, immunofluorescence intensity in the two channels was measured by using photoshop and ImageJ Biophotonic programs for each cotransfection 15 cells were considered for quantification. The results are given as mean±SD (Standard deviation).

Preparation of cell extracts, immunoprecipitation SDS-PAGE and Western immunoblotting.
Cells were lysed with 10mM Tris-HCl pH 7.4/150mM NaCl/ 1mM EDTA pH 8.0/ 1% Triton X-100. For all the experiments on transfected HEK293, 6 x 106 cells were lysed and used for each coimmunoprecipitation. For the experiment on HPBALL cells, 100 x 106 cells were used for each coimmunoprecipitation. Immunoprecipitation was performed by over-night incubation with OKT-8, a conformation-sensitive antibody anti-CD8α, followed by adding Protein A-Sepharose beads (Pharmacia). Immunoprecipitated pellet were washed, treated for SDS-PAGE and resolved on a 10% polyacrylamide gels. For each experiment aliquots of the lysate (100 μg total protein/each aliquot) were also precipitated with acetone and treated for SDSPAGE. Next, proteins were transferred to nitrocellulose filters, which were then incubated with primary antibodies diluted in blocking buffer (5% non-fat dry milk, 0.1% Tween-20 in PBS), followed by peroxidase-conjugated secondary antibodies. For anti-LNX1p80 and anti-LNX2 antibodies western blot was performed in PBS- 1% BSA. After washing, bound antibodies were detected by ECL (Amersham Biosciences). CD8α degradation was detected by previously treating cells with or without 90μM chloroquine for 16 hours.

1.4 RESULTS.

1.4.1 CD8α binds the LNX proteins LNX2 and LNX1p80.

To confirm the interaction between LNX2 and CD8α, LNX2 cDNA was *in vitro* transcribed and translated and the radioactively labeled protein was incubated with either the CD8α cytosolic C-terminal tail or its ΔYV-mutant fused to the GST (see Materials and methods). The bound proteins were separated by SDS-PAGE and revealed by autoradiography. As shown in Fig.1D, LNX2 associates *in vitro* with the cytosolic C-terminal tail of CD8α (lane 2), but not with its ΔYV-mutant (lane 3).
LNX2 is closely related to the p80 isoform of LNX1, another member of the LNX protein family [Fig.1C, ***(Dho et al. 1998; Rice et al. 2001)***]. However, in contrast to LNX2, the function of LNX1p80 as E3 ligase has been partially explored ***(Kansaku et al. 2006; Takahashi et al. 2009)***. For these reasons, we decided to test whether LNX1 is a CD8α binding protein. On the other hand, we were not surprised that this protein was not found in our two-hybrid assay, since LNX1p80 is poorly expressed in human liver cells ***(Dho et al. 1998)***. As observed for LNX2, *in vitro* transcribed and translated LNX1p80 was also able to interact with the CD8α cytosolic C-terminal tail fused to the GST (Fig.1D, lane 5). The removal of the C-TVM from CD8α decreased such interaction (Fig.1D, lane 6).
CD8α protein is usually present in T and NK cells, but, unfortunately, the low level of endogenous CD8α protein did not allow us to co-immunoprecipitate LNX proteins from this cell fraction. Therefore, we used the human HPB-ALL T-cell line and we demonstrated that in these cells, LNX1p80 and LNX2 were pulled down by CD8α (Fig.2A, lanes 2 and 4). Therefore, these data suggested that such interactions are also occurring in the physiological context of the T cell coreceptor CD8α. In order to further characterize this interaction, we decided to shift to a heterologous expression system that could be more easily handled and allow higher level of protein expression. Therefore, GFP and GFP-tagged versions of LNX1p80 and LNX2 were generated, transfected with CD8α in HEK293 cells and then immunoprecipitated from cell lysates by an anti-GFP antibody. The presence of CD8α in the precipitates was tested by immunoblotting. Fig.2B shows that, consistently with the previous data, GFPLNX1p80 (lane 2) and GFP-LNX2 (lane 3), but not GFP (lane 1), were able to coimmunoprecipitate CD8α. Likewise, CD8α pulled-down GFP-LNX2 (Fig.2C, lane 1) and GFP-LNX1p80 (Fig.2C, lane 5). In the absence of CD8α C-TVM LNX2 interaction was completely lost (Fig.2C, lane 4), while LNX1p80 interaction decreased (Fig.2C, lane 8). Therefore, CD8α *in vitro* and *in vivo* interacts with LNX2 and LNX1p80 and these interactions require its C-TVM.
It has been previously shown that LNX1p80 interacts with the junctional proteins JAM-4 via the second PDZ domain ***(Kansaku et al. 2006)*** and the first

two PDZ domains of LNX2 are required for binding to the cell surface coxsackievirus and adenovirus receptor (CAR) ***(Sollerbrant et al. 2003)***. To identify regions of LNX1p80 and LNX2 important for CD8α recognition, we generated a series of truncation mutants, containing separately the distinct domains and tested their ability to bind CD8α cytosolic C-terminal tail or its ΔYV-mutant fused to the GST (Fig.S2). Consistently with the results of the two-hybrid assay, the N-terminal fragment of LNX2 including RING domain, NPAY signal and the first two PDZ domains was able, although to a less extent, to interact with CD8α tail in YV-dependent manner. However, neither the RING domain nor the NPAY motif alone interacted as the full-length protein. In contrast, we found that the fragment including all the four PDZ domains was indispensable for a proper interaction to CD8α.
Indeed, its *in vitro* binding efficiency was comparable to the one observed for the fulllength protein (Fig.S2). Moreover, when expressed in HEK293 cells, it was coimmunoprecipitated by CD8α (Fig.S3A, lane 3). Among the four PDZ domains of LNX2, the first 2 appeared to have a major role, since they were sufficient, although to a lesser extent, to bind CD8α tail in YV-dependent manner. Similar results were overall observed for the LNX1p80 protein (Fig.S2 and S3A), thus fully confirming the observation that LNX1p80 and LNX2 interact with CD8α via their four PDZ domains.

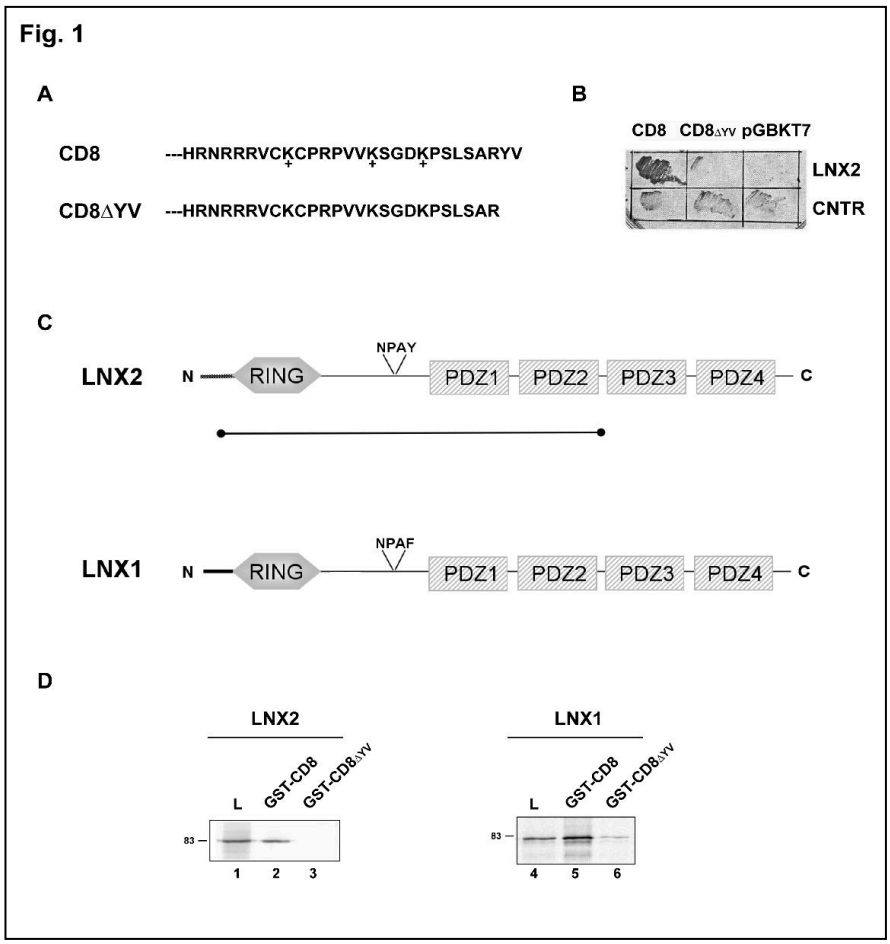

Fig.1: Identification and characterization of LNX2 and LNX1p80 as interacting partner of CD8α.

(A) The amino acidic sequences of CD8α wild type and ΔYV-mutant cytosolic Cterminal tail used as baits in the two-hybrid assay. (B) Identification of the N-terminal fragment of LNX2 by two-hybrid assay: yeast colony expressing the N-terminal fragment was able to grow on high-stringency selection plate when co-transformed with plasmid expressing the CD8α wild type cytosolic tail. No growth was detected when either a control plasmid (pGBKT7, vector with the GAL4 DNA binding domain) or a plasmid expressing the ΔYV-mutated tail was cotransformed. CNTR represents yeast colony transfected with the vector expressing only the GAL4 activation domain, which grew at low extent in all the transformations. (C) Schematic representation of LNX2 and LNX1p80. LNX proteins contain a RING finger domain, an NPAY/NPAF motif for interaction with Numb protein and 4 PDZ domains. The line underneath LNX2 indicates the fragment obtained by two-hybrid assay. (D) *In vitro* interaction between either LNX2 or LNX1p80 and the cytosolic tail of CD8α. Glutathione-sepharose beads, loaded with GST fused to CD8α wild type (lanes 2 and 5) or ΔYV mutant cytosolic tail (lanes 3 and 6), were incubated with 35S-methioninelabelled *in vitro*-translated LNX2 (lanes 2 and 3) or LNX1p80 (lanes 5 and 6). Bound proteins were eluted from the beads and analyzed together with the loaded samples (L, lanes 1 and 4) by SDS-PAGE and autoradiography. Numbers indicate molecular mass (kDa).

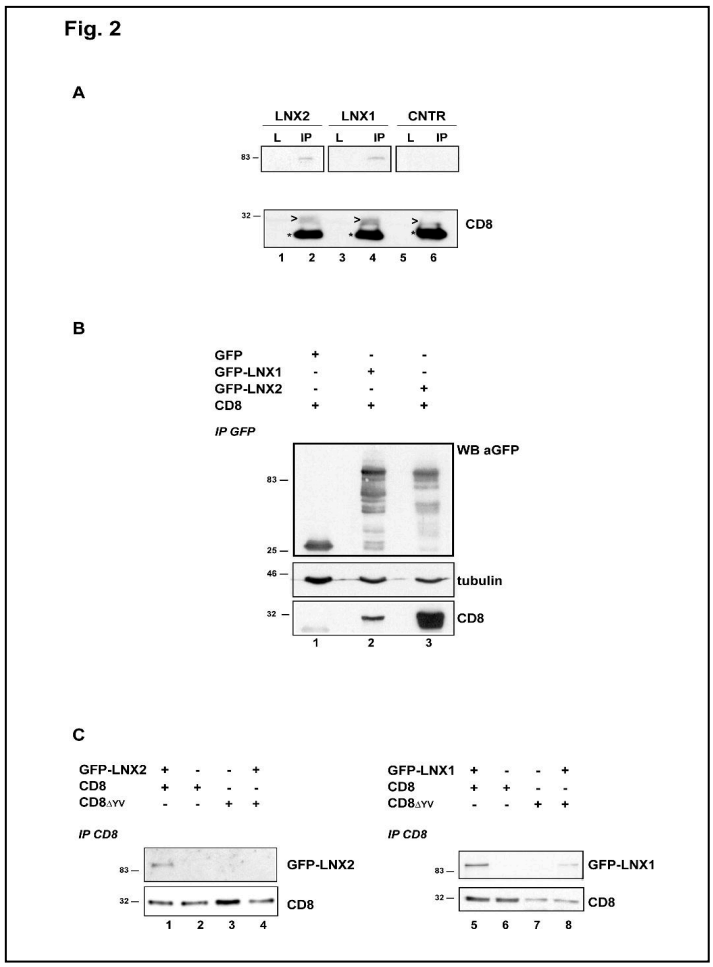

Fig.2: *In vivo* interaction between CD8α and either LNX2 or LNX1p80.
(A) CD8α was immunoprecipitated from human HPB-ALL T cells lysates and visualized by immunoblotting. A control was also performed by using mouse IgGs. Arrowheads point CD8α, which was immunoprecipitated with the mouse OKT-8 antibody (lane 2 and 4), but not with mouse IgGs (lane 6). The presence of either LNX1p80 (lane 4) or LNX2 (lane 2) in the immunoprecipitates was revealed with specific antibodies. In the control immunoblotting was performed by comcomitantly using anti-LNX1p80 and anti-LNX2 antibodies (lane 6). Aliquots (100 µg) of total proteins were precipitated and loaded (L). However, CD8α and LNX proteins (lanes 1,3 and 5) were poorly detectable in these fractions. Asterisks mark the immunoglobulin light chains revealed by immunoblotting. (B) CD8α was expressed with GFP (lane 1), GFP-LNX1p80 (lane 2) or GFP-LNX2 (lane 3) in HEK293 cells. After 24-hrs transfection, LNX proteins were immunoprecipitated from cell lysates by an anti-GFP antibody and visualized by immunoblotting. The presence of CD8α in the immunoprecipitates was revealed with with anti-CD8α antibody. Lysates were also analysed by imunoblotting with anti-tubulin antibody as loading control. (C) CD8α or CD8α-ΔYV was expressed alone (lanes 2,3,6,7) or together with either GFP-LNX2 (lanes 1,4) or GFP-LNX1p80 (lanes 5,8) in HEK293 cells. After 24-hrs transfection, CD8α was immunoprecipitated from cell lysates and visualized by immunoblotting. The presence of LNX proteins in the precipitates was revealed with an anti-LNX2 (lanes1-4) or anti-GFP (lanes 5-8) antibody. Numbers indicate molecular mass (kDa).

1.4.2 CD8α expression leads to redistribution of LNX1p80 or LNX2 to the plasma membrane.

In order to identify the intracellular localization of LNX1p80 and LNX2 in mammalian cells, GFP- or HA-tagged constructs of the two proteins were generated and expressed in HEK293 cells. GFP-LNX1p80 exhibited both a cytosolic and nuclear localization (Fig.3a), as previously described ***(Zheng et al. 2010)***. In contrast, GFP-LNX2 was exclusively cytosolic (Fig.3i). Remarkably, we found that this localization was changed upon simultaneous expression of wild type CD8α, since both GFP-LNX1p80 (Fig.3, c-e) and GFP-LNX2 (Fig.3, k-m) appeared to redistribute at the plasma membrane, where CD8α localized as well. In addition, GFP-LNX2 was also recruited by CD8α at the Golgi complex (Fig.3, k-m, arrowheads). Interestingly, HA-tagged fragments containing the four PDZ domains of either LNX1p80 or LNX2 were also relocated at the plasma membrane upon CD8α coexpression (Fig.S3B, a-c, g-i). Moreover, as expected, expression of the CD8-ΔYV did not have any affect on the intracellular distribution of all these chimeric proteins (Fig.3, f-h, n-p, and Fig.S3B, d-f, j-l). These results confirmed that CD8α interacts in live cells with LNX1p80 and LNX2, strongly suggesting a functional role of these interactions.

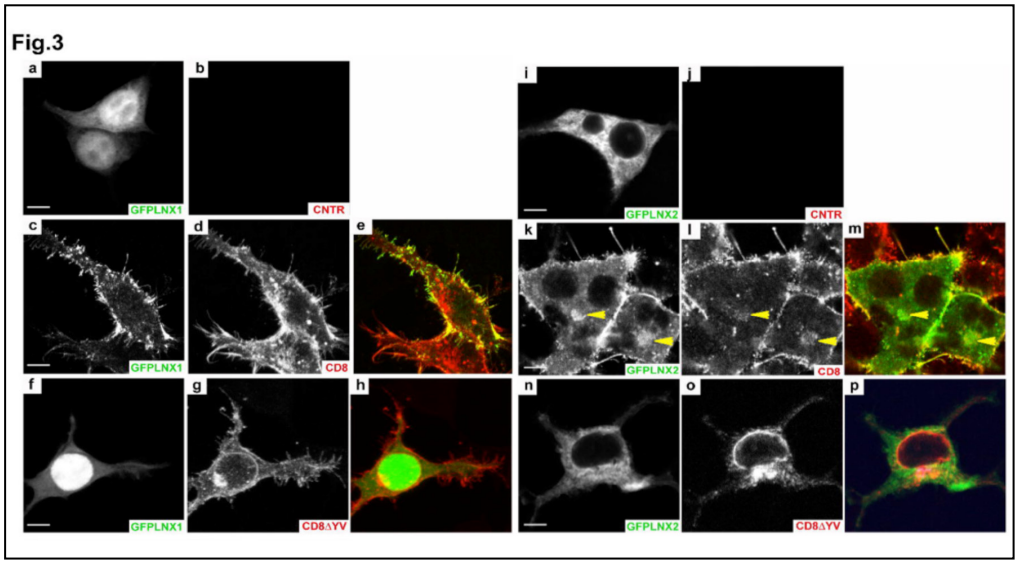

Fig.3: CD8α expression leads to redistribution of LNX1p80 or LNX2 to the plasma membrane.
GFP-LNX1p80 (green, a-h) or GFP-LNX2 (green, i-p) was expressed in HEK293 cells alone (a-b, i-j) or together with either CD8α (c-e, k-m) or CD8-ΔYV (f-h, n-p). After 24- hrs transfection, cells were fixed and immunostained for CD8α (red). (e, h, m, p) merge. Yellow arrowheads in k-m indicate colocalization between CD8α and GFP-LNX2, presumably at the Golgi complex. A single confocal section is shown. Scale bar, 3 μm.

1.4.3 LNX1p80 and LNX2 promote ubiquitination of CD8α.

Next, we examined whether LNX1p80 was able to ubiquitinate CD8α, as previously described for claudin ***(Takahashi et al. 2009)***, and whether also LNX2 was equipped of ubiquitination activity. For this purpose, we coexpressed CD8α, HA-tagged ubiquitin and either GFP, GFP-LNX1p80 or GFP-LNX2 in HEK293 cells (Fig.4). After 24-hrs transfection, CD8α was immunoprecipitated from cell lysates and its level of ubiquitination was analyzed by immunoblotting with an anti-HA antibody (Fig.4). In contrast to the control (lane 1), a pattern of HA signal was found in the presence of the coexpressed GFP-LNX1p80 (lane 2) or GFP-LNX2 (lane 3). Since the cytosolic tail of CD8α has three potential Lys residues for ubiquitination (Fig.1A), the lower bands visualized by the anti-HA antibody (asterisks) might correspond to monoubiquitination of a single, double or triple Lys residues, respectively. Higher bands, possibly corresponding to polyubiquitinated forms, and a smear pattern were detected exclusively when CD8α was coexpressed with LNX2 (lane 3). These results clearly indicated that both LNX1p80 and LNX2 induce CD8α ubiquitination.

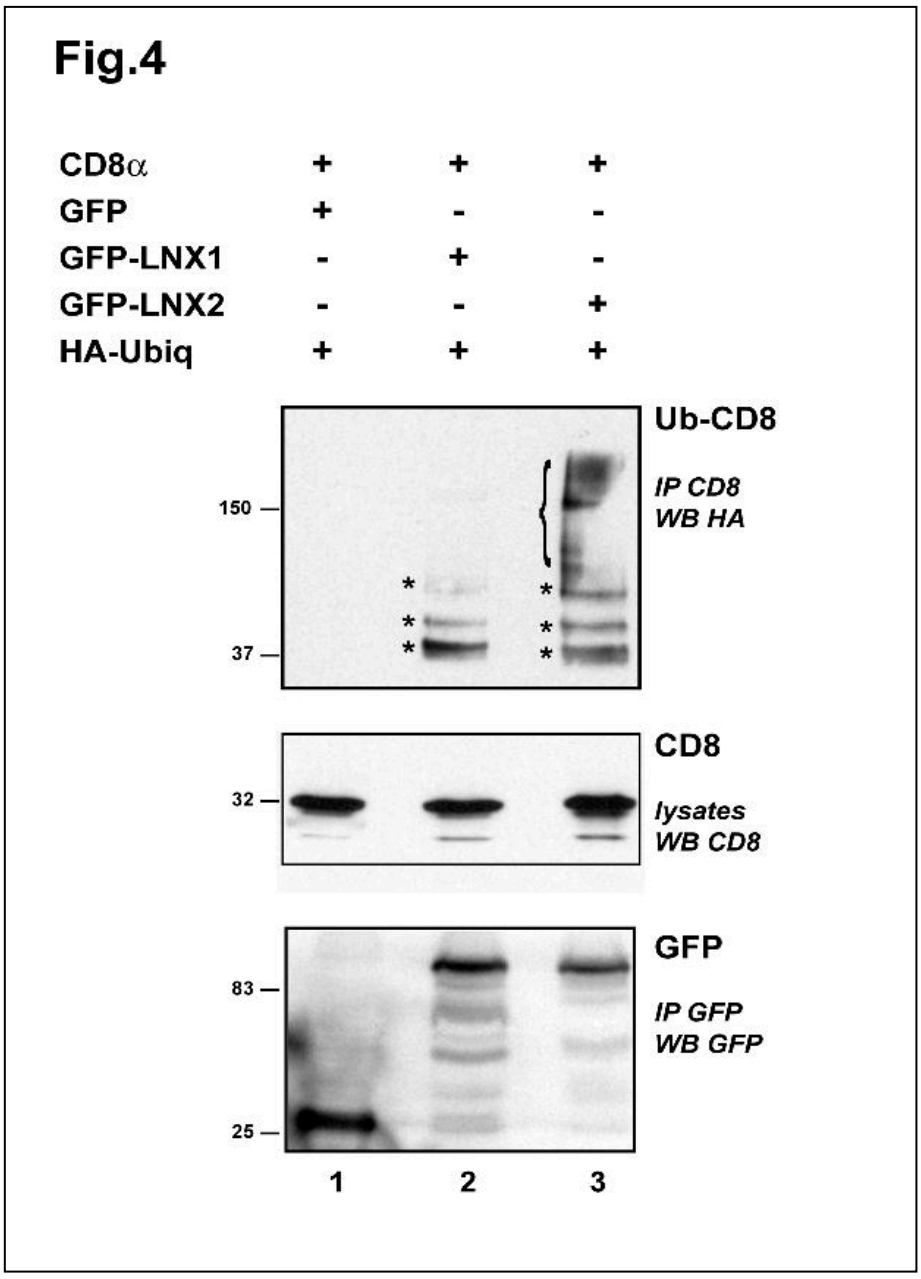

Fig.4: LNX1p80 and LNX2-dependent ubiquitination of CD8α.
Plasmids expressing CD8α, HA-tagged ubiquitin and GFP, GFP-LNX1p80 or GFPLNX2 were transiently co-transfected in HEK293 cells. After 24 hrs, CD8α was immunoprecipitated and the ubiquitinated CD8α fraction (Ub-CD8) was revealed by an anti-HA antibody. Total lysates were also analyzed by immunoblotting with anti-CD8α antibody. GFP-tagged LNXs were immunoprecipitated with a GFP mAb and revealed with an anti-GFP pAb. The asterisks indicate ubiquitinated CD8α bands, which might correspond to monoubiquitination of single, double or triple Lys residues, respectively. The parenthesis indicates the smear pattern and higher molecular weight ubiquitinated CD8α forms detected only in the presence of LNX2. Numbers indicate molecular mass (kDa).

1.4.4 LNX1p80 and LNX2 control CD8α localization at the plasma membrane.

While we were performing the immunofluorescence experiments on HEK293 cells, we observed a strong reduction of CD8α level at the PM in cells that expressed high levels of LNX proteins expression (data not shown). In order to verify and clearly visualize this effect, we decided to shift to the human hepatoma cell line Huh-7, because these cells are bigger and more spread than the HEK293, allowing a better visualization of protein localization at the PM. Moreover, we changed our transfection procedure by initially transfecting cells with GFP-LNX1p80, GFP-LNX2 or GFP and, only after 24 hrs, with CD8α. This allowed us to accumulate high level of LNX proteins in cells already before CD8α expression. Then, after further 24 hrs, cells were fixed and, before detergent permeabilization, directly treated with an anti-CD8 polyclonal antibody to uniquely label CD8α fraction localized at the PM. Cells were then permeabilized and the CD8α intracellular fraction was revealed by using an anti-CD8 monoclonal antibody. As shown in Fig.5, upon coexpression with either GFP-LNX1p80 (e-h) or GFP-LNX2 (i-l), the amount of CD8α localized at the PM was strongly decreased in comparison to cells expressing CD8α alone (f, j) or together with GFP (a-d). We quantified this decrease by measuring the ratio between the PM (extra) and intracellular (intra) signal detected by immunofluorescence (for quantification see Materials and methods). As shown in Fig.5, in respect to the control CD8/GFP coexpression, only ~50% of CD8α at the PM was detected upon GFP-LNX1p80 or GFP-LNX2 coexpression. Therefore, we concluded that LNX1p80 and LNX2 modulate CD8α protein level at the plasma membrane.

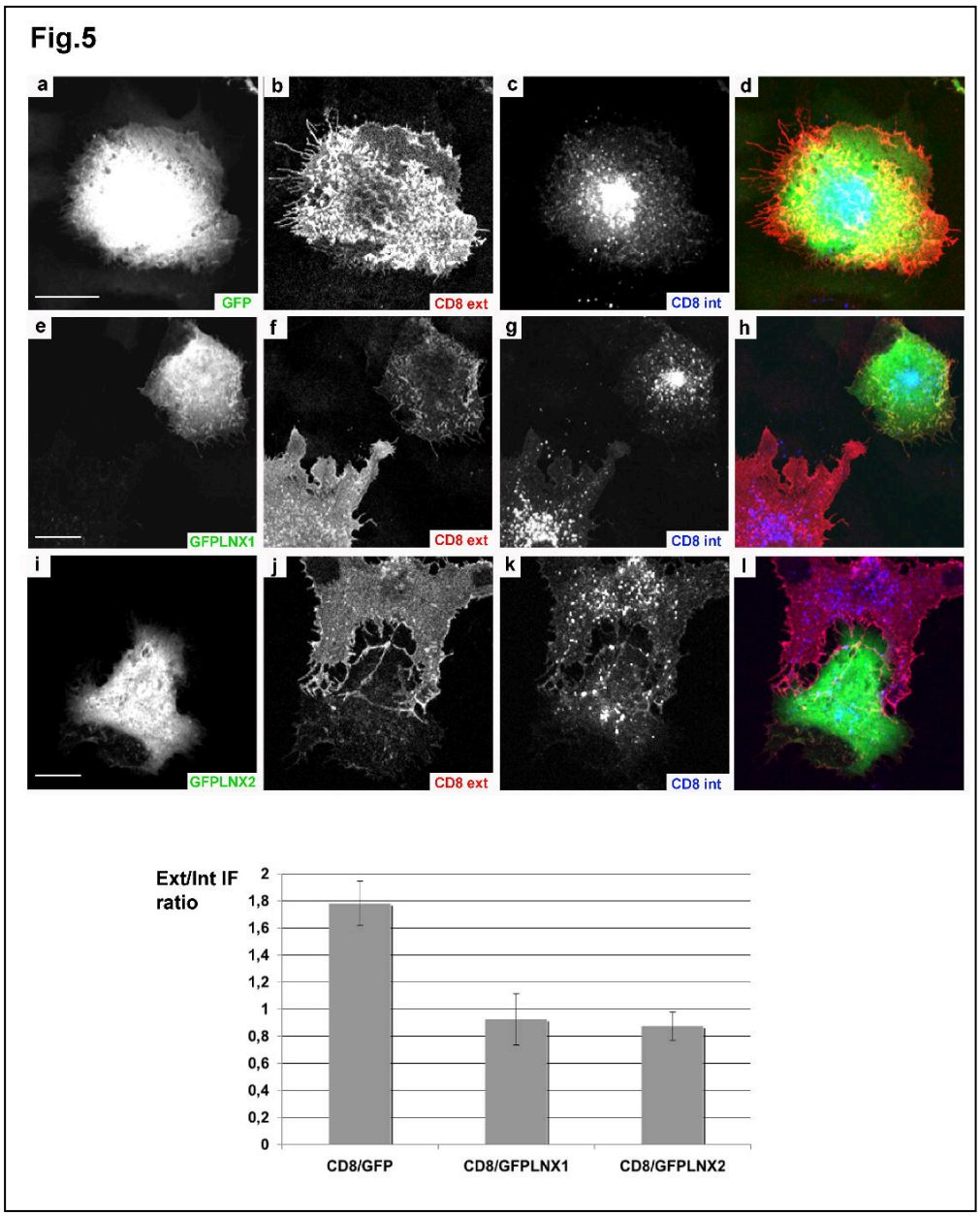

Fig.5: High expression level of GFP-LNX1p80 and GFP-LNX2, but not GFP, induces CD8α downregulation from the plasma membrane.
Huh-7 cells expressing by the new transfection procedure CD8α and high level of GFP (a-d), GFP-LNX1p80 (e-h) or GFP-LNX2 (i-l) were fixed and analyzed by indirect immunofluorescence. (b, f, j) cells stained for CD8α before permeabilization in order to label the CD8α fraction localized on the PM (CD8 ext, red); (c, g, k) cells stained for CD8α after permeabilization to label the CD8α intracellular fraction (CD8 int, blue). (d, h, l) merge. GFP (a, green), GFP-LNX1p80 (e, green) or GFP-LNX2 (i, green) expression is shown. On the bottom, the ratio between the external and the internal CD8α fraction quantified for the three distinct cotransfections as described in Materials and methods. A single confocal section is shown. Scale bar, 3 μm.

1.4.5 LNX1p80 and LNX2 are involved in endocytic trafficking and degradation of CD8α.

The monoubiquitination of CD8α and its downregulation from the PM in the presence of LNX1p80 and LNX2 strongly suggested that the two LNX proteins are involved in CD8α internalization and degradation. To address this hypothesis, Huh-7 cells expressing by the new transfection procedure high level of GFP-LNX1p80, GFP-LNX2 or GFP together with CD8α were examined by immunofluorescence using antibodies specific for an early endosomes marker EEA1 and a lysosomal marker, LAMP1, in order to detect the accumulation of CD8α into endocytic compartments. We found that in the presence of either GFP-LNX1p80 (Fig.6 and 7, e-h) or GFP-LNX2 (Fig.6 and 7, i-l), concomitantly to its downregulation from the PM, a fraction of CD8α accumulated in EEA1 or LAMP1-positive compartments (Fig.6 and 7, e-l, arrowheads). In contrast, when transfected alone (Fig.6, f, j) or with GFP (Fig.6 and 7, a-d), CD8α was not significantly detected in endocytic structures and mostly visualized at the PM. Similar results were also observed in HEK293 cells (data not shown).

Next, we examined whether CD8α downregulation from the PM observed by the new transfection procedure resulted in the coreceptor degradation. We have previously observed that simultaneous cotransfection of CD8α and GFP-LNX proteins induced CD8α ubiquitination but did not decrease the total amount of CD8α in the whole lysate (Fig.4, lanes 1-3). In contrast, Fig.8 clearly shows that, on equal conditions of cotransfection efficiency and input protein level (tubulin protein level), when GFPLNX1p80 (lane 2) or GFP-LNX2 (lane 3) are highly expressed, the total amount of CD8α in the whole lysate was smaller than that of GFP-coexpressing cells (lane 1).

Remarkably, such effect on CD8α was not observed, when CD8α was coexpressed with the HA-tagged PDZ domains of either LNX1p80 or LNX2 (lanes 4 and 5), which bind CD8α (Fig.S2 and Fig.S3), but lack the RING domains. To understand whether this degradation takes place into the lysosomes, we treated cells with the lysosome inhibitor chloroquine (Fig.8, lanes 6-10) and found that the amount of CD8α in the whole lysate was significantly increased by this treatment (lanes 7 and 8). These data strongly suggest that LNX1p80 and LNX2 induce CD8α transport to the lysosomes and degradation.

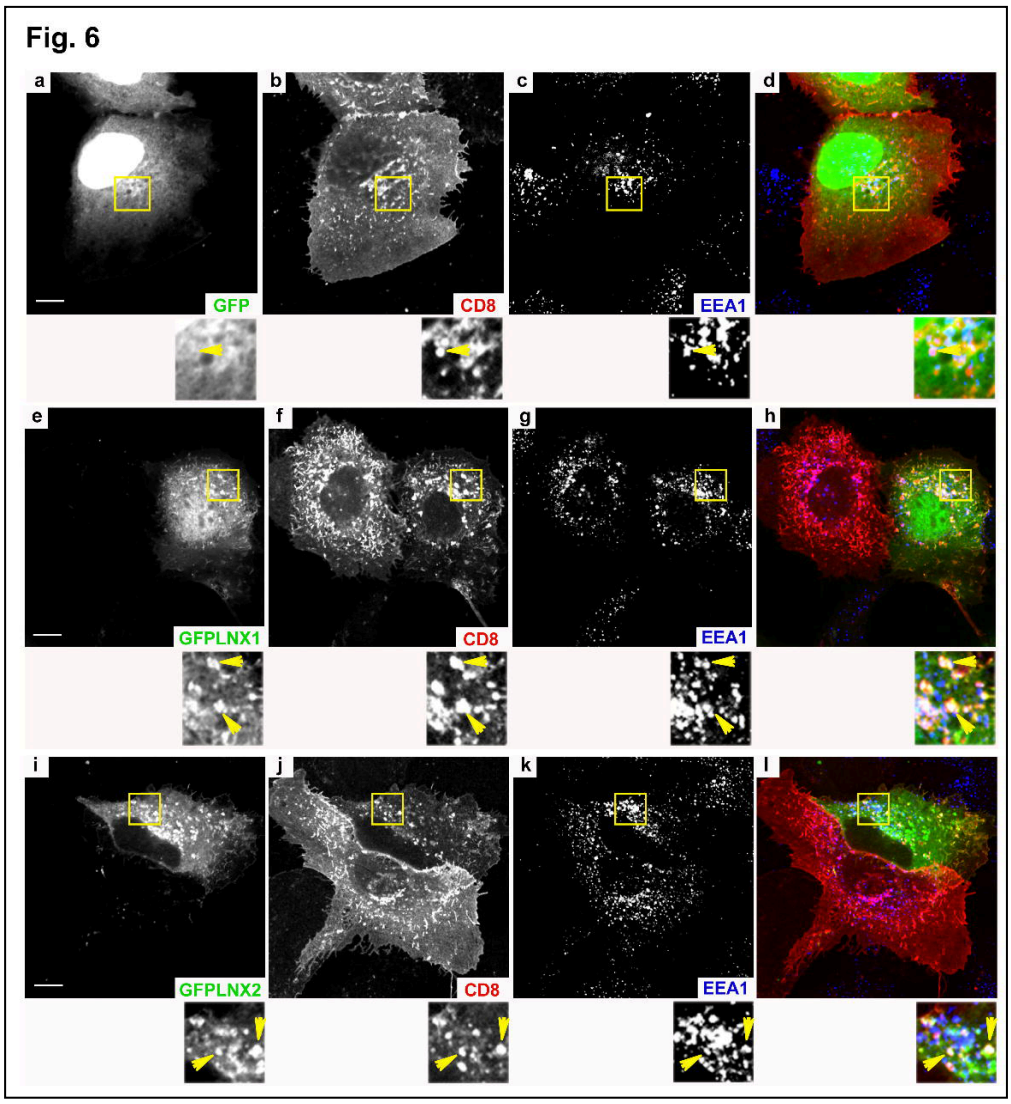

Fig.6: High expression level of GFP-LNX1p80 and GFP-LNX2, but not GFP, promotes CD8α transport to the early endosomes.
Huh-7 cells expressing by the new transfection procedure CD8α and high level of GFP (a-d), GFP-LNX1p80 (e-h) or GFP-LNX2 (i-l) were fixed and stained for CD8α (b, f, j, red) and the early endosomes marker EEA1 (c, g, k, blue). (d, h, l) merge. Higher magnification of the cell areas marked in panels by the yellow lines is shown at the bottom. Arrowheads indicate endocytic structures where CD8α colocalizes with GFPLNX1p80 or GFP-LNX2, but not GFP. A single confocal section is shown. Scale bar, 3 µm.

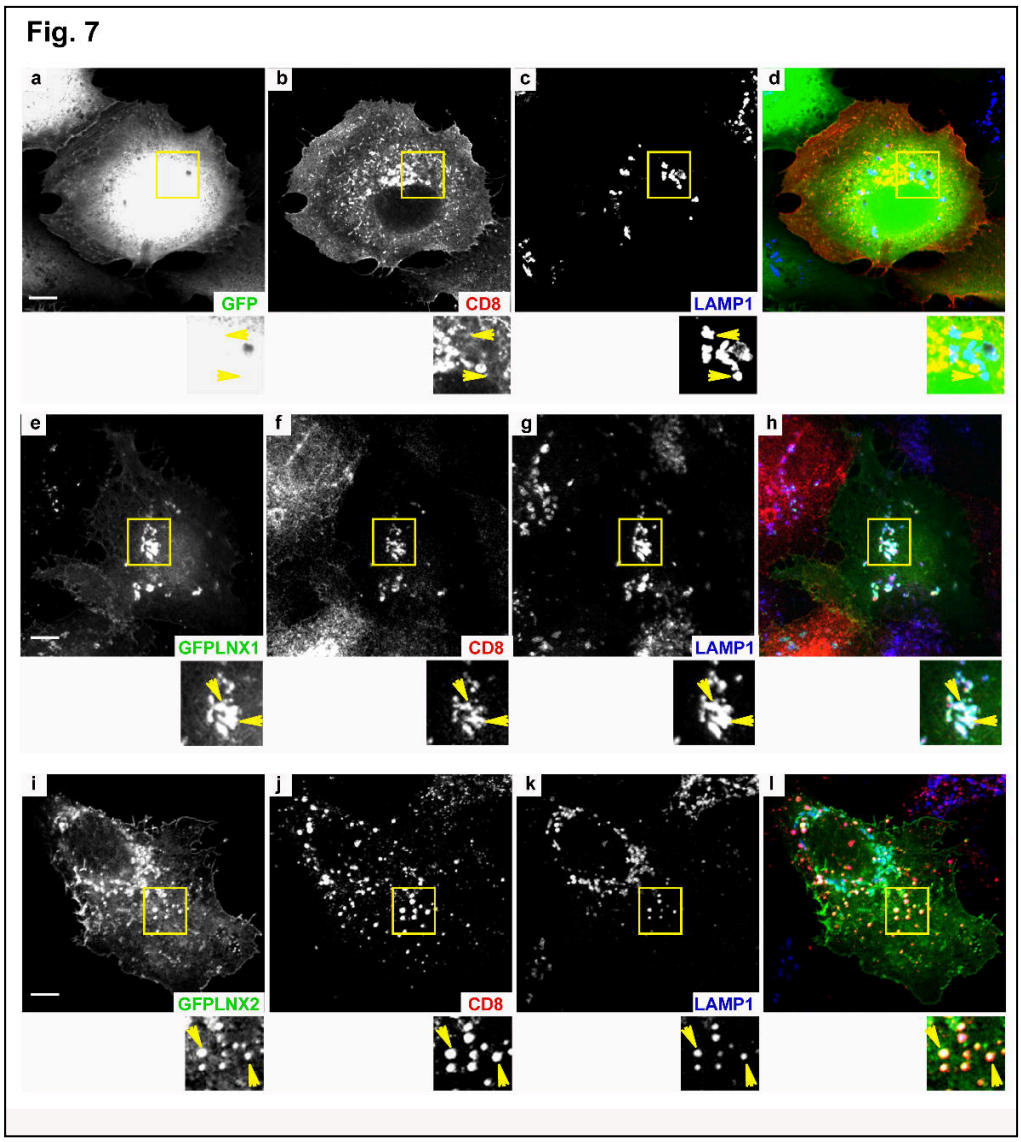

Fig.7: High expression level of GFP-LNX1p80 and GFP-LNX2, but not GFP, promotes CD8α transport to the lysosomes.
Huh-7 cells expressing by the new transfection procedure CD8α and high level of GFP (a-d), GFP-LNX1p80 (e-h) or GFP-LNX2 (i-l) were fixed and stained for CD8α (b, f, j, red) and the lysosomal marker LAMP1 (c, g, k, blue). (d, h, l) merge. Higher magnification of the cell areas marked in panels by the yellow lines is shown at the bottom. Arrowheads indicate endocytic structures where CD8α colocalizes with GFPLNX1p80 or GFP-LNX2, but not GFP. A single confocal section is shown. Scale bar, 3µm.

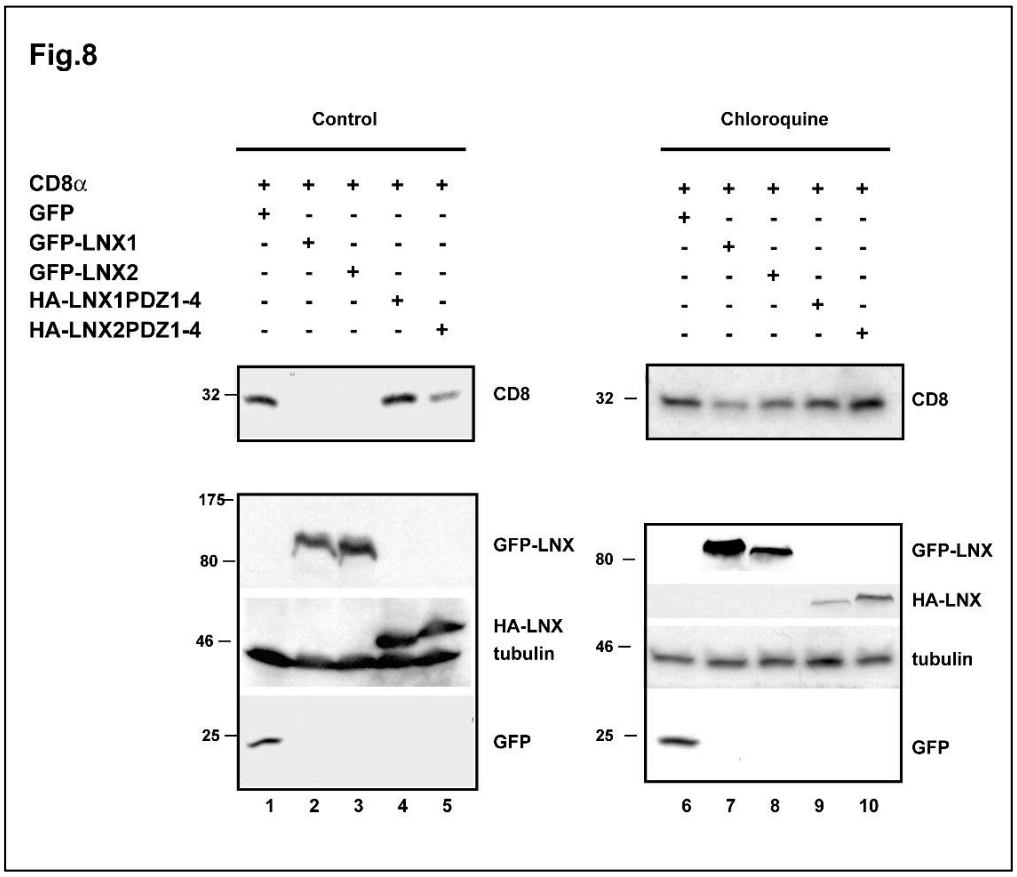

Fig.8: Lysosomal degradation of CD8α protein in cells highly expressing either GFP-LNX1p80 or GFP-LNX2.

HEK293 cells expressing, by the new transfection procedure, CD8α and high level of GFP (lanes 1 and 6), GFP-LNX1p80 (lanes 2 and 7), GFP-LNX2 (lanes 3 and 8), Hatagged PDZ1-4 domains of LNX1p80 (lanes 4 and 9) or LNX2 (lanes 5 and 10), were cultured with or without chloroquine treatment. After cell lysis, CD8α protein was immunoprecipitated from equal cell lysate aliquots and revealed by immunoblotting. In parallel, equal cell lysate aliquots were used to reveal GFP and GFP-tagged LNX proteins with an anti-GFP mAb, and HA-tagged PDZ domains of LNX1p80 and LNX2 with an anti-HA mAb. Lysates were also analyzed by immunoblotting with anti-tubulin antibody as loading control. Numbers indicate molecular mass (kDa).

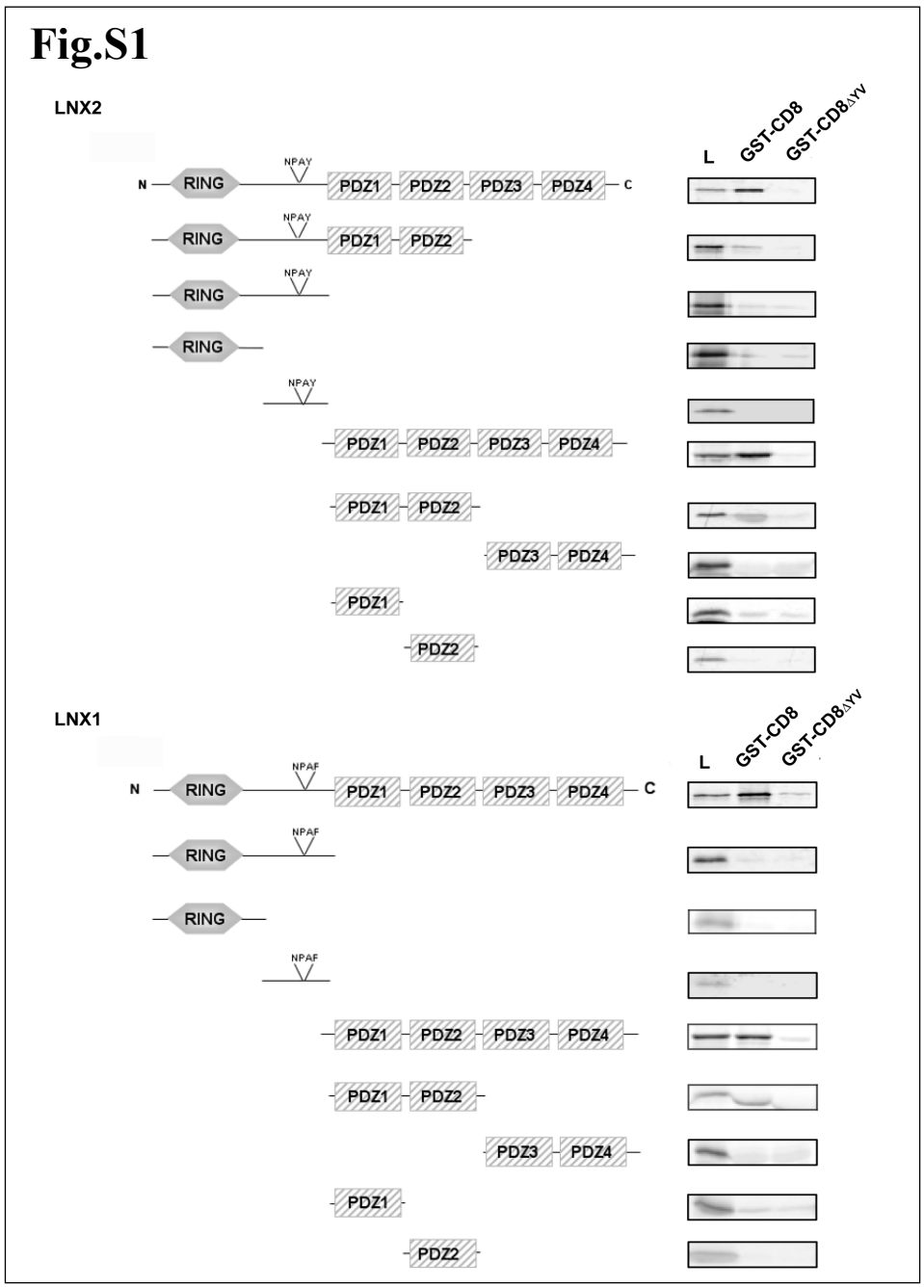

Fig.S1: The four PDZ domains of either LNX1p80 or LNX2 mediate *in vitro* the interaction with CD8α.

List of the LNX2 and LNX1p80 constructs generated and *in vitro* tested for their ability to interact with GST-fused either to the wild type or to the ΔYV-mutant cytosolic tail of CD8α. Bound proteins were eluted from the beads and analyzed together with the loaded samples (L) by SDS-PAGE and autoradiography.

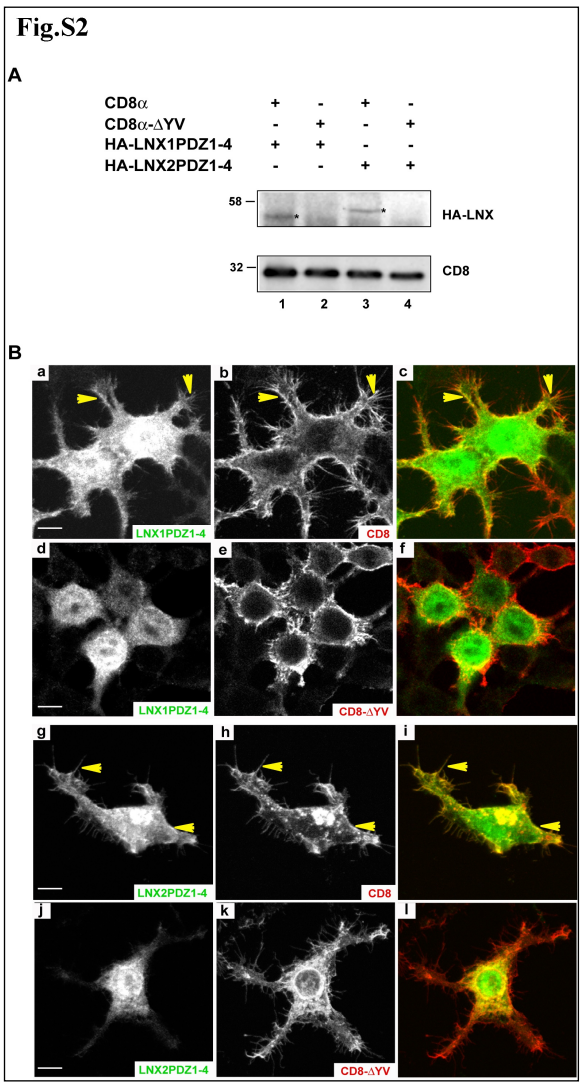

Fig.S2: CD8α interacts *in vivo* with the four PDZ domains of either LNX1p80 or LNX2.

(A) *In vivo* interaction between CD8α and the four PDZ domains of either LNX1p80 or LNX2. CD8α (lanes 1,3) or CD8-ΔYV (lanes 2,4) was expressed together with HA-tagged PDZ domains of either LNX1p80 (lane 1,2) or LNX2 (lane 3,4) in HEK293 cells. After 24-hrs transfection, CD8α was immunoprecipitated from cell lysates and visualized by immunoblotting. The presence of LNX1p80 or LNX2 fragments in the precipitates was revealed with an anti-HA antibody. Numbers indicate molecular mass (kDa).
(B) CD8α expression redistributes the four PDZ domains of either LNX1p80 or LNX2 to the plasma membrane. HA-tagged PDZ domains of either LNX1p80 (a-f) or GFP-LNX2 (g-l) were expressed in HEK293 cells together with either CD8α (a-c, g-i) or CD8-ΔYV (d-f, j-l). After 24-hrs transfection, cells were fixed and immunostained for CD8α (red) and HA (green). (c, f, i, l) merge. Yellow arrowheads indicate colocalization at the plasma membrane. A single confocal section is shown. Scale bar, 3 mm.

1.5 CONCLUSION.

In this work, we identify and characterize the interaction between the human coreceptor CD8α and LNX1p80 and LNX2 proteins. These results show that this binding occurs *in vitro* and *in vivo* and mutually affects the localization of each partner: CD8α recruits LNX1p80 or LNX2 from the cytosol to the plasma membrane, while, remarkably, LNX1p80 or LNX2 expression leads to CD8α ubiquitination, downregulation from the PM, endocytosis and degradation. RING-based E3 ligases confer specificity to ubiquitination by recognizing target substrates. Accordingly, they have been linked to the control of many cellular processes and to multiple human diseases. However, despite their relevance, the functional characterization of most of them remains at a rudimentary stage ***(Deshaies and Joazeiro 2009).*** The activity of LNX1 as E3 ubiquitin ligase has been recently explored. Two splicing variants of LNX1 exist, the p70 and p80. The LNX1p70 binds the junctional protein JAM4 and its overexpression facilitates JAM4 endocytosis ***(Kansaku et al. 2006).*** On the other hand, LNX1p80 is an interacting partner of claudin-1 and promotes its ubiquitination, removal from the tight junctions and transport to the lysosomes ***(Takahashi et al. 2009).*** Interestingly, LNX1 downregulation has been associated to gliomas ***(Chen et al. 2005)*** and to the cardiovascular Kawasaki infectious disease ***(Burgner et al. 2009)***, indicating its indispensable relevance for the proper functionality of distinct tissues and organs. In contrast to LNX1, LNX2 has been poorly studied and the only interacting protein so far identified was the cell surface coxsackie- and adenovirus receptor (CAR) ***(Mirza et al. 2006).*** No information was available to date whether LNX2 behaves, similarly to LNX1, as an E3 ubiquitin ligase in mammalian cells. Here, we shed much light on the function of both LNX proteins: we demonstrate that they are expressed in human T lymphocytes and we identify an important novel partner for them, the human TCR coreceptor CD8α. This finding suggests that LNX proteins play a role in the regulation of T-cell tolerance and immunity, as the E3 ligase c-Cbl, which also has a RING finger domain ***(Jeon et al. 2004, Naramura et al. 2002).*** Future work will be addressed to test this interesting hypothesis. While the anterograde transport of CD8α and β chains along the exocytic pathway has been described ***(D'Angelo et al. 2009, Erra et al. 1999, Goldrath et al. 1997, Pascale et al. 1992)***, whether and how CD8 localization at PM is regulated by endocytic trafficking and which signals and cellular machineries are involved is so far largely unknown. The identification of the LNX ubiquitin ligases as interacting protein of CD8α, their redistribution at the PM upon CD8α expression and the effect of LNX protein expression on CD8α localization and expression contribute to answer these questions and it will help to understand how impairment of CD8 function and localization at the PM might lead to immune diseases. It will be interesting to investigate whether and how LNX proteins regulate the localization of CD8 αβ heterodimer as well. Despite the strong similarity between LNX1p80 and LNX2 structure and function, potentially interesting differences may distinguish them. In contrast

to LNX1p80, LNX2 is recruited by CD8α also to the Golgi complex; its interaction is more severely dependent on the C-TVM of CD8α, and LNX2 expression induces also a smear pattern of ubiquitination, which might correspond to CD8α polyubiquitinated forms. Intriguingly, while mono- or multimono-ubiquitination has been notably involved in endocytosis ***(Mukhopadhyay and Riezman 2007)***, polyubiquitination has been also associated to direct sorting from the Golgi to the vacuole of the yeast protein Gap1 ***(Soetens et al. 2001).*** Therefore, LNX2 might be also involved in the regulation of CD8α transport to, through or from the Golgi complex, which has been already shown to be strongly dependent on the C-TVM of the co-receptor ***(D'Angelo et al. 2009).*** Further work is required to verify such hypothesis.
In conclusion, our results identify two major interacting partners of the human coreceptor CD8α, providing the first link between the possible regulation of the function of CD8α at the plasma membrane of lymphocytes and ubiquitination, endocytosis and lysosomal degradation.

CHAPTER II

Alpha B-Crystallin over-expression reverts the dominant negative effect of mutant Frizzled4 L501fsX533 (disease gene for a dominant form of familial exudative vitreoretinopathy).

2.1.1 Abstract.

Familial exudative vitreorethinopaty (FEVR) is an hereditary ocular disorder caused by an insufficient vascularization of the periferal retina during development. The resulting hypoxia actives a compensatory vascularization but the new vessels are prone to rapture causing exudates and bleeding followed by scarring, retinal detachment and blindness. Mutations in Frizzled4 (Fz4), a member of the cell surface Wnt family receptors, were found in many FEVR patients. In a autosomal dominant form of FEVR (the most frequent and henceforth referred as Fz4-FEVR), the deletion of two nucleotides leads to the synthesis of a completely different and truncated cytosolic tail (L501fsX533). This receptor is retained in the ER and somehow traps Fz4 by oligomerization, thus performing its dominant effect.
We confirmed the ER retention of Fz4-FEVR in transfected cells and observed the formation of oligomers of high molecular weigth in a time dependent manner, suggesting that oligomerization plays a role in the localization of the mutant. Interestingly, when we replaced the cytosolic tail of the G glycoprotein coded by the ts-045 mutant strain of VSV (VSVG) with the tail of wilde-type or mutant receptor, the chimeric VSVG-Fz4-FEVR was completely retained in the ER, whereas VSVG-Fz4 exited from the ER. Thus, the Fz4-FEVR tail is sufficient to determine ER localization. In addition, performing a competition experiment, we found that overexpression of a peptide coding FEVR tail resulted in the recovery of the cell surface expression of Fz-FEVR, suggesting that its retention in the ER is protein-mediated.
Most importantly, we found with a proteomic approach a new interactor of both Fz4wt and Fz4-FEVR, the αB-Crystallin protein. This interaction was not tail dependent, suggesting that the three cytosolic loops of the receptor may be involved. αB-Crystallin overexpression promoted cell surface expression of Fz4-FEVR and prevented its dominant negative effect on the wild-type counterpart. Thus, αB-Crystallin might represent an important tool to contrast FEVR. Current effort is focused to identify the specific interactor(s) responsible of the retention in the ER of Fz4-FEVR in order to identify others possible therapeutic target(s).

2.1.2 Exit from the ER.

Although the secretory pathway in eukaryotic cells has been intensively studied, fundamental issues, such as the molecular mechanisms of ER exit, still remain elusive. Two different models have been proposed: *cargo capture* and *bulk flow*. In the cargo capture model, proteins are recognized by cargo receptors and concentrated in ER exit sites and COPII vesicles. According to the bulk flow model, secretory proteins move out of the ER as part of the bulk fluid or membrane of departing vesicles in a receptor independent manner, although both are COPII dependent ***(Belinda A. et al. 2001).*** The fundamental difference between the two models is that in the *cargo capture,* cargo proteins are selectively recognized and their transport is actively promoted ***(Wieland F.T. et al. 1987).*** In contrast, resident proteins are tought to remain into the ER because mostly excluded from COPII vesicles by weak (lateral) interaction with variety of proteins in the lumen of the ER forming a sort of "matrix". Most of the resident proteins into the ER are chaperones involved in the assisting of the folding newly synthesized proteins.
Numerous signal motifs can tightly regulate the export process from the ER. To date, several classes of ER export motifs have been identified in the cytosolic tails of transmembrane proteins. These export signals, characterized in non-GPCR transmembrane proteins, can be divided into several classes. Among them, diacidic motifs DxE or ExD, have been identified in the cytosolic C-termini of the vesicular stomatitis viral glycoprotein (VSVG), cystic fibrosis transmembrane conductance regulator (CFTR), Kir2.1 potassium channel, Angiotensin II Receptors ***(Nishimura N. et al. 1997, Ma D. et al. 2001, Xiaoping Zhang et al. 2011)*** and many other proteins ***(Melanie Mikosch and Ulrike Homann. 2009).*** The DxE motif directs the concentration of the cargo molecule during ER export, thereby enhancing the rate of its exit from the ER. Mutation of the DxE motif to AxA does not affect VSVG molecule assembly but slow down the ER exits of about 10-fold ***(Nishimura N. et al. 1999)***. Adding DxE motif confers transport ability to sufficiently direct the export of other proteins, which are normally retained in the ER. Specifically, this motif is required for the interaction of VSVG with Sec23/24 in a ternary pre-budding complex consisting of Sar1-GTP, cargo, and Sec23/24 ***(Nishimura N., Balch W.E. 1997).*** More recently, it has been identified a new diacidic export motif ExxD that facilitates ER export of SYP31 and may function for type I and type II proteins in plants ***(Laurent Chatre et al. 2009).*** Similarly, the double phenylalanine motif (FF), is required for efficient transport of the p24 family proteins and ERGIC-53 from the ER to the Golgi ***(O. Nufer et al. 2002, O. Nufer et al. 2003).*** Notably, the substitution of FF motif with a di-hydrophobic signal as VV, LL, VL, IL, IV, or V alone, produces the same ER export capacity for ERGIC-53 ***(O. Nufer et al. 2003).*** NKCC2 requires the tri-hydrophobic motif LLV in the distal COOH terminus for the ER exit and cell surface expression ***(Nancy Zaarour et al. 2009).*** Furthermore, a single C-terminus alanine in the cytosolic tail of Major

histocompatibility complex class I (MHC-I) molecole is crucial for its correct cell surface expression, as well as a single C-terminal valine of the cytosolic tail of Frizzled 4 and 7 where its removal strongly slow down the exiting form the ER ***(Sunglim Cho et al. 2011, Heike Hering, Morgan Sheng. 2002, Giovanni D'Angelo et al. 2009).*** Thus, all these evidences demonstrate that the export from the ER is selectively regulated by specific aminoacids, although the deletion or substitution of these residues doesn't abrogate the capacity to exit from the ER, **according to the *bulk flow model* described above *(Belinda A et al. 2001).*** Increasing evidences suggest that the phosphorylation signal plays a critical role in protein targeting to the plasma membrane. For example, extracellular signalling that activates phosphoinositide 3-kinase (PI3K) causes a significant increase in the surface expression of voltage-gated calcium channels and transient receptor potential channels ***(Viard P. et al. 2004, Bezzerides V.J. et al. 2004).*** In the KCNK3 potassium channel, the deletion of a 14-3-3 binding motif (SWTY) results in a substantial loss of surface expression, implicating the influence of the phosphorylation signal on the cargo protein ***(O'Kelly I. et al. 2002, Rajan S. et al. 2002).*** Indeed, 14-3-3 binding to the SWTY motif is dependent on phosphorylation and thus relies on the activity of kinases that phosphorylate this motif. In particular, Akt, a downstream kinase of PI3K, directly phosphorylates the SWTY sequence under fetal bovine serum or growth factor stimulation, and recruits 14-3-3, which subsequently confers the cell surface expression of the SWTY-carrying reporter potassium channel ***(Jean-Ju Chung et al. 2009).*** Similarly, 14-3-3 promotes cell surface expression of GPR15, a G protein-coupled receptor (GPCR) that serves as a co-receptor for HIV. Also in this case, the binding of14-3-3 to this receptor requires a phosphorylation of the S359 residue in cytosolic tail ***(Yukari Okamoto and Sojin Shikano 2010).***

2.1.3 Export trafficking of G protein-coupled receptors.

G protein-coupled receptors (GPCRs) are a superfamily of cell-surface receptors that regulate a variety of cell functions by responding to a myriad of ligands. The superfamily includes the Frizzled receptors which have a similar structure to GPCRs although clearly distinct functional properties (see Frizzled receptors section). GPCR expression level at the cell surface is a balance of three highly regulated, dynamic intracellular trafficking processes, namely export, internalization and degradation.
Recent efforts to elucidate the mechanism underlying GPCR export from the ER have led to the identification of several motifs in the membrane-proximal carboxyl termini which play a critical role in their export from the ER ***(Schulein R. et al. 1998).***

The export motifs can be grouped in different classes:

- **$E(x)_3LL$ motif:** The role of the LL motif has been controversial, although it has been demonstrated that the LL motif together with an upstream glutamate (E) residue [$E(x)_3LL$] in the carboxyl terminus of the vasopressin V2 receptor is essential for its cell surface expression ***(Matthew T. et al. 2005).***
- **$F(x)_3F(x)_3F$ motif:** A triple phenylalanine motif [$F(x)_3F(x)_3F$] has been identified in the membrane-proximal carboxyl terminus of the dopamine D1 receptor that is required for its cell-surface expression ***(Jason C. Bermak et al. 2001).***
- **$FN(x)_2LL(x)_3L$ motif:** Recently, it has been demonstrated that a dileucine and surrounding hydrophobic residues, namely upstream phenylalanine (F) and asparagine (N) and downstream leucine (L), constitute an ER-export motif [$FN(x)_2LL(x)_3L$] within the membrane-proximal carboxyl terminus of the human vasopressin V1b/V3 receptor. Mutations of one or more of these five hydrophobic residues reduce receptor expression at the plasma membrane, indicating that the integrity of $FN(x)_2LL(x)_3L$ motif is required for receptor export from the ER ***(J. Robert et al. 2005).***
- **$F(x)_6LL$ motif:** Utilizing a strategy of progressive truncation and alanine-scanning mutagenesis, it has been demonstrated that F_{436} and $I_{443}L_{444}$ in the carboxyl terminus of α_{2B}-AR and F_{309} and $L_{316}L_{317}$ in the carboxyl terminus of AT1R are required for receptor export from the ER ***(M.T. Duvernay et al. 2004).***

These motifs are required for GPCR export from the ER. However, the molecular mechanism underlying their function remains unclear. There are several possibilities regarding their role in GPCR ER export. First, similarly to DxE and FF motifs, these motifs may function as independent ER-export signals, autonomously mediating receptor export from the ER. Consistent with this possibility, the $F(x)_3F(x)_3F$, $FN(x)_2LL(x)_3L$ and $F(x)_6LL$ motifs confer transport capabilities to the ER-retained proteins. However, unlike the DxE and

FF motifs, there is no evidence that any of these motifs directly associate with the components of the COPII vesicles. Second, the motifs may be involved in proper receptor folding in the ER. In order to pass through the ER quality control, GPCRs have to be correctly folded. Incompletely folded or misfolded receptors cannot pass the ER quality control mechanism are targeted for degradation. Accordingly, the $F(x)_3F(x)_3F$ motif mediates the interaction of the dopamine D1 receptor with the ER chaperone protein DRiP78 ***(Jason C. et al. 2001).*** Although the intrinsic structural determinants for the export trafficking of G protein-coupled receptors (GPCRs) have been mainly identified in the N- and C-terminus of the receptors, recently it has been identified a single Leu residue, present in the first intracellular loop, that is essential for the export of α2B-AR, β2-AR, AT1R and α1B-AR from the ER (REFF).

2.1.4 ER localization mediated by recycling.

The ER lumen contains a variety of soluble proteins that perform essential functions related to protein folding and assembly. Munro and Pelham were the first to show that ER resident proteins are distinguished by the presence of a C-terminal KDEL sequence (HDEL in yeast) that prevents their secretion ***(Munro, S. and Pelham, H.R. 1987).*** The finding that KDEL-proteins can be modified by post-ER enzymes indicated that these proteins are retrieved from Golgi cisternae ***(Pelham H.R. 1988, Dean N. and Pelham H.R. 1990).*** Thus, the ER retention is a dinamic process mostly based on the continous recyling from downstream compartment of proteins "erroneously" escaped form the ER. Following the discovery of the KDEL signal, and the first KEDL receptor (KDELR) ***(Lewis M.J. et al. 1992; Heli I. et al. 2011)*** many variants of the signal have been described. Recently, 35 variants of KDEL signal, along with the specificity code of the three human KDEL receptors have been identify ***(Heli I. et al. 2011).*** These authors proposed a PROSITE motif for ER localization that is currently [KRHQSA]-[DENQ]-E-L. In humans, a distinction between the various signals is achieved by differential specificities of the three KDELRs. Although some overlap exists, it appears that each KDEL receptor mediates the retrieval of a subgroup of soluble ER proteins ***(Lewis M.J. et al. 1992).*** The KDELR was shown to be present in purified COPI vesicles, and to colocalize with coatomer in buds and vesicles of permeabilized cells, GTPγS treated. In contrast to cargo proteins, uptake of the KDELR into COPI vesicles does not depend on the hydrolysis of GTP, underlining its role as machinery rather than cargo ***(Wilson D.W. et al. 1993).*** Sorting of membrane proteins into COPI vesicles often depends on cytosolic signals that mediate their binding to coat components. The best characterized is the carboxy-terminal di-lysine motif K(X)KXX, found in some ER-resident proteins and in cycling proteins that function at the ER-Golgi interface (ERGIC53/ p58, and in p25) ***(Teasdale R.D., Jackson M.R. 1996).*** Several studies suggest that the efficiency of the KKXX signal depends on both the X residues and on the distance of the signal from the membrane ***(Vincent M.J. et al. 1998).*** The potency of the K(X)KXX motif, in conjunction with the efficiency of ER exit, determines whether at steady state a protein is mainly ER-localized, or whether it distributes between the ER, ERGIC and Golgi compartments. The dilysine motif interacts with coatomer, and this interaction is required for the retrieval of tagged proteins to the ER ***(Stornaiuolo M et al. 2003).*** In particular, in the Wbp1 protein, dilysine motif was found to interact with a subcomplex of coatomer consisting of the α-, β'- and ε-COP subunits ***(Letourneur F. et al. 1994).*** Subsequently, two-hybrid assays and functional analysis showed that the binding is mediated by the N-terminal WD40 propeller domains of the α- and β'-COP subunits ***(Eugster A. et al. 2004).***
Arginine (Arg)-based motifs represent an additional important class of ER localization signals conforming to the consensus [YΩR]–R–X–R (where Y/Ω is an aromatic or bulky hydrophobic residue) ***(Michelsen K. et al. 2005).*** First

identified in the invariant chain of the major histocompatibility complex class II (MHC-II), this signal is often found on subunits of multimeric complexes such as cell-surface receptors and ion channels ***(Lotteau V. et al. 1990, Schutze M.P. et al. 1994).*** It couples complex assembly to cell-surface transport by maintaining unassembled subunits in the ER; upon correct assembly, the signal is inactivated, allowing for ER export. Several mechanisms have been proposed for signal inactivation: steric masking by intersubunit interaction following proper assembly, hindrance of the signal by multivalent binding of 14-3-3 proteins, binding of PDZ-domain proteins, protein phosphorylation ***(Yuan H. et al. 2003, Mrowiec T. and Schwappach B. 2006, Oliver Nufer and Hans-Peter Hauri. 2003).*** Unlike KXKXX signals, the positioning of Arg-based signals is not confined to the extreme C-terminus, and the signal may appear in multiple copies along the cytosolic domains of membrane proteins. The ability of Arg signals to interact with coatomer suggests that ER localization is due to COPI-mediated retrieval transport ***(Rohan D. Teasdale and Michael R. Jackson. 1996).*** Recent studies in yeast identified two highly conserved stretches in the β- and δ-COP subunits of coatomer that are required collectively for the binding of Arg-based motifs ***(Michelsen K. Et al. 2005).***

2.1.5 Oligomerization: export or retention in the ER?

Protein–protein interactions are crucial to the organizational structure and function of cell signalling networks. Many classes of receptors and other signal transducer polypeptides form constitutive or regulated dimers and/or higher order oligomers ***(P.J. Woolf, J.J. Linderman 2004).***
Several studies have demonstrated the capacity of G protein-coupled receptors (GPCRs) to form homo-dimers/oligomers. These interactions are important for cell surface delivery. Moreover, the organizational structure of the complexes may also be central for the molecular mechanisms leading to G protein binding and activation. Recently, the potential for hetero-dimeric/oligomeric interactions between different GPCRs has also been explored by co-expression. The results indicate that the interactions can influence ligand pharmacology, the type of the generated signals and cellular trafficking of the complexes. Several evidences suggest that GPCR dimerization occurs at the level of protein synthesis in the endoplasmic reticulum or during protein maturation in the Golgi apparatus ***(Graeme Milligan et al. 2007).*** Dimerization/ oligomerization of both gonadotropin receptors FSH and LH is a pre-requisite for cell surface expression of the complex and it occurs constitutively in the early biosynthetic pathway ***(Tao Y.X. et al. 2004, Thomas R.M. et al. 2007, Guan R. et al. 2009, Guan R. et al. 2010).*** However, misfolded human LHR mutants are retained in the ER and, in addition to homodimerization, they may also form heterodimers with the Wt receptor thus acting as a dominant negative ***(Guan R. et al. 2009).*** Thus, in this case oligomerization favor the absence of the ER export. Accordingly, the introduction of a ER retention motif into GPCRs not only results in lack of cell surface delivery of the modified receptor but can also inhibits cell surface delivery of a co-expressed unmodified receptor. For example, the replacement of the C-terminal tail of β2-adrenoceptor with the equivalent region of the GABAb-R1 subunit, which contains a well-characterized arginine-based ER retention signal, results in ER trapping of the modified β2-adrenoceptor. This modification also limits cell surface delivery of co-expressed wild type β2-adrenoceptor. In addition to the introduction of ER retention motifs into GPCRs, mutations in a variety of positions can eliminate or limit cell surface trafficking of a receptor and the mutants may act as dominant negatives for cell surface delivery of wild type receptors ***(Salahpour A. et al. 2004).***
Interestingly, at variance with above results, gap junction Connexin 43 (Cx43), which is able to form multimeric channels, exit from the ER as a monomer and subsequently oligomerizes in the Golgi complex. This seems to be due to a 29-kDa thioredoxin-family protein (ERp29) that, acting as a chaperone, helps to stabilize the monomeric form of Cx43 in the ER. When Cx43 reaches the Golgi complex, ERp29 leaves Cx43 and is recycled to the ER thanks to KDEL-based retrieval motif ***(Shamie Das et al. 2009).***
All together, these data indicate that the oligomerization status of the receptors is crucial for their delivery to the plasma membrane and in particular for the

export from the ER. Interestingly, in some cases, oligomeric status is crucial for masking specific ER retention motifs or to form a stable complex that is capable to escape the quality control in order to exit from the ER. In contrast, oligomeric complex can be the cause of the dominant negative effect of mutated receptor retained in the ER.

Importantly, several ER-retained GPCR mutants can be rescued by treatment with chemical or pharmacological chaperones, an approch that has potential therapeutic implications in all diseases associated with ER-retained receptor mutants ***(J.H. Robben et al. 2006, Tao Y.X. 2006).*** In addition, beyond to the chemical and pharmacological chaperones, cell surface expression of some receptor, like Cardiac Potassium Channel hERG, can be rescued by growing the cells that express these receptors to a lower temperature ***(Eckhard Ficker et al. 2003, Jayasri Nanduri et al. 2009).***

2.1.6 Frizzled receptors.

Frizzleds (Fzs), are cell surface receptors involved in a variety biological processes during development as well as in adult life. Human as well as mouse genome has 10 different genes that codify for 10 different receptors. The primary structure of all ten mammalian Fzs display many landmarks observed in virtually all G protein-coupled receptors, including an ectosolic N-terminus that is N-glycosylated, seven hydrophobic transmembrane segments predicted to form α-helixes, and three intracellular and extracellular loops, and a cytosolic tail that harbor potential sites of protein phosphorylation (Fig10). Putative glycosylation sites on the extracellular loops of Fzs could be involved in ligand binding and have been shown to be important for receptor maturation in ER, which is regulated in a specific manner by the protein Shisa ***(Yamamoto A. et al. 2005).*** Sequence and mutational analyses revealed the presence of two PDZ (**P**SD-95/**d**ics large/**Z**O-1 homologous) binding domain in the cytosolic tail, providing a protein-interacting interface for the receptor. The juxtamembrane KTxxxW motif is conserved among all 10 Fz receptors, while the second PDZ-binding motif, at the C-terminus of the receptors, is present only in Fz-1, -2, -4, -7 ***(Annouck Luyten et al. 2008)*** (Fig.10). The extracellular domain of Fzs can bind several secreted molecules and some are considered to be cognate ligands. The primary endogenous agonists are the WNT proteins, of which there are 19 mammalian forms. These proteins are able to trigger most of the Fz-mediated signaling pathways.
However, recent findings suggest that at least three other protein families can directly bind Fzs and activate downstream signaling: soluble Frizzled-related proteins (soluble FRPs), R-spondin and Norrin. R-spondin and Norrin were shown to interact with the CRD (**c**ystein **r**each **d**omain), while sFRPs were initially seen as WNT scavengers that prevented WNT binding to Fzs. However, recent studies support the idea of direct binding of sFRPs to Fz-CRDs, probably by CRD dimerization followed by receptor activation, as in the case of sFRP1-mediated activation of Fz2 ***(Rodriguez, J. et al. 2005)***.

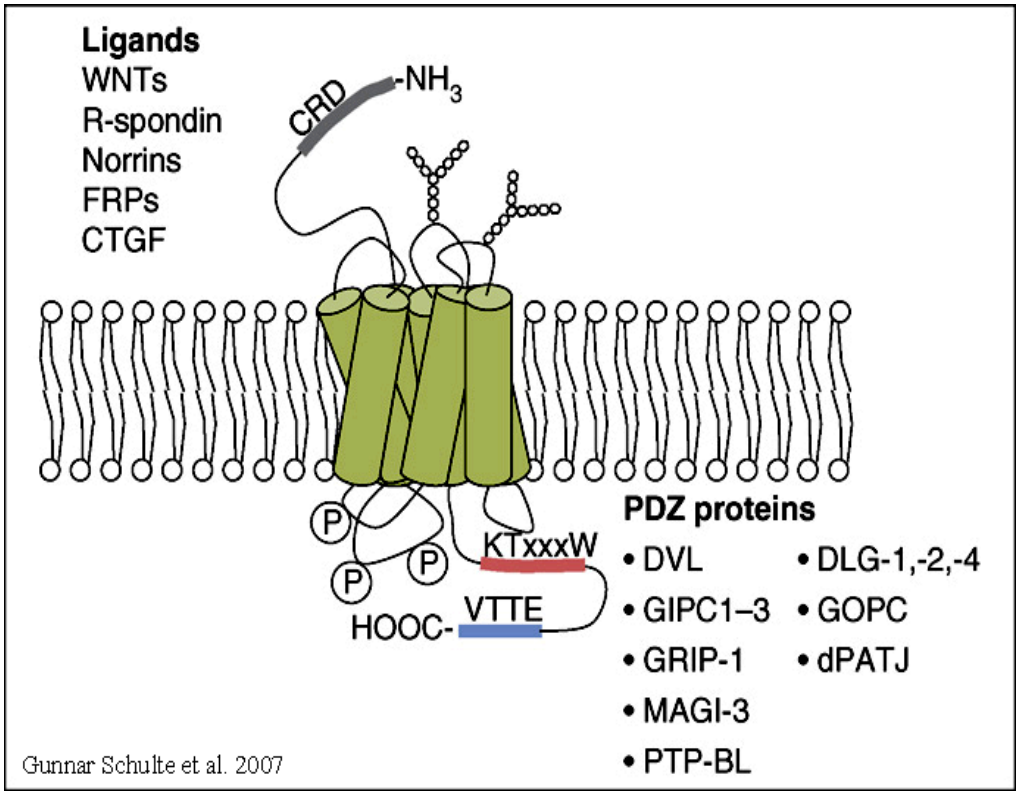

Fig.10: Schematic view of the assembly in the membrane of Fz receptors: The model indicates extra and intracellular interacting proteins, putative glycosylation and phosphorylation sites. The N-terminal CRD is the primary binding site for ligands. The red stretch in the C terminus indicates the internal PDZ-interacting motif (KTxxxW), which is absolutely conserved in the different Fz isoforms and necessary for DVL binding and signaling. The blue stretch at the C-terminus indicates the presence of a classical, less well-conserved PDZ-ligand sequence present in a subset of Fz.

The main signaling pathways (Fig.11) activated by all 10 Frizzled receptors are:

1. ***Fz/β-catenin pathway:*** agonist stimulation results in the activation of the phosphoprotein Dishevelled (DVL), leading to inhibition of a constitutively active glycogen-synthase kinase 3 within a destructive complex consisting of APC (adenomatous polyposis coli) and axin, which regulates the phosphorylation and destruction of b-catenin. The b-catenin thus spared is translocated to the nucleus, where it cooperates with TCF/LEF transcription factors tomodify gene transcription ***(Gordon M.D. and Nusse R. 2006).***
2. ***Fz/Ca2+ pathway:*** The agonists induce elevation of intracellular calcium levels in a G-protein-dependent manner either directly, through activation of phospholipases ***(Slusarski D.C. 1997),*** or indirectly, via a decrease in intracellular cyclic GMP ***(Ma L. and Wang H.Y. 2006)***, resulting in activation of calcium-dependent kinases, such as calciumdependent protein kinase (PKC) and Ca2+/calmodulin-dependent protein kinase.
3. ***Fz/PCP (planar cell polarity) pathway:*** The information is believed to be transduced via DVL to the small GTPases RHO and RAC and their effectors, which are mainly ROCK (RHO kinase) and the c-jun-Nterminal kinase-c-jun-AP1 pathway ***(Seifert J.R. and Mlodzik M. 2007).***

Mutagenesis has revealed that several residues in the intracellular loops and in the C-terminal domain of Fzs are crucial for signaling. Specifically, the mutation of the highly conserved internal KTxxxW motif in the C terminus, or single amino acid exchanges in the first (R340A) or the third (L524A) intracellular loops of human Fz5, completely abolished Fz signaling. Importantly, identical mutations completely ablated the binding of DVL (DSH in Xenopus and Drosophila) and its membrane recruitment by Fzs ***(Cong F. et al. 2004).***

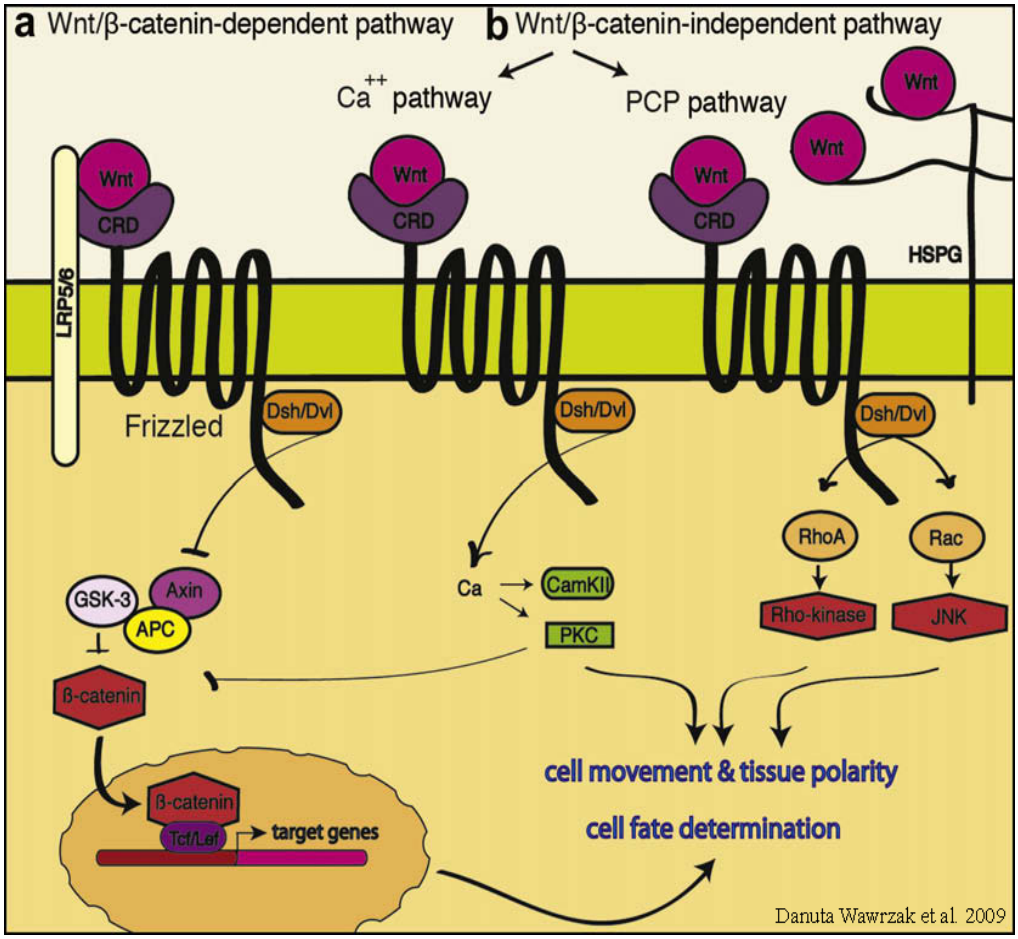

Fig.11: Schematic representation of the Wnt signaling pathways:
(a) The canonical, Wnt/b-catenin pathway. Binding of the Wnt ligand to the Fz and to the co-receptor of the LRP family leads to phosphorylation of Dishevelled (Dsh/Dvl), and to titration of Axin away from the β-catenin degradation complex, composed of APC, GSK-3 and Axin itself. As a consequence, the degradation complex cannot assemble, β-catenin is stabilized and translocates to the nucleus where, together with transcription factors of the Tcf/Lef family, it activates Wnt target genes, such as c-myc and cyclin D1. (b) The non-canonical, β-catenin independent pathways: the PCP and the Ca^{2+} pathway. A main branch of the PCP downstream of Dsh/Dvl involves the small GTPases of the Rho family, Rac and c-Jun N-terminal kinase (JNK). Dsh/Dvl can also stimulate calcium flux and protein kinase C (PKC) and calmodulin-dependent protein kinase II (CAMKII). The non-canonical Wnt signaling controls cell movement and tissue polarity. Heparan sulfate proteoglycans (HSPG) are known to bind and to concentrate Wnt at the cell surface and to influence Wnt signaling.

2.1.7 Familial exudative vitreoretinophaty (FEVR).

Familial exudative vitreoretinopathy (FEVR) is characterized by failure of peripheral retinal vascularization. The visual problems and variable phenotype associated with FEVR result from secondary complications caused by retinal ischemia. The retinal avascularity is probably present from birth and generates sequelae that stabilize in early adult life or progress in later life. Expressivity may be asymmetric and is highly variable, ranging from mild or asymptomatic to severe (e.g., registered as blind) within the same family. The diagnosis of FEVR is based on bilateral peripheral retinal avascularity diagnosed by indirect ophthalmoscopy and fundus fluorescein angiography. Four genes are known to be associated with FEVR: FZD4, encoding for Fz4 receptor, LRP5, encoding for low-density lipoprotein receptor-related protein 5 ***(Johane Robitaille, et al. 2002)***, NDP, encoding for the secreted protein Norrin, that is one of the principal agonist Fz4 ligands ***(Katherine B Sims, MD. 2009)*** and TSPAN12, a member of the tetraspanin superfamily ***(James A. Poulter et al. 2010).*** In all cases, mutations affect the activation of the pathway promoted by Fz4 receptor. As it as been shown that Fz4 signaling regulates endothelial cells (EC)/mural cells (MC) interactions and is essential for vascular integrity in the retina and cerebellum ***(Xin Ye et al. 2009).*** Furthermore, Fz4 is present throughout the developing and adult vasculature, and its inactivation results in severe vascular disorganization. It has been shown, cultured Fz4-/- retinal embrional cells (RECs) are unable to form capillary-like structures but can integrate into these structures when they are formed by WT RECs. Moreover, Norrin/Fz4/Lrp signaling controls a transcriptional program in endothelial cells that is, at least partially, mediated by Sox17. These results establish Norrin/Fz4/Lrp signaling as a central regulator of REC development, and they indicate that the hypovascularization responsible for FEVR, Norrie disease or osteoporosis-pseudoglioma syndrome arises from the impairment of a specific transcriptional program. They also suggest that Fz4/Lrp signaling could play a role in vascular growth, remodeling, and maintenance in a variety of normal and pathologic contexts beyond the retina ***(Xin Ye et al. 2009).***
Among all described mutations associated to the FEVR, only the Fz4 L501fsX533 is associated to the dominant form, that is also the relatively most frequent ***(Kondo H. et al. 2003).*** This mutation consists in a deletion of a di-nucleotide (*ct*) in 1501-1502 position in exon2 of the FZD4 gene that results in a frameshift mutation that starts at the *leucine* in position 501 and finishes in position 533 where it introduces an early stop codon. In transfected cells, the effect of this mutation is the total absence of the mutant receptor on the plasma membrane ***(Johane Robitaille et al. 2002).*** Most importantly, in the same condition, the mutant receptor acts as a dominant negative by trapping the wild-type counterpart in the ER by oligomerization ***(Kaykas A. et al. 2004).***

2.2 Aim of the study.

It was previously shown that the C-terminal PDZ binding motif of the receptor Fz4 is crucial for its efficient cell surface expression ***(D'Angelo et al. 2009).*** However, the removal of the two last C-terminal *valine* residues, part of the C-terminal PDZ binding motif, resulted only in the rediction of cell surface expression of the wild-type receptor (about 60%). This result was due to the loss of the interaction with the GRASP proteins which is crucial for the correct and sequential transport of the receptor to and throught the Golgi complex. Such interaction is lost also by the mutant Fz4-FEVR that, surprisingly, is completely absent from the plasma membrane and mostly retained in the ER. Thus, the loss of the interaction with GRASPs only partially explain the ER retention of Fz4-FEVR, suggesting the existence of a further mechanism to prevent cell surface expression of the mutant receptor. The aim of the present work was to identify this molecular mechanism and to define approaches for obtaining cell surface expression of functional Fz4 receptors in Fz4/Fz4-FEVR expressing cells, i.e. a first step to envisage therapeutic perspectives for the cure of adFEVR.

2.3 Materials and methods.

All culture reagents were obtained from Sigma-Aldrich (Milan, Italy). Solid chemicals and liquid reagents were obtained from E. Merck (Darmstadt, Germany), Farmitalia Carlo Erba (Milan, Italy), Serva Feinbiochemica (Heidelberg, Germany), Delchimica (Naples, Italy) and BDH (Poole, United Kingdom). The radiochemicals were obtained from Perkin Elmer (Bruxelles, Belgium). Protein A-Sepharose CL-4B and the ECL reagents were from Amersham Biosciences (Milan, Italy). Protease Inhibitor Cocktail was obtained from Roche (Milan, Italy).

Antibodies
The following antibodies were used: mouse monoclonals anti-GFP and anti-HA (Santa Cruz Biotechnology Inc.); rabbit polyclonal anti-HA (Sigma Aldrich); mouse monoclonal anti-FLAG (Sigma Aldrich); mouse monoclonal anti-γTubilin (Santa Cruz Biotechnology Inc.); rabbit polyclonals anti-Calnexin (StressGene), anti-GM130 (Marra et al., 2001), rabbit anti-Sec31 (Marra et al., 2001); mouse monoclonals anti-ERGIC53 (Marra et al., 2001) anti-CRYAB (Enzo Life Sciences) anti-CD7107a **(**LAMP1) (Biolegend); Peroxidase-conjugated goat anti-mouse and anti-rabbit IgG (Sigma-Aldrich, Milan, Italy). Texas-Red-conjugated goat anti-mouse or rabbit IgG, FITC-conjugated goat anti-mouse or rabbit IgG and Cy5-conjugated goat anti-mouse IgG (Jackson Immunoresearch Laboratories, West Grove, PA, USA).

cDNA cloning and plasmid construction
The construct pCDNA5-HA-Fz4 was kindly provided by M. MacDonald and M.R. Hayden. The mutant L501fsX533 (Fz4-FEVR) was obtained by site direct mutagenesis using the following oligos:

Fz4-FEVR
Fw: 5'-TGGTCTGCCAAAACTTCACACGTGGCAGAAG-3'
Rv: 5'-AGTTTTGGCAGACCAAATCCACATG-3'

The expression vector pCMV6-XL5 for human alpha Crystallin B-chain (hCRYAB) (ID NM_001885.1) protein was obtained from I.M.A.G.E. Consortium.

To obtain the construct 3xFLAG-hCRYAB, the cDNA coding for the human alpha crystallin B-chain was amplified by PCR using the following oligos containing HindIII/XbaI flanking restriction sites:

Fw (HindIII): 5'-AAGCTTATGGACATCGCCATCCACCACCC-3'
Rv (XbaI): 5'-TCTAGACTATTTCTTGGGGGCTGCGG-3'

To obtain the construct 3xFLAG-hCRYAB (R120G) in which the R_{120} was substituted with a glycine (G), the construct 3xFLAG-hCRYAB was used as a template and the site direct mutagenesis assay was performed according to the manufacturer instruction (Roche) using the following oligos:

Fw: 5'-CTCCAGGGAGTTCCACGGGAAATACCGGATCCCAG-3'
Rv: 5'-GTGGAACTCCCTGGAGATGAAACC-3'

To obtain the constructs 3xFLAG-Fz4-wt or FEVR tails, the region encoding for the tails of the Fz4-wt or Fz4-FEVR were isolated from the cDNAs of the proteins and subcloned in the 3xFLAG-CMV-7.1 expression vector by using the following oligos containing BglII/XbaI flanking restriction sites:

Fz4-wt tail
Fw (BglII): 5'-AGATCTATGGACATCGCCATCCACCACCC-3'
Rv (XbaI): 5'-TCTAGACTATTTCTTGGGGGCTGCGG-3'

Fz4-FEVR tail
Fw (BglII): 5'-AGATCTATGGACATCGCCATCCACCACCC-3'
Rv (XbaI): 5'-TCTAGACTATTTCTTGGGGGCTGCGG-3'

To obtain the constructs 3xFLAG-VSVGts045-Fz4wt tail and 3xFLAG-VSVGts045-Fz4-FEVR tail, the regions encoding for the ectodomain and transmembrane domain (LTM) of VSVG and the tailes of Fz4wt or Fz4-FEVR were isolated from the cDNAs of the respective proteins and subcloned in the 3xFLAG-CMV-7.1 expression vector by using the following oligos:

VSVG (LTM)
Fw (HindIII): 5'-AAGCTTAAGTTCACCATAGTTTTTCC-3'
Rv (BglII): 5'-AGATCTGAGAACCAAGAATAGTCC-3'

Fz4-wt tail
Fw (BglII): 5'-AGATCTATGGACATCGCCATCCACCACCC-3'
Rv (XbaI): 5'-TCTAGACTATTTCTTGGGGGCTGCGG-3'

Fz4-FEVR tail
Fw (BglII): 5'-AGATCTATGGACATCGCCATCCACCACCC-3'
Rv (XbaI): 5'-TCTAGACTATTTCTTGGGGGCTGCGG-3'

Cell culture, transfection and immunofluorescence.
Human HEK293T, Huh-7 and COS-7 cells were routinely grown at 37ºC in Dulbecco's Modified Essential Medium (DMEM), containing 10% fetal bovine serum (FBS) and transfected by using FuGene 6.0 according to the manifacturer instruction (Roche).
To obtained the dominant negative effect of Fz4-FEVR on the wild-type counterpart, COS-7 cells were transiently transfected as previously described (Kaykas A. et al. 2004). Indirect immunofluorescence was performed as previously described (Mottola G., et al., 2000). Single confocal images were acquired at 63x and 100x magnification on a LSM510 Zeiss Confocal Microscope (Carl Zeiss, Jena, Germany).
To separately stain Fz4 proteins on either cell surface (extra) or intracellular membranes (intra), indirect immunofluorescence was performed as previously described (Mottola et al., 2000; D'Agostino M., et al. 2011). In order to measure the ratio between plasma membrane and intracellular staining, the immunofluorescence intensity in the two channels was measured by using photoshop and ImageJ Biophotonic programs. For each transfection, 10 cells were considered for quantification. The results are given as mean±SD (Standard Deviation).

Preparation of cell extracts, immunoprecipitation SDS-PAGE and Western immunoblotting.
Cells were lysed in B-Buffer (10mM Tris-HCl pH 7.4, 150mM NaCl pH 8.0, 1% Triton X-100) for 30 minutes on ice. 6 x 10^6 HEK293T cells were lysed and used for each co-immunoprecipitation. Immunoprecipitation was performed by over-night incubation with mouse monoclonal or rabbit polyclonal anti-HA antibody followed by Protein A-Sepharose beads (Pharmacia). The immunoprecipitated pellet were washed, treated at 37°C for 15 minutes for SDS-PAGE and resolved on a 10% polyacrylamide gels. For each experiment aliquots of the lysate (100 µg total protein/each aliquot) were precipitated with acetone and treated for SDS-PAGE. Proteins were subsequently transferred to nitrocellulose filters (D'Agostino M., et al. 2011), which were incubated with primary antibodies diluted in blocking buffer (5% non-fat dry milk in PBS1X), followed by peroxidase-conjugated secondary antibodies. After washing, bound antibodies were detected by ECL (Amersham Biosciences).

Pulse-Chase & EndoH assay.
HEK293T cells, transiently transfected with HA-Fz4 and HA-Fz4-FEVR for 48hrs, were starved with a modified DMEM without CYS/MET aminoacids, containing 1% FBS. After 30 minutes the cells were incubated (PULSE) for 20 or 30 minutes with the same modified DMEM containing ^{35}S-CYS/MET (100μci/ml). After washing with PBS1X the cells were incubated (CHASE) for 2 and 4hrs with the unmodified DMEM 10% FBS containing cycloheximide (inhibitor of protein biosynthesis). After washing with PBS1X, HA-Fz4 and HA-Fz4-FEVR proteins were immonoprecipitated by using a mouse monoclonal anti-HA antibody for 16hrs at 4°C followed by Protein A-Sepharose beads (Pharmacia). After washing with the buffer used for the lysis, the immunoprecipitated proteins were treated with EndoH enzyme, according to the manufacturer's instructions, and analyzed by SDS-PAGE.

Velocity gradient.
Cell lisates, diluted in glycerol at the final concentration of 6%, were loaded on the top of discontinuous 20 to the 40% glycerol gradients (5ml final volume). After ultracentrifugation in the SW40.1 rotor at 45000 rpm of 16hrs, 13 fractions were collected from the bottom of the gradient. All fraction were precipitated in 15% TCA for 2hrs at 4°C. After 30 minutes of centrifugation, the pellets were washed two times with *ice cold acetone*, solubilized in Laemmli Buffer and analyzed by SDS-PAGE.

Temperature shift assay.
Huh-7 cells were cultured on coverslips and transfected with different VSVG constructs. After 2hrs at 37°C, cells were incubated at the non permessive temperature of 40°C for 16hrs. After this period, the first coverslips were fixed in *formaldehyde* 3,7% while the others were cultured at 10°C or 15°C for 2hrs before the fixation. Huh-7 cells, transiently transfected with Fz4 and its mutant Fz4-FEVR, were culture for 48hrs at 37°C and then incubated at 10°C or 15°C for 2hrs before fixation.

Competition assay in-vivo.
Huh-7 cells were transiently transfected with HA-Fz4 or HA-Fz4-FEVR alone or togheter 3xFLAG-Fz4wt tail or 3xFLAG-Fz4-FEVR tail and after 48hrs at 37°C were fixed and processed for immunofluorescence analysis.

2.4 RESULTS.

2.4.1 Intracellular localization of Fz4-FEVR.

In order to precisely determine the intracellular site(s) of accumulation of Fz4-FEVR along the secretory pathway, HuH7 cells ***(Mottola G. et al. 2002; Stornaiuolo M. et al. 2003)*** were transiently transfected (Fig.S3 A1, A2) and analyzed by confocal immunofluorescence microscopy. The extent of colocalization with proteins marker of the ER, ERES, IC, Golgi and endosomal compartment was measured. As illustrated in Fig.12A, Fz4 resulted scarcely present in the ER and ERES, more in the IC and mostly in the Golgi complex, as expected for a cell surface protein (comprising a trace amount in the endosomal compartment). In contrast, Fz4-FEVR appeared almost entirely confined in the ER and not significantly present in any other compartment of the secretory pathway. The results obtained by confocal immunofluorescence were strongly supported by pulse-chase labeling experiments followed by Endo H resistance assays performed in HEK293T cells (Fig.12B). Fz4 reached a 50% resistance after a 4 hours chase, indicating its transit through the trans-Golgi en-route toward the plasma membrane; while Fz4-FEVR did not acquire any resistance to Endo H digestion within the 4 hours chase. Therefore, we concluded that a peculiar and very strong molecular mechanism must determine the tight localization in the ER of Fz4-FEVR.

Fig.12

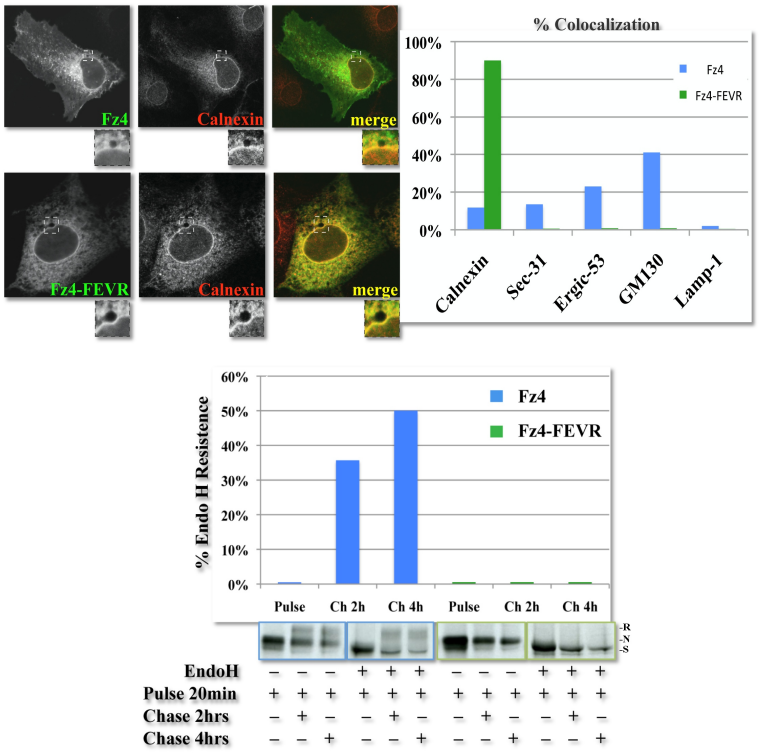

Fig.12: Fz4 is retained in the endoplasmatic reticulum.
A) Fz4-FEVR is almost entirely located in the ER of transfected Huh7 cells. Confocal immunofluorescence analysis of the localization of Fz4, Fz4-FEVR N-terminally tagged with HA epitope in comparison to markers of the intracellular compartments: Calnexin (ER), Sec-31 (ERES), ERGIC-53 (ERGIC), GM130 (cis-Golgi), Lamp-1 (late endosomes). Inset magnification of the box area. The percent of colocalization is shown in the upper-right punnel.
B) Fz4-FEVR is not exported to the Golgi complex in transfected HEK293T cells. Lysates from cells pulse-chase labeled with S^{35}-CYS and -MET as indicated were treated with Endoglycosidase H and analyzed on SDS-gels after immunoprecipitation. The position on the gel of the Endo H resistant (R) and sensitive (S) and native (N) of forms of Fz4 constructs is indicated on the right.

2.4.2 Fz4-FEVR forms with time oligomers of high molecular weight in the ER.

Based on the evidence that Fz4-FEVR traps its wild-type counterpart in the ER by oligomerization, and that chimaeric wild-type receptor, forced to form aggregates, is totaly retained in the ER ***(Kaykas A. et al. 2004)***, we speculated that an abnormal oligomerization could explain the lack of export from the ER of the mutant receptor.
In order to investigate the oligomerization grade of Fz4 and Fz4-FEVR, HEK293T cells were transiently transfected (Fig.S3 A1, A2). After 48hrs the cells were collected, detergent lysed and aliquots of the lysates were loaded on the top of glycerol gradients prepared and analyzed as described in the material and methods section. In the Fig.13A are shown the sedimentation profiles of BSA and thyreoglobulin (hTG), used as standard molecular weight. Given that the molecular weight of the BSA is very similar to that of the monomeric form of Fz4 receptor, we considered the receptor present in the fractions 1-6 as monomeric, while that present in fractions 7-13 oligomeric (either homo- and heteroligomeric). Thus, Fz4 was mostly present as a monomer while Fz4-FEVR formed oligomers of high molecular weight. In contrast, as shown in the Fig.13B, when the newly syntesized forms of Fz4 and Fz4-FEVR were analyzed after 30 min pulse with ^{35}S-Met and -Cys, a clearly different result was obtained: the sedimentation profiles of Fz4 and Fz4-FEVR were very similar, showing the presence of about 50% of both monomeric and oligomeric forms. This result is conceivable with the notion that the folding of complex transmembrane proteins may require time and the interaction with a number of chaperone proteins present in the lumen of the ER. Therefore, a likely conclusion is that the form of Fz4 component for ER export is the monomeric one, which is acquired with time by the newly synthesized chain. Indeed, the results of Endo-H analysis after pulse-chase labeling are fully in support of this hypothesis, showing a slow transport of Fz4 to the medial/trans Golgi (50% in 4 hours). According to this view, the absence of Fz4-FEVR export from the ER would not be caused by its oligomerization: in contrast, the oligomerization shown by the mutant at steady-state would be the conseguence of the severely impaired transport.

Fig.13

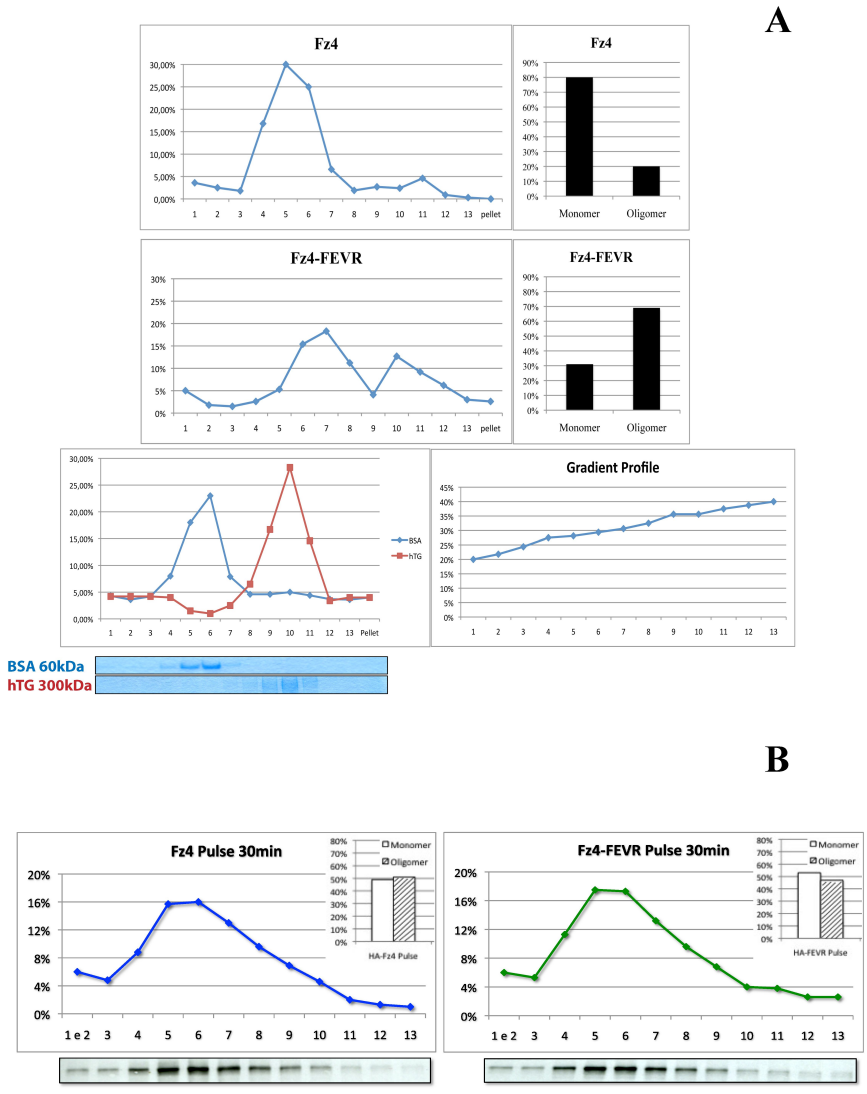

Fig.13: Oligomerization state of Fz4 and Fz4-FEVR.
A) Fz4-FEVR accumulates mostly as oligomeric complexes in transfected HEK293T cells. Aliquots of cell lysates were analyzed on 20-40% glycerol gradients followed by SDS-gels. BSA and human thyreoglobulin (hTG) were used as MW markers for the gradient. B) Newly synthesized Fz4 and Fz4-FEVR show the same extent of oligomerization. Transfected cells were pulse-labeled for 30 minutes and the lysates analyzed as in (A). Fz4 constructs of each fractions were immunoprecipitated, resolved on SDS-gel, and revealed by autoradiografy.

2.4.3 The cytosolic C-terminal tail of Fz4-FEVR is sufficient for the ER localization of a reporter protein.

If the lack of ER export of Fz4-FEVR would not primarily depend on its abnormal oligomerization, the first candidate would clearly be the new cytosolic tail acquired with the frame-shift mutation. To address this question, we generated chimaeric proteins between the VSVG glycoprotein coded by the ts-045 mutant strain (Fig.S3.B1) ***(Balsh et al. 2006)*** and the cytosolic tail of Fz4 and Fz4-FEVR as indicated in Fig.S3.B3 and B4. Given that Fz4-FEVR misses the C-TVM, a motif that highly improves cell surface expression of Fz4 receptor ***(D'Angelo et al. 2009)***, to better analyze the effect of the Fz4-FEVR tail on the VSVG reporter we used the mutant VSVG form in which its cytosolic diacidic motif is substituted with alanine residues (VSVG-AXA) (Fig.S3.B2) ***(D'Angelo et al. 2009).*** As shown in Fig.14B and D, this mutant was less present on the surface of transfected Huh-7 cells in comparison to VSVG.

Most interestingly, when the cytosolic tail of VSVG-AXA was substituted with the Fz4 counterpart, a similar accumulation of the chimaera at the cell surface was detected (VSVG-Fz4 tail, Fig.14C and D); but almost no expression of the Fz4-FEVR tail containing chimaera was measured at the cell surface (VSVG-Fz4-FEVR tail, Fig.14C and D).

Finally, to demonstrate that the Fz4-FEVR tail was impairing the ER to Golgi transport of the chimaeric proteins, we first accumulated the transfected proteins in the ER by incubating the cells at 40°C and then shifted the temperature to 32°C for 20 min. As shown in Fig.14E, the VSVG-Fz4-FEVR protein did not exit from the ER as well as the VSVG tail-less mutant (Fig.S3.B5), while the VSVG-Fz4 protein behaved very similarly to the VSVG-GFP. In conclusion, these results indicated strongly that the cytosolic C-terminal tail of Fz4-FEVR is sufficient to determine ER localization of a very different transmembrane protein (VSVG, type-I single transmembrane domain; Fz4-FEVR, multi-spanning 7 transmembrane domains).

Fig.14

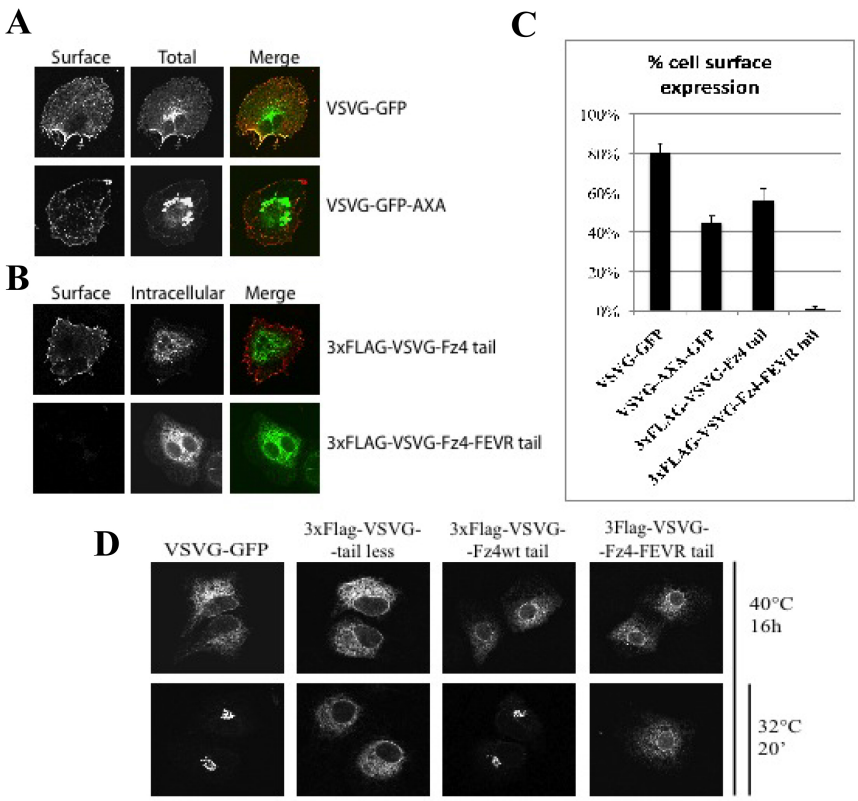

Fig.14: The Fz4-FEVR tail is sufficient for ER retention of a reporter protein.

A) Huh-7 cells, transiently transfected with ts0-45 VSVG-GFP or VSVG-AXA-GFP were grown at the permissive temperature of 32°C and fixed and analyzed by indirect immunofluorescence after 48hrs. The extracellular staining was evaluated using a anti-VSVG rabbit polyclonal antibody before permeabilization (surface), while total staining was evaluated by the GFP signal (total). B) Huh-7 cells, transiently transfected as in (A) with indicated chimeric constructs. Extracellular staining was obtained using a anti-FLAG mouse monoclonal before permeabilization (surface); the total expression was evaluated using the same antibody after permeabilization (total). C) Grafic rappresentation of the percent of cell surface expression of the experiments shown in (A,B).

D) Parallel cultures Huh-7 cells were transfected with indicated constructs and incubated for 16hrs at 40°C. The cells were fixed before or after 20 minutes of incubation at 32°C. 3xFLAG-VSVG-tail less was used as a negative control.

2.4.4 The ER localization mechanism of Fz4-FEVR is saturable.

Given that the cytosolic tail of Fz4-FEVR was sufficient to determine ER localization, two main hypothesis could be advanced to explain the tight localization of the mutant receptor in the ER. First, it may drive a massive self interaction of Fz4-FEVR chains excluding their entry into the COPII. Second, it may mediate the interaction with other protein(s) that would determine ER localization. In principle, the main difference of the 2 envisaged mechanisms is that only the second is saturable. To address this hypothesis, the cytosolic tail of Fz4 and Fz4-FEVR were engineered in 3xFLAG expression vectors (Fig.S3.C1 and C2) and expressed by co-transfection as cytosolic peptides together with full-lenght Fz4 or Fz4-FEVR assembled in the ER membrane. As shown in Fig.15, almost no effect on cell surface expression level was observed when Fz4 was transfected alone or with either one of the two 3xFLAG plasmids; in contrast, in the presence of its competing tail, Fz4-FEVR was clearly expressed on the cell surface, scoring about 1/3 of the value of Fz4 alone. Most importantly, this effect was specific, as shown by the total absence of Fz4-FEVR surface expression in the presence of the Fz4 tail (Fig.15). Thus, the most likely explanation for this results is that Fz4-FEVR has acquired the capacity to interact with novel partner protein(s) that are responsible for its ER localization.

Fig.15

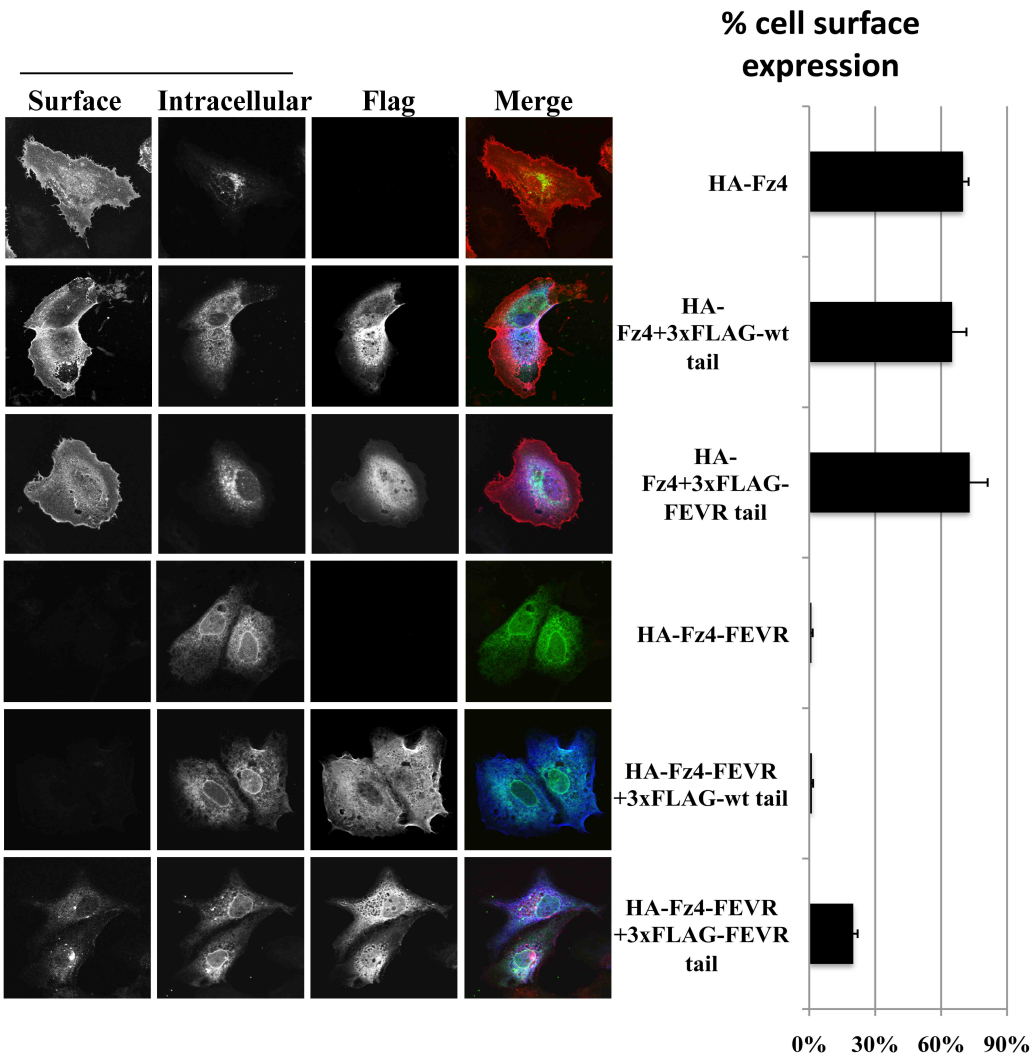

Fig.15: The ER localization mechanism of Fz4-FEVR is saturable.
Huh-7 cells were transiently transfected with indicated constructs for 48hrs and processed for triple indirect immunofluorescence microscopy. On the right, the histrogram shows the percent of cell surface expression of full length Fz4 receptors obtained as specified in material and methods.

2.4.5 Possible mechanism for ER retention of Fz4-FEVR.

As shown in Fig.12A, Fz4-FEVR colocalized almost only with calnexin, marker of the ER, while Fz4 was detected at the ERES, intermediate compartment and Golgi complex, as expected for a protein *en route* toward the plasma membrane. These results suggest that a retention, rather than a recycling mechanism, would trap Fz4-FEVR in the ER. However, based on the slow rate of export to the Golgi complex of (Fig.12B) it is also possible that the tight ER localization of Fz4-FEVR could be the result of a reduced export rate followed by an efficient recycling mechanism to the ER. To check this hypothesis, Huh-7 cells were transiently transfected with the chimeric proteins VSVG-Fz4, VSVG-FEVR, VSVG-GFP or VSVG-AXA-GFP and incubated at 10°C or 15°C for 2 hrs, after 16hrs at the non permessive temperature of 39,5°C required for the ER accumulation. It is well documented that at 10°C the export from the ER is blocked at the ERES and visualized by immunofluorescence with an increased co-localization with COPII proteins ***(D'Angelo G. et al. 2009).*** Similarly, at 15°C, the transport to the Golgi complex is arrested in the ERGIC, clearly recognizable for its accumulation of ERGIC-53 proteins ***(D'Angelo G. et al. 2009).*** Thus, if Fz4-FEVR would at least in part exit from the ER and recyle from the ERGIC and the cis-Golgi, it should be trapped (and visualized) at low temperature in the respective localization. As shown in Fig.16, after 2hrs at 10°C, the chimeric VSVG-Fz4 tail showed a significant score of co-localization with Sec-31 as well as VSVG-AXA-GFP. More important, the chimeric VSVG-Fz4-FEVR tail showed a significant percent of co-localization with Sec-31, thus showing its entry in the ERES. Intriguingly, after 2hrs at 15°C, while both VSVG-AXA-GFP and VSVG-Fz4wt tail were significantly detected in ERGIC-53 positive structures, about no signals of VSVG-Fz4-FEVR was detectable (Fig.17). Prompted by these results, Huh-7 cells were transiently transfected with HA-Fz4 and HA-Fz4-FEVR, incubated at 37°C for 48hrs and then shifted at 10°C or 15°C for 2hrs in order to validate the result obtained with the chimaeric constructs. As shown in Fig.18A, Fz4-FEVR was significantly detected in Sec-31 positive structures after 2hrs at 10°C, but much less in ERGIC-53 positive compartment at 15°C (Fig.18B).
Therefore, these findings support the view that Fz4-FEVR is not prevented to exit from the ER and that is quickly recycled back by a retrogade vesicular traffic operating not further than the intermediate compartment. Most likely, the tight localization in the ER shown at 37°C would be the result of retention and reclying, and further work is needed to evaluate the contribution of these two mechanisms in Fz4-FEVR localization.

Fig.16

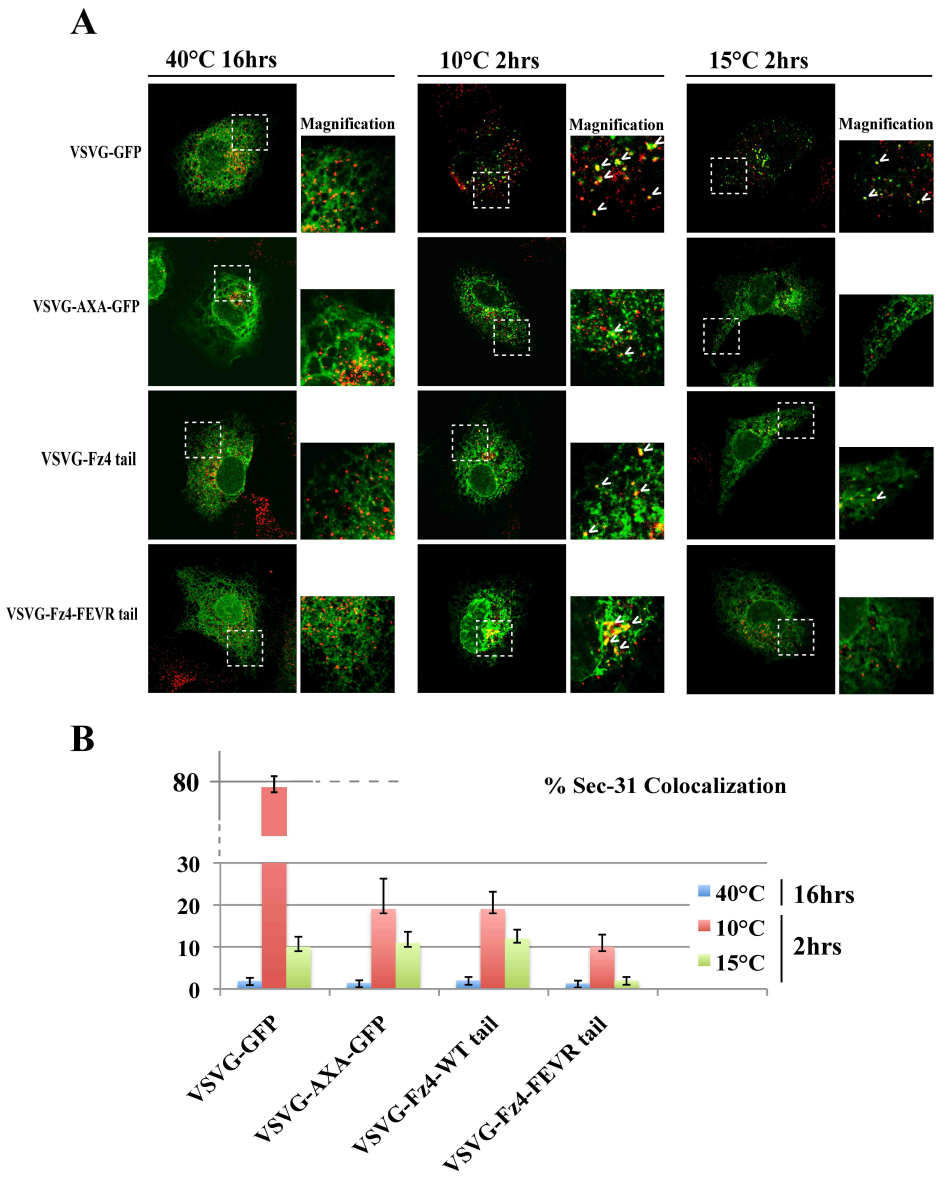

Fig.16: Accumulation of chimeric VSVG-Fz4-FEVR tail at the ERES as revealed by incubation 10°C and colocalization with Sec-31.
A) Huh-7 cells, transiently transfected with indicated constructs were incubated for 16hrs at non-permessive temperature of 40°C and precessed for immunofluorescence analysis before or after incubation for 2hrs at the temperature of 10°C or 15°C. B) The histogram shows the persent of colocalization with Sec-31 protein, marker of ERES.

Fig.17

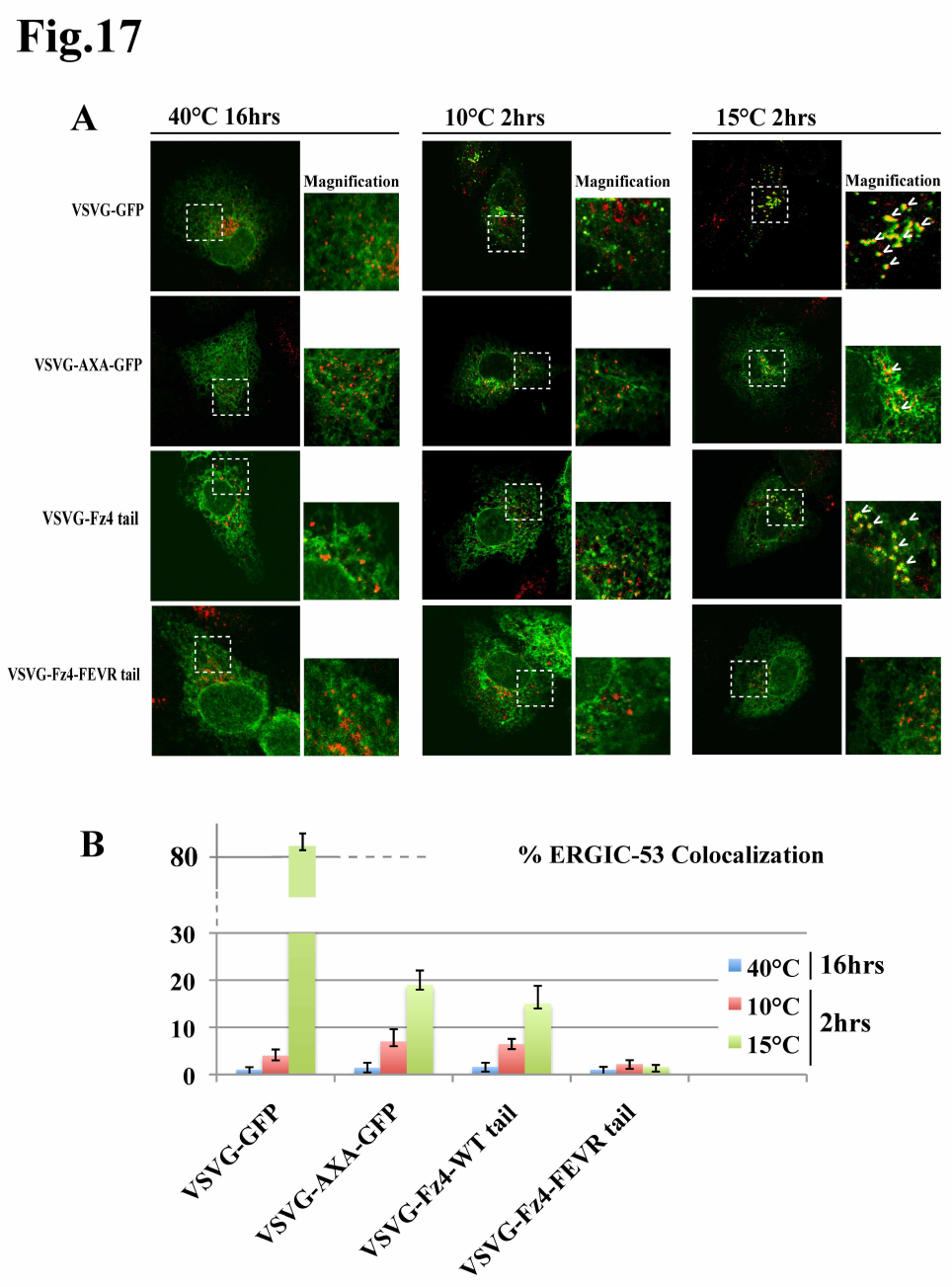

Fig.17: Absence of accumulation of chimeric VSVG-Fz4-FEVR tail at the ERGIC as revealed by incubation 15°C and colocalization with ERGIC-53.

A) Huh-7 cells, transiently transfected with indicated constructs were incubated for 16hrs at non-permessive temperature of 40°C and precessed for immunofluorescence analysis before or after incubation for 2hrs at the temperature of 10°C or 15°C. B) The histogram shows the persent of colocalization with ERGIC-53 protein, marker of ERGIC.

Fig.18

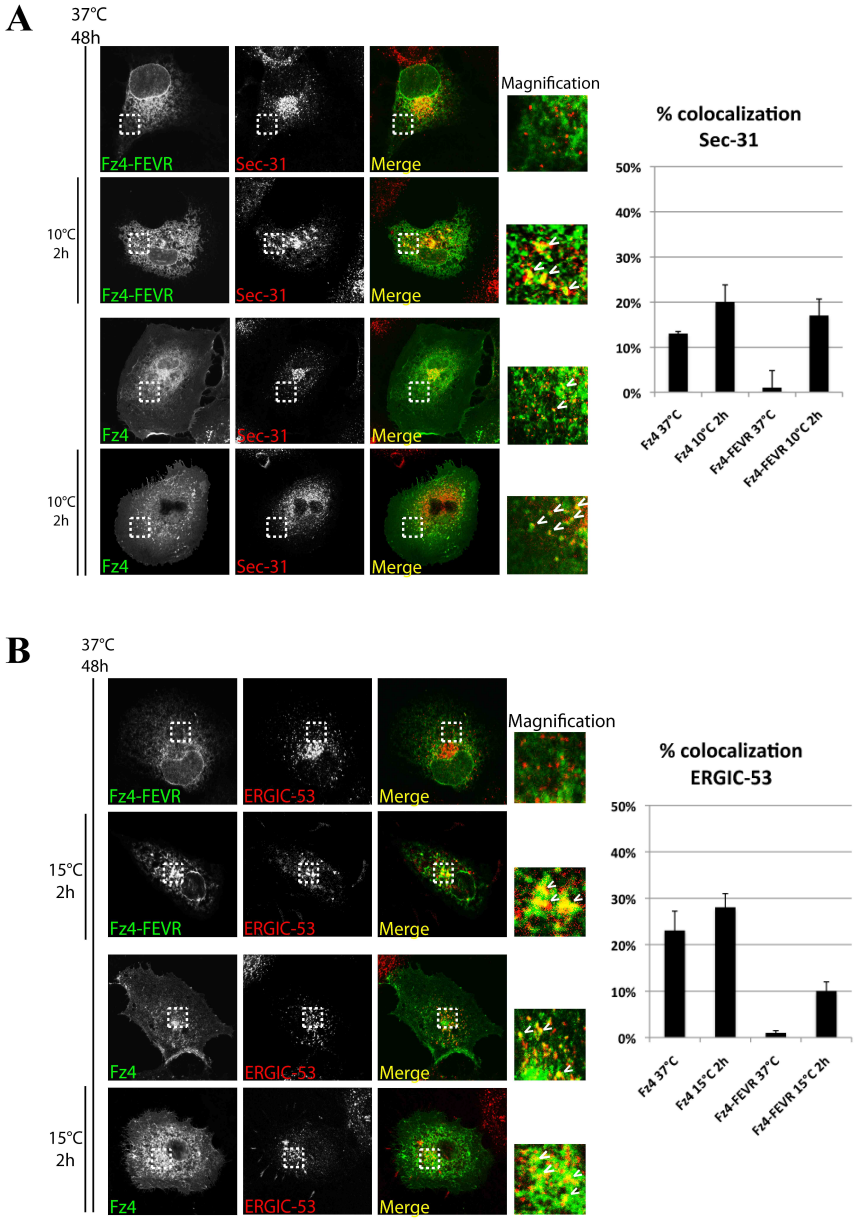

Fig.18: Accumulation full lenght of Fz4-FEVR at ERES and ERGIC as revealed by incubation 10°C and 15°C and colobeling with Sec-31 and ERGIC-53 proteins.

A,B) Huh-7 cells, transiently transfected with indicated constructs, incubated for 48hrs at 37°C and fixed and processed for immunoflourescence microscopy before or after an 2hrs of incubation at 10°C or 15°C. The persentage of colocalization is shown on the right.

2.4.6 Alpha Crystallin B-chain is a new interactor of Fz4 and its mutant Fz4-FEVR.

In order to idenfy specifics interactors for the mutant receptor Fz4-FEVR, HEK293T cells were transiently transfected with cDNAs encoding for N-terminal HA-tagged Fz4 or Fz4-FEVR and after 48hrs, detergent-lysed and immunoprecipitated mouse monoclonal anti-HA antibody.
The immunoprecipitaed proteins were resolved by SDS-PAGE and analyzed by mass spectrometry. This approch gave a number of potential interactor proteins. Among them was alpha crystallin B-chain (CRYAB). It belongs to the small hit shock family protein (sHSP), it is a major lens protein but it is also expressed in numerous non-lens tissues of vertebrates, consistently with its chaperone function ***(Bhat SP et al. 1989; Sax CM, Piatigorsky J. 1994; Van Noort JM et al. 1995; Renkawek K et al. 1999; Arrigo AP. 1995).*** Patients who carry a missense mutation in αB-crystallin (R120G) develop desmin-related myopathy and cataracts ***(Vicart P., et al. 1998).*** It is likely that maintaining genomic integrity is important in the lens since the anterior lens epithelial cells are held in the G0 phase of the cell cycle throughout life ***(Reddan JR. 1982; Gao CY et al. 1999).*** One study suggested that αB-crystallin may be an important component of the cellular machinery involved in maintaining genomic stability ***(Andley UP et al. 2001).*** The reduced thermal stability and the dominant negative effects of the mutant αB-crystallin may be the direct cause of cataract because αB-crystallin null mice have clear lenses ***(Brady JP et al. 2001).*** α-Crystallins, especially CRYAB, are expressed in several other tissues under stress conditions. α-Crystallin A-chain appears to function as a molecular chaperone in prevention of stress-induced precipitation of β- and λ-crystallins ***(Dawson DW et al. 1999).*** Being a small heat shock protein, CRYAB can be constitutively expressed and increased in response to cellular stresses ***(Samali A, Orrenius S. 1998).***
In order to investigate whether CRYAB specifically interacts with Fz4-FEVR, we transiently transfected HEK293T wih cDNAs encoding for N-terminal 3xFLAG-tagged CRYAB (Fig.S3.D1) , and N-terminal HA-tagged Fz4, Fz4-FEVR or Fz4-tail less (Fz4-Δ35) (Fig.19B) (Fig.S3.A3). After 48hrs the cells were lysated, the proteins were immunoprecipitated with a rabbit polyclonal anti-HA antibody and the co-immoprecipitated proteins were detected by western blot with a mouse monoclonal anti-FLAG antibody. As it is shown in Fig.19B and C, CRYAB was co-immunoprecipitated by both wild-type and mutant receptor. In addiction, CRYAB was co-immunoprecipitated also by Fz4-tail less, suggesting that it interacts with the cytosolic loops of Fz4.

Fig.19

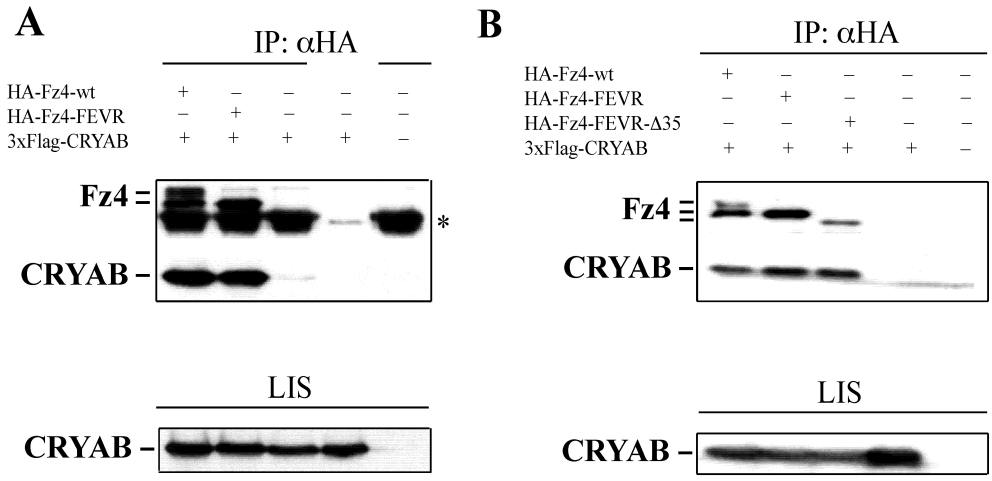

Fig.19: CRYAB interacts with Fz4 receptor in tail independent manner.
A,B) HEK293T cells were co-transfected with indicated constructs for 48hrs. The lysates were immunoprecipitated and revealed by western blot after SDS-gel. The content of relevant protein experiment in which the Fz4 receptor were immunoprecipitated by a rabbit anti-HA antibody while the co-immunoprecipitated CRYAB was detected by a mouse anti-FLAG muose. Fz4 receptor used for the experiment are denscribed in B.

2.4.7 The overexpression of CRYAB promotes the cell surface expression of Fz4-FEVR.

In order to investigate the functional role of CRYAB on Fz4 and Fz4-FEVR, Huh-7 cells were transiently transfected wih 3xFLAG-CRYAB, HA-Fz4 or HA-Fz4-FEVR expression vectors. After 48hrs, the cells were fixed and the intracellular localization of the proteins was analyzed by indirect immunofluorescence. Preliminary results showed that the overexpression of CRYAB does not influence the localization of Fz4 receptor; in contrast, the localization of Fz4-FEVR drastically changed, as shown by an intracellular labeling much more similar to Fz4 and by the possible expression on the cell surface (data not shown). This result suggested the intriguing hypothesis that CRYAB overexpression could rescue cell surface expression of Fz4-FEVR. To check and to quantify this effect, Huh-7 cells were transiently transfected with HA-Fz4 and HA-Fz4-FEVR alone or together 3xFLAG-CRYAB, and analyzed for surface and intracellular labeling. Interestingly, as shown in Fig.20, CRYAB overexpression promotes a strong recovery of cell surface expression of Fz4-FEVR (about 50% of Fz4, either expressed alone or with CRYAB). In contrast, the recovery of Fz4-FEVR on plasma membrane was much less efficient when co-transfected with the mutant CRYAB (R120G) (Fig.S3.D2), defective for its chaperone activity ***(Joseph Horwitz 2002; Ste´phanie Simon et al. 2007).*** This result strongly indicates that the chaperone activity of CRYAB is able to overcome the tight mechanism of retention of Fz4-FEVR in the ER.

Fig.20

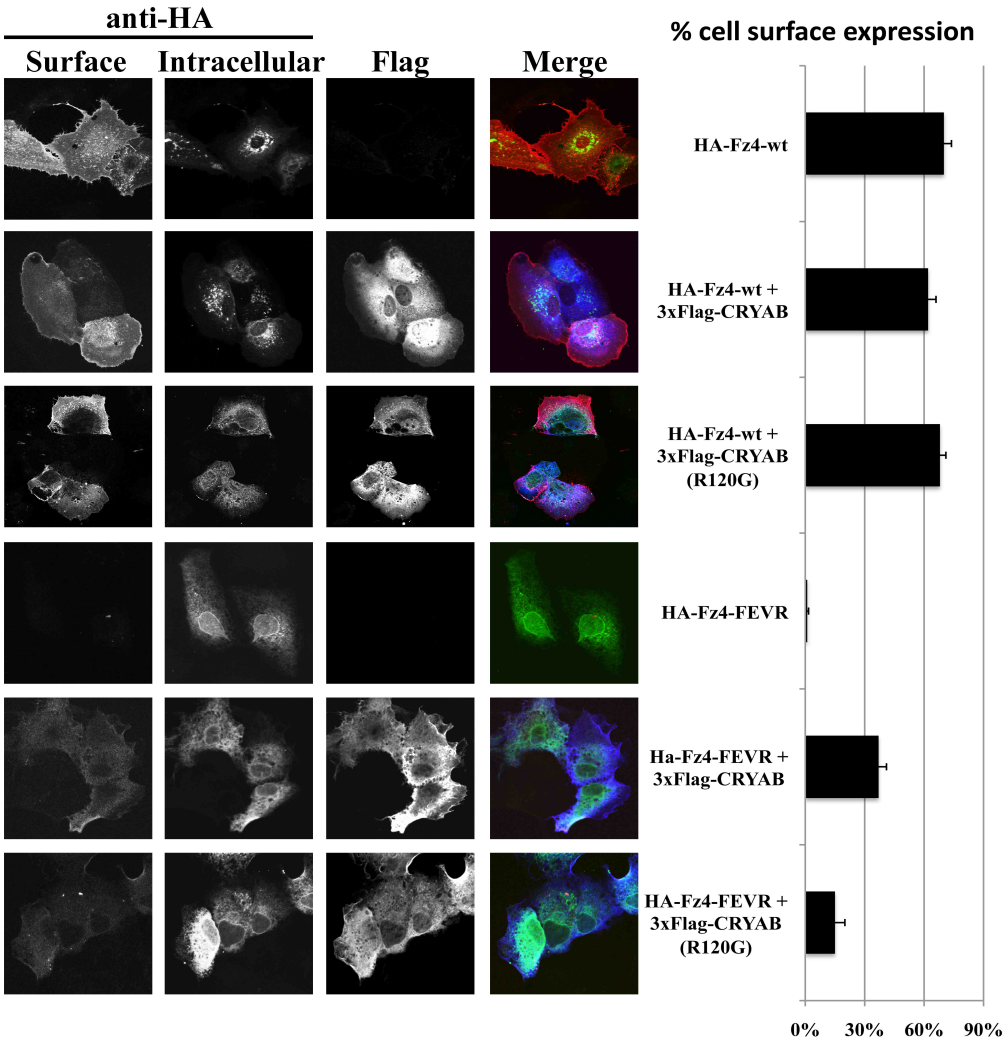

Fig.20: CRYAB over-expression promotes cell surface expression of Fz4-FEVR.
Huh-7 cells were transfected with the indicated construts for 48hrs and processed for triple indirect imunofluorescence microscopy as denscribed in materials and methods section. The percent of cell surface expression was evalueted and is shown on the right.

2.4.8 CRYAB over-expression reverts the dominant negative effect of Fz4-FEVR on cell surface expression of Fz4.

Based on the evidence that CRYAB over-expression rescues cell surface expression of Fz4-FEVR, we asked whether this over-expression can inhibit the dominant negative effect of Fz4-FEVR on cell surface expression of Fz4. First of all, we reproduced the dominant effect in COS-7 cells transiently transfected with Fz4 and Fz4-FEVR at a 1 to 5 ratio, respectivly **(*Kaykas A. et al. 2004*).** As shown in Fig.21A, Fz4 receptor expressed alone is mostly located on cell surface while the co-expression with Fz4-FEVR results in its tight localization in the ER, colocalizing with Fz4-FEVR and calnexin (Fig.21B). More intriguingly, CRYAB overexpression results on the relocalization of Fz4 on the cell surface, preventing its trapping in the ER (Fig.21A); but, apparently, it does not rescues anymore Fz4-FEVR expression on the cell surface (Fig.21A). In addiction, we observed that the intracellular staining of Fz4, Fz4-FEVR and calnexin changes in the cells expressing the dominance negative phenotype (Fig.21A and B). further work is needed to explain these apparent discrepancies. Howerver, the most important outcome of the results shown in Fig.20 and 21 is that CRYAB may represent an important target to develope a therapeutical approach to target the dominant form of FEVR determined by Fz4-FEVR.

Fig.21

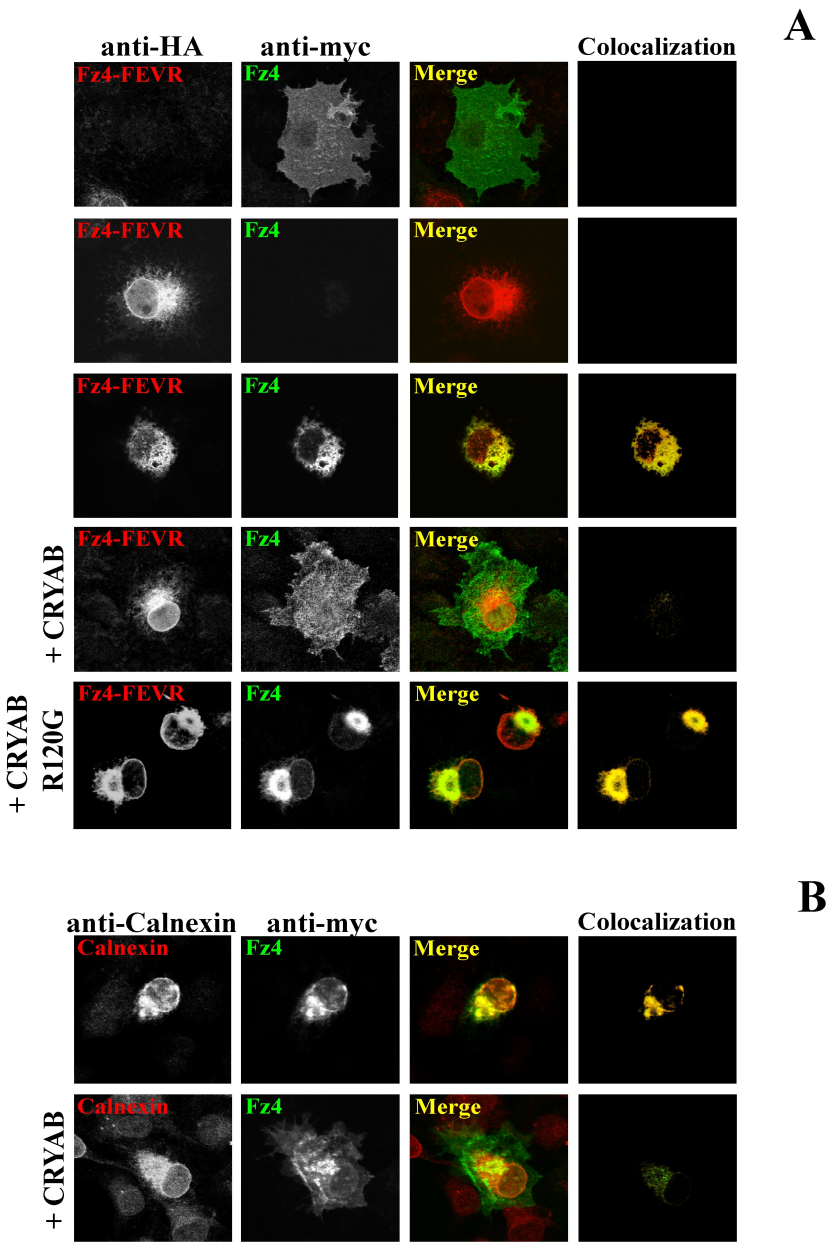

Fig.21: CRYAB overexpression reverts the dominant negative effect of Fz4-FEVR on Fz4.

A) COS-7 cells were transiently transfected with myc-tagged Fz4, HA-Fz4-FEVR, 3xFlag-CRYAB or its mutant 3xFlag-CRAYB(R120G) as indicated. 48 hours post-transfection the cells were fixed and processed for immunofluorescence microscopy.

B) Colocalization of myc-Fz4 transfected in COS-7 cells and the endogenous Calnexin protein, in the the presence or in the absence of cotransfected 3xFlag-CRAYB. Cells were manipulated as in A.

Fig.S3

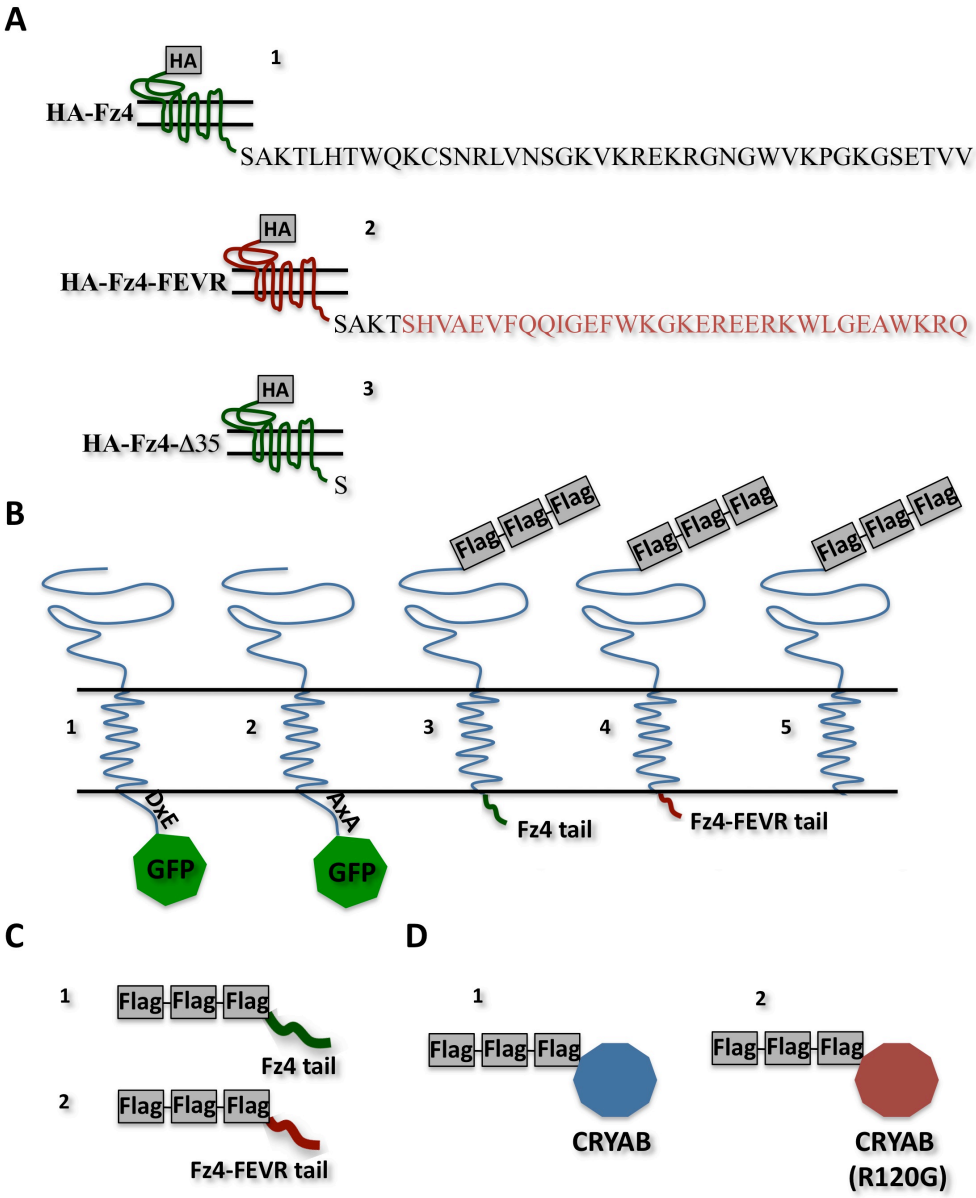

Fig.S3: Schematic representation of the constructs used.

2.5 CONCLUSION.

In the present work we characterized the mutant receptor Frizzled4 (L501fsX533) associated to the dominant form of *famialial exudative vitreoretinopathy*. As previously described the mutant Fz4-FEVR is not expressed on the plasma membrane of transfected cells but is retained in the endoplasmatic reticulum where it traps the wild-type counterpart by oligomerization ***(Johane Robitaille et al. 2002; Kaykas A. et al. 2004).*** Our data shed much light on the intracellular localization of the mutant receptor. At the steady state, Fz4-FEVR shows an almost exclusive ER localization by confocal immunofluorescence microscopy, as evidenciated by a complete colocalization with *calnexin.* More importantly, this localization is most likely mediated by specific protein(s) interacting with its new cytosolic tail, as indicated by the acquired ER localization of VSVG-Fz4-FEVR tail constructs and by the rescue of cell surface expression of Fz4-FEVR in the presence of competing Fz4-FEVR tail expressed as a cytosolic peptide. Finally, temperature shift experiments performed on chimeric constructs or Fz4 and Fz4-FEVR indicates that an efficient recycling mecchanism most likely contributes to the ER localization of Fz4-FEVR.
Interenstingly, the ER localization of Fz4-FEVR triggers its oligomerization. Indeed, velocity gradients show that Fz4 wild-type, that was mostly located on the plasma membrane, is almost exlusively in monomeric forms at steady state, while Fz4-FEVR, that is tightly located in the ER at steady state, forms mainly oligomers. However, newly synthesized Fz4 and Fz4-FEVR shows a similar level of oligomerization, about 50% suggesting that monomeric Fz4 forms do exit from the ER, while monomeric Fz4-FEVR are impaired to exit the ER and form with time more and more oligomeric forms that would contribute to the ER localization. Noteworthy, oligomerization in the ER is the crucial step required for the export of many transmembrane receptors or channels ***(Tao Y.X. et al. 2004, Thomas R.M. et al. 2007, Guan R. et al. 2009, Guan R. et al. 2010)***, but it can determine ER retention of others ***(Shamie Das et al. 2009).***

In addiction, we have identified CRYAB as an interactor of both Fz4 and Fz4-FEVR. Alpha-Crystallins, the major eye lens protein, belong to small heat shock protein (sHSP) family, due to structural and functional similarities ***(Klemenz R. et al. 1991; Crabbe M.J.C. et al. 2001).*** Alpha-Crystallins consist of alphaA and alphaB subunits of 20 kDa each and exists as a polydisperse oligomer with an average molecular mass of 600-800 kDa ***(Groenen P.J.T.A. et al. 1999).*** More recently, alpha-Crystallins have been shown to be present in a number of non-lenticular tissues, suggesting that they may have a more general cellular function. Like all other sHSP, alpha-Crystallins act as a molecular chaperone by preventing the aggregation of proteins denatured by heat or other stress conditions ***(Horwitz J. et al 1992; Horwitz J. et al. 1998).*** Although, the mechanism of chaperone function of alpha-Crystallins is not fully understood, it was shown that they specifically recognize aggregation-prone, non-native structures that occur early on the denaturation pathway of

protein. Numerous studies have shown that the chaperone activity of alpha-Crystallins is dependent on the presence of surface-exposed hydrophobic patches ***(Raman B. et al.1994; Das K.P. et al. 1995; Sharma, K.K. et al.1998).*** Interestigly, the interaction between Fz4 and CRYAB does not depend on the presence of both wild-type or mutant tail of the receptor, suggesting that the recognition is mediated by the cytosolic loops of the receptor. CRYAB over-expression does not influence the subcellular distribution of Fz4 in transfected cell and we have no clues at the moment on the functional relevance of this interaction; in contrast, it significantly influences the localization of Fz4-FEVR, as evidenced by the difference intracellular distribution and the abundant recovery of the mutant receptor on cell surface. According to the previous results exstensively described in literature on its chaperone activity ***(G. Bhanuprakash Reddy et al. 2002)***, CRYAB prevents or resolves the aggregation of several cytosolic proteins. For this reason, we think that the recovery to the cell surface of Fz4-FEVR may be due to the chaperone activity of CRYAB that would inhibit the oligomerization of the mutant receptor, thus allowing its export from the ER and localization on plasma membrane. In support of this conclusion is the finding that a mutated CRYAB, devoid of chaperone activity, has very minor effect on Fz4-FEVR intracellular transport. At the best of our knowledge, this is the first evidence that CRYAB acts as a chaperone for transmembrane proteins. Moreover, and mostly importantly, CRYAB over-expression reverted the dominant negative effect of Fz4-FEVR on Fz4 previosly described in literature ***(Kaykas A. et al. 2004).*** Our results indicate that CRYAB is able to free Fz4 receptor from the oligomer formed with Fz4-FEVR, promoting its export and delivery to the plasma membrane. Further work is required to verify that the Fz4 forms that have reached the cell surface in these condition are able to elicit signal transduction in response to Norrin. Moreover, it will be interesting to investigate whether CRYAB may act as chaperone on other mutated transmembrane receptors that are retained in the ER. Indeed, a number of mutated receptors act as dominat negative on their wild-type counterparts impairing their ER export ***(Tao Y.X. et al. 2004, Thomas R.M. et al. 2007, Guan R. et al. 2009, Guan R. et al. 2010).***

In conclusion, the most interesting outcome of this work is the possibility that CRYAB may open new therapeutic approches for the autosomal dominant form of *familial exudative vitreoretinopathy*.

3. Aknowledgments.

I want to thank:

The full professor Stefano Bonatti, for giving me the opportunity to join his group and to develop these projects in his lab and for guiding me with patience and willingness in my first steps as a young scientist and, more important, for encouraging me in my down moments.

The full professor Maria Vittoria Barone to put to use the confocal microscopy LSM510 Ziess.

The full professor Andrè le Bivic to give me the opportunity to work, undre the guide Dr Giovanna Mottola, in his group at the IBDML institute in Marseille.

The full professor Antonella De Matteis to give me the opportunity to work, under the guide of the Dr Giovanni D'Angelo, in his group at the Mario Negri Sud institute in Santa Maria Imbaro.

Dr Giusy Tornillo for everything she taught me with great patience and dedication.

Dr Valentina Lemma for helping me in performing the experiments.

Dr Massimo Mallardo and Dr Giovanna Mottola for their scientific assistance.

Dr Gabriella Caporaso for her helpful collaboration.

Patrizio Sesti and Enzo Brescia for their technical assistance.

Funding:

This work was supported by grants from Ministero Università Ricerca Scientifica e Tecnologica to S.B.; and from Telethon Italia [grant number GGP09029].

4. References.

Amandio V. Vieira, Christophe Lamaze, Sandra L. Schmid (1996) *Control of EGF Receptor Signaling by Clathrin-Mediated Endocytosis.* Science **274**:2086-2088.

Anderson RG. (1998) *The caveolae membrane system.* Annu. Rev. Biochem. **67**:199-225.

Andley UP, Song Z, Wawrousek EF, Brady JP, Bassnett S, Fleming TP. (2001) *Lens epithelial cells derived from aB-crystallin knockout mice demonstrate hyperproliferation and genomic instability.* FASEB J. **15**:221-229.

Annouck Luyten et al. (2008) *The Postsynaptic Density 95/Disc-Large/Zona Occludens Protein Syntenin Directly Interacts with Frizzled 7 and Supports Noncanonical Wnt Signaling.* Molecular Biology of the Cell. **19**:1594-1604.

Appenzeller C., Andersson H., Kappeler F. and Hauri H.P. (1999) *The lectin ERGIC-53 is a cargo transport receptor for glycoproteins.* Nat. Cell Biol. **1**:330-334.

Aridor M., Bannykh S. I., Rowe T. & Balch W. E. (1995) *Sequential coupling between COPII and COPI vesicle coats in endoplasmic reticulum to Golgi transport.* J. Cell Biol. **131**:875-893.

Arrigo AP. (1995) *Expression of stress genes during development.* Neuropathol Appl Neurobiol **21**:488-91.

Balch, W.E. (2006) *Structure of the Sec13/31 COPII coat cage*. Nature **439**:234-238.

Belinda A. Phillipson, Peter Pimpl, Luis Lamberti Pinto daSilva, Andrew J. Crofts, J. Philip Taylor, Ali Movafeghi, David G. Robinson, Jurgen Denecke. (2001) *Secretory Bulk Flow of Soluble Proteins Is Efficient and COPII Dependent.* The Plant Cell, Vol. **13**:2005-2020.

Beck R., M. Ravet, F.T. Wieland, D. Cassel (2009) *The COPI system: Molecular mechanisms and function.* FEBS letter, **583**:2701–2709.

Ben Amara, A., Ghigo, E., Le Priol, Y., Lepolard, C., Salcedo, S. P., Lemichez, E., Bretelle, F., Capo, C. and Mege, J. L. (2010). *Coxiella burnetii, the agent of Q fever, replicates within trophoblasts and induces a unique transcriptional response.* PLoS One **5**:5315.

Benado, A., Nasagi-Atiya, Y. and Sagi-Eisenberg, R. (2009). *Protein trafficking in immune cells.* Immunobiology **214**:403-421.

Bezzerides VJ, Ramsey IS, Kotecha S, Greka A & Clapham DE. (2004) *Rapid vesicular translocation and insertion of TRP channels.* Nat Cell Biol **6**:709-720.

Bhat SP, Nagineni CN. (1989) *aB subunit of lens specific protein acrystallin is present in other ocular and non-ocular tissues.* Biochem Biophys Res Commun **158**:319-25.

Bhanuprakash G. Reddy, Sriram Narayanan, P. Yadagiri Reddy, Ira Surolia (2002) *Suppression of DTT-induced aggregation of abrin by KA-*

and KB-crystallins: a model aggregation assay for K-crystallin chaperone activity in vitro. FEBS Letters **522**:59-64.

Bhoj, V. G. and Chen, Z. J. (2009). *Ubiquitylation in innate and adaptive immunity.* Nature **458**:430-437.

Bielli, A., Haney, C.J., Gabreski, G., Watkins, S.C., Bannykh, S.I. and Aridor, M. (2005) *Regulation of Sar1 NH2 terminus by GTP binding and hydrolysis promotes membrane deformation to control COPII vesicle fission.* J. Cell Biol. **171**:919-924.

Bi, X., Corpina, R.A. and Goldberg, J. (2002) *Structure of the Sec23/24-Sar1 pre-budding complex of the COPII vesicle coat*. Nature **419**:271-277.

Bockaert J, Fagni L, Dumuis A, Marin P (2004) *GPCR interacting proteins (GIP).* Pharmacol Ther **103**:203-221.

Boll W., Iris Rapoport, Christian Brunner, Yorgo Modis, Siegfried Prehn, Tomas Kirchhausen (2002) *The μ2 Subunit of the Clathrin Adaptor AP-2 Binds to FDNPVY and YppØ Sorting Signals at Distinct Sites.* Traffic **3**: 590-600.

Brady JP, Garland DL, Green DE, Tamm ER, Giblin FJ, Wawrousek EF. (2001) *αB-crystallin in lens development and muscle integrity: a gene knockout approach.* Invest Ophthalmol Vis Sci **42**:2924-2934.

Brady AE, Limbird LE (2002) *G protein-coupled receptor interacting proteins: emerging roles in localization and signal transduction.* Cell Signal **14**:297-309.

Brandizzi and Patrick Moreau. (2009) *A novel di-acidic motif facilitates ER export of the syntaxin SYP31.* Journal of Experimental Botany **11**:3157-3165.

Burgner, D., Davila, S., Breunis, W. B., Ng, S. B., Li, Y., Bonnard, C., Ling, L., Wright, V. J., Thalamuthu, A., Odam, M. (2009). *A genome-wide association study identifies novel and functionally related susceptibility Loci for Kawasaki disease.* PLoS Genet **5**:1000319.

Cancino, J. *et al.* (2007) *Antibody to AP1B adaptor blocks biosynthetic and recycling routes of basolateral proteins at recycling endosomes.* Mol. Biol. Cell **18**, 4872–4874.

Cao TT, Deacon HW, Reczek D, Bretscher A, von Zastrow M (1999) *A kinase-regulated PDZ-domain interaction controls endocytic sorting of the β2-adrenergic receptor.* Nature **401**:286-290.

Catherine L. Jackson. (2009) *Mechanisms of transport through the Golgi complex.* Journal of Cell Science **122**, 443-452.

Chen, J., Xu, J., Zhao, W., Hu, G., Cheng, H., Kang, Y., Xie, Y. and Lu, Y. (2005). *Characterization of human LNX, a novel ligand of Numb protein X that is downregulated in human gliomas.* Int. J. Biochem Cell Biol. **37**:2273-2283.

Chiang, Y. J., Kole, H. K., Brown, K., Naramura, M., Fukuhara, S., Hu, R. J., Jang, I. K., Gutkind, J. S., Shevach, E. and Gu, H. (2000). *Cbl-b regulates the CD28 dependence of T-cell activation.* Nature **403**:216-220.

Clague MJ. (1998) *Molecular aspects of the endocytic pathway*. Biochem. J. **336**(Pt 2), 271-82.

Cong, F. et al. (2004) *Wnt signals across the plasma membrane to activate the beta-catenin pathway by forming oligomers containing its receptors, Frizzled and LRP.* Development **131**:5103–5115.

Crabbe M.J.C. and Hepburne-Scott H.W. (2001) Curr. Pharm. Biotechnol. **2**:77-111.

Dawson DW, Volpert OV, Bouck NP. (1999) *Pigment Epithelium-Derived Factor: A Potent Inhibitor of Angiogenesis.* Science **285**:245-248.

Dean, N. and Pelham, H.R. (1990) *Recycling of proteins from the Golgi compartment to the ER in yeast.* J. Cell Biol. **111**:369–377.

De la Calle-Martin, O. Hernandez, M. Ordi, J. Casamitjana, N. Arostegui, J. I. Caragol, I. Ferrando, M. Labrador, M. Rodriguez-Sanchez, J. L. and Espanol T. (2001). *Familial CD8 deficiency due to a mutation in the CD8 alpha gene.* J. Clin. Invest. **108**:117-123.

Deshaies, R. J. and Joazeiro, C. A. (2009). *RING domain E3 ubiquitin ligases.* Annu. Rev. Biochem **78**:399-434.

Dho, S. E., Jacob, S., Wolting, C. D., French, M. B., Rohrschneider, L. R. and McGlade, C. J. (1998). *The mammalian numb phosphotyrosine-binding domain. Characterization of binding specificity and identification of a novel PDZ domaincontaining numb binding protein, LNX.* J. Biol. Chem. **273**:9179-9187.

Di Guglielmo M.G., Le Roy C., Goodfellow A.F. and Wrana J.L. (2003) *Distinct endocytic pathways regulate TGF-β receptor signalling and turnover.* Nature Cell Biology **3**:410-421.

Duvernay M.T., Zhou F., Wu G. (2004) *A conserved motif for the transport of G protein-coupled receptors from the endoplasmic reticulum to the cell surface* J. Biol. Chem. **279**:30741-50.

Eckhard Ficker, Adrienne T. Dennis, Lu Wang and Arthur M. Brown. (2003) *Role of the Cytosolic Chaperones Hsp70 and Hsp90 in Maturation of the Cardiac Potassium Channel hERG*. Circ. Res. **92**:87-100.

Eileithyia Swanton, Andrew Holland, Stephen High, and Philip Woodman. (2005) *Disease-associated mutations cause premature oligomerization of myelin proteolipid protein in the endoplasmic reticulum.* PNAS **102**:4342-4347.

Erra M. C., Iodice L., Lotti L. V. and Bonatti S. (1999). *Cell fractionation analysis of human CD8 glycoprotein transport between endoplasmic reticulum, intermediate compartment and Golgi complex in tissue cultured cells.* Cell Biol. Int. **23**:571-577.

Eugster, A., Frigerio, G., Dale, M. and Duden, R. (2004) *The α- and β'- COP WD40 domains mediate cargo-selective interactions with distinct dilysine motifs.* Mol. Biol. Cell **15**, 1011-1023.

Fadi F. Hamdan, Moulay Driss Rochdi, Billy Breton, Delphine Fessart, Douce E. Michaud, Pascale G. Charest, Ste´phane A. Laporte, and Michel Bouvier (2007) *Unraveling G-Protein-coupled-Receptor*

Endocytosis Pathways Using Real-time Monitoring of Agonist-promoted Interaction between β-Arrestins and AP-2. **28**2:29089-29100.

Fath S, Mancias JD, Bi X, Goldberg J. (2007) *Structure and organization of coat proteins in the COPII cage.* Cell **129**:1325-1336.

Ferguson SS, Zhang J, Barak LS, Caron MG (1998) *Molecular mechanisms of G protein-coupled receptor desensitization and resensitization.* Life Science **62**:1561-1565.

Folsch, H. (2005) *The building blocks for basolateral vesicles in polarized epithelial cells.* Trends Cell Biol. **15**, 222–228.

Fred S. Gorelick, Christine Shugrue (2001). *Exiting the endoplasmic reticulum*. Molecular and Cellular Endocrinology **177**, 13–18.

Fumiko Itoh, Nullin Divecha, Lenny Brocks, Lauran Oomen, Hans Janssen, Jero Calafat, Susumu Itoh and Peter ten Dijke (2003) *The FYVE domain in Smad anchor for receptor activation (SARA) is sufficient for localization of SARA in early endosomes and regulates TGF-β/Smad signalling.* Genes to Cells **7:**321-331.

Fung-Leung W. P., Schilham M. W., Rahemtulla A., Kundig T. M., Vollenweider M., Potter J., van Ewijk W. and Mak T. W. (1991). *CD8 is needed for development of cytotoxic T cells but not helper T cells.* Cell **65**:443-449.

Gage RM, Kim KA, Cao TT, von Zastrow M (2001) *A transplantable sorting signal that is sufficient to mediate rapid recycling of G protein-coupled receptors.* J Biol Chem **276**:44712-44720.

Gangadharan, D. and Cheroutre, H. (2004). *The CD8 isoform CD8alpha/alpha is not a functional homologue of the TCR co-receptor CD8alpha/beta.* Curr. Opin. Immunol **16**:264-270.

Gao CY, Rampalli AM, Cai HC, He HY, Zelenka PS. (1999) *Changes in cyclin dependent kinase expression and activity accompanying lens fiber cell differentiation.* Exp Eye Res **69**:695-703.

Giovanni D'Angelo, Liana Prencipe, Luisa Iodice, G. Beznoussenko, Marco Savarese, Pier Francesco Marra, Giuseppe Di Tullio, Gianluca Martire, Maria Antonietta De Matteis, and Stefano Bonatti. (2009) *Grasp65 And Grasp55 Sequentially Promote The Transport Of C-Terminal Valine Bearing Cargoes To And Through The Golgi Complex.* J. Bio. Chem.

Goldrath A. W., Hogquist K. A. and Bevan M. J. (1997). *CD8 lineage commitment in the absence of CD8.* Immunity **6**:633-642.

Gomez-Martin D., Diaz-Zamudio M. and Alcocer-Varela J. (2008). *Ubiquitination system and autoimmunity: the bridge towards the modulation of the immune response.* Autoimmun Rev. **7**:284-290.

Gordon, M.D. and Nusse, R. (2006) *Wnt signaling: multiple pathways, multiple receptors, and multiple transcription factors.* J. Biol. Chem. **281**, 22429–22433.

Graeme Milligan. (2007) *G protein-coupled receptor dimerisation: Molecular basis and relevance to function.* Biochimica et Biophysica Acta **1768**, 825-835.

Groenen P.J.T.A., Merck K.B., de Jong W.W. and Bloemendal H. (1994) Eur. J. Biochem. **225**:1-19.

Gronski M. A., Boulter J. M., Moskophidis D., Nguyen L. T., Holmberg K., Elford A. R., Deenick E. K., Kim H. O., Penninger J. M., Odermatt B. (2004). *TCR affinity and negative regulation limit autoimmunity.* Nat. Med. **10**:1234-1239.

Guan, R., Feng, X., Wu, X., Zhang, M., Zhang, X., Hebert, T.E., Segaloff, D.L. (2009) *Bioluminescence resonance energy transfer studies reveal constitutive dimerization of thehumanlutropin receptor and a lack of correlation between receptor activation and the propensity for dimerization.* J. Biol. Chem. **284**:7483-7494.

Guan R., Wu X., Feng X., Zhang M., Hébert T.E., Segaloff D.L. (2010) *Structural determinants underlying constitutive dimerization of unoccupied human follitropin receptors.* Cell. Signal. **22**:247-256.

Harald W. Platta and Harald Stenmark (2011) *Endocytosis and signaling.* Current Opinion in Cell Biology **23**:393-403.

Harvey T.M. and Emmanuel Boucrot (2011) *Molecular mechanism and physiological functions of clathrin-mediated endocytosis.* Nature Review **12**:517-533.

Heike Hering, Morgan Sheng. (2002) *Direct interaction of Frizzled-1, -2, -4, and -7 with PDZ domains of PSD-95.* FEBS Letters **521**:185-189.

Heli I. Alanen, Irina B. Raykhel, Marja J. Luukas, Kirsi E.H. Salo and Lloyd W. Ruddock. (2011) *Beyond KDEL: The Role of Positions -5 and -6 in Determining ER Localization*. J. Mol. Biol. **7**:62966.

Hershko A. and Ciechanover A. (1992). *The ubiquitin system for protein degradation.* Annu. Rev. Biochem. **61**:761-807.

Hopkins C.R., Miller K. and Beardmore J. M. (1985) *Receptor-mediated endocytosis of transferrin and epidermal growth factor receptors: a comparison of constitutive and ligand-induced uptake.* J. Cell Sci. **3**:173-186.

Hsien-yu Wang, Tong Liu, Craig C. Malbon. (2006) *Structure-function analysis of Frizzleds.* Cellular Signalling **18**:934-941.

Kaykas A., Yang-Snyder J., Héroux M., Shah K.V., Bouvier M. and Randall T.Moon. (2004) *Mutant Frizzled 4 associated with vitreoretinopathy traps wild-type Frizzled in the endoplasmic reticulum by oligomerization.* Nature Cell Biology **6**.

Kansaku A., Hirabayashi S., Mori H., Fujiwara N., Kawata A., Ikeda M., Rokukawa C., Kurihara H. and Hata Y. (2006). *Ligand-of-Numb protein X is an endocytic scaffold for junctional adhesion molecule 4.* Oncogene **25**:5071-5084.

Kappeler F., Klopfenstein D.R., Foguet M., Paccaud J.P. and Hauri H.P. (1997) *The recycling of ERGIC-53 in the early secretory pathway.*

ERGIC-53 carries a cytosolic endoplasmic reticulum-exit determinant interacting with COPII. J. Biol. Chem. **272**:31801–31808.

Katherine B Sims, MD. (2009) *NDP-Related Retinopathies*. Gene reviews.

Kawabata K., Nagasawa M., Morio T., Okawa H. and Yata J. (1996). *Decreased alpha/beta heterodimer among CD8 molecules of peripheral blood T cells in Wiskott-Aldrich syndrome.* Clin. Immunol Immunopathol **81**:129-135.

Kristian Prydz, Gunnar Dick and Heidi Tveit (2008) *How Many Ways Through the Golgi Maze?* Traffic review, **9**:299–304.

Kondo H., Hayashi H., Oshima K., Tahira T., Hayashi K. (2003) *Frizzled 4 gene (FZD4) mutations in patients with familial exudative vitreoretinopathy with variable expressivity.* Journal Ophthalmol, **87**:1291-1295.

Kota Saito, Koh Yamashiro, Yuki Ichikawa, Patrik Erlmann, Kenji Kontani, Vivek Malhotra, and Toshiaki Katada. (2011) *cTAGE5 mediates collagen secretion through interaction with TANGO1 at endoplasmic reticulum exit sites.* Moll. Bio. Cell.

James A. Poulter, Manir Ali, David F. Gilmour, Aine Rice, Hiroyuki Kondo, Kenshi Hayashi, David A. Mackey, Lisa S. Kearns, Jonathan B. Ruddle, Jamie E. Craig, Eric A. Pierce, Louise M. Downey, Moin D. Mohamed, Alexander F. Markham, Chris F. Inglehearn, and Carmel Toomes. (2010) *Mutations in TSPAN12 Cause Autosomal-Dominant Familial Exudative Vitreoretinopathy.* The American Journal of Human Genetics **86**:248-253.

Jason C. Bermak, Ming Li, Clayton Bullock and Qun-Yong Zhou. (2001) *Regulation of transport of the dopamine D1 receptor by a new membrane-associated ER protein. Nature Cell Biology* **3**:492-498.

Jayasri Nanduri, Pamela Bergson, Ning Wang, Eckhard Ficker, and Nanduri R. Prabhakar. (2009) *Hypoxia inhibits maturation and trafficking of HERG K^+channel protein: Role of Hsp90 and ROS. Biochem Biophys Res Commun*. **388**(2):212-216.

Jean-Ju Chung, Yukari Okamoto, Brian Coblitz, Min Li, Yun Qiu and Sojin Shikano. (2009) *PI3K/Akt signalling-mediated protein surface expression sensed by 14-3-3 interacting motif.* The FEBS Journal.

Jeon M. S., Atfield A., Venuprasad K., Krawczyk C., Sarao R., Elly C., Yang C., Arya S., Bachmaier K., Su L. (2004). *Essential role of the E3 ubiquitin ligase Cbl-b in T cell anergy induction.* Immunity **21**:167-177.

Johane Robitaille, Marcia L.E. MacDonald, Ajamete Kaykas, Laird C. Sheldahl, Jutta Zeisler, Marie-Pierre Dubé, Lin-Hua Zhang, Roshni R. Singaraja, Duane L. Guernsey, Binyou Zheng, Lee F. Siebert, Ann Hoskin-Mott, Michael T. Trese, Simon N. Pimstone, Barkur S. Shastry, Randall T. Moon, Michael R. Hayden, Y. Paul Goldberg3, Mark E. Samuels. (2002) *Mutant frizzled-4 disrupts retinal angiogenesis in familial exudative vitreoretinopathy.* Nature genetics **32**.

Joseph Horwitz (2003) *Alpha-crystallin.* Experimental Eye Research **76**:145-153.

Iodice L., Sarnataro S. and Bonatti S. (2001). *The carboxyl-terminal valine is required for transport of glycoprotein CD8 alpha from the endoplasmic reticulum to the intermediate compartment.* J. Biol. Chem. **276**:28920-28926.

Irie H. Y., Ravichandran K. S. and Burakoff S. J. (1995). *CD8 beta chain influences CD8 alpha chain-associated Lck kinase activity.* J. Exp. Med. **181**:1267-1273.

Laurent Chatre, Vale´rie Wattelet-Boyer, Su Melser, Lilly Maneta-Peyret, Federica Sunglim Cho, Jeongmin Ryoo, Youngsoo Jun, and Kwangseog Ahn. (2011) *Receptor-Mediated ER Export of Human MHC Class I Molecules Is Regulated by the C-Terminal Single Amino Acid.* Traffic **12**, 42–55.

Lederkremer, G.Z., Cheng, Y., Petre, B.M., Vogan, E., Springer, S., Schekman, R., Walz, T. and Kirchhausen, T. (2001) *Structure of the Sec23p/24p and Sec13p/31p complexes of COPII.* Proc. Natl. Acad. Sci. USA **98**:10704-10709.

Lee, M.C., Orci, L., Hamamoto, S., Futai, E., Ravazzola, M. and Schekman, R. (2005) *Sar1p N-terminal helix initiates membrane curvature and completes the fission of a COPII vesicle.* Cell **122**:605-617.

Letourneur, F., Gaynor, E.C., Hennecke, S., Demolliere, C., Duden, R., Emr, S.D., Riezman, H. and Cosson, P. (1994) *Coatomer is essential for retrieval of dilysine-tagged proteins to the endoplasmic reticulum.* Cell **79**:1199-1207.

Levkowitz G, Waterman H, Zamir E (1998) *c-Cbl/Sli-1 regulates endocytic sorting and ubiquitination of the epidermal growth factor receptor.* Genes Dev **12**:3663-3674.

Lewis, M.J. and Pelham, H.R. (1992) *Sequence of a second human KDEL receptor.* J. Mol. Biol. **226**:913-916.

Lotteau, V., Teyton, L., Peleraux, A., Nilsson, T., Karlsson, L., Schmid, S.L., Quaranta, V. and Peterson, P.A. (1990) *Intracellular transport of class II MHC molecules directed by invariant chain.* Nature **348**:600-605.

Luttrell L.M., Lefkowitz R.J. (2002) *The role of beta-arrestins in the termination and transduction of G-protein-coupled receptor signals.* J. Cell Science, **115**:455.

Ma D., Zerangue N., Lin Y.F., Collins A., Yu M., Jan Y.N., Jan L.Y. (2001) *Role of ER export signals in controlling surface potassium channel numbers.* Science, **291**:316-319.

Ma L. and Wang H.Y. (2006) *Suppression of cyclic GMP-dependent protein kinase is essential to the Wnt/cGMP/Ca2+ pathway.* J. Biol. Chem. **281**:30990-31001.

Madshus I.H. and Espen Stang (2009) *Internalization and intracellular sorting of the EGF receptor: a model for understanding the mechanisms of receptor trafficking.* J.Cell.Science **122**:3433-3439.

Malhotra V. (2009) *TANGO1 facilitates cargo loading at endoplasmic reticulum exit sites.* Cell, **136**:891-902.

Marchese A, Benovic JL (2001) *Agonist-promoted ubiquitination of the G protein-coupled receptor CXCR4 mediates lysosomal sorting.* J. Biol. Chem. **276**:45509-45512.

Mariano Stornaiuolo, Lavinia V. Lotti, Nica Borgese, Maria-Rosaria Torrisi, Giovanna Mottola, Gianluca Martire, and Stefano Bonatti. (2003) *KDEL and KKXX Retrieval Signals Appended to the Same Reporter Protein Determine Different Trafficking between Endoplasmic Reticulum, Intermediate Compartment, and Golgi Complex.* Mol. Biol. Cell. **14**(3):889-902.

Marsh M, McMahon HT. (1999) *The structural era of endocytosis.* Science. **285**:215-20.

Martire G., Mottola G., Pascale M. C., Malagolini N., Turrini I., Serafini-Cessi F., Jackson M. R. and Bonatti S. (1996). *Different fate of a single reporter protein containing KDEL or KKXX targeting signals stably expressed in mammalian cells.* J. Biol. Chem. **271**:3541-3547.

Matthew T. Duvernay, Catalin M. Filipeanu, Guangyu Wu. (2005) *The regulatory mechanisms of export trafficking of G protein-coupled receptors.* Cellular Signalling **17**:1457–1465.

Matthew T. Duvernay, Chunmin Dong, Xiaoping Zhang, Melanie Robitaille, Terence E. Hebert and Guangyu Wu. (2009) *A Single Conserved Leucine Residue on the First Intracellular Loop Regulates ER Export of G Protein-Coupled Receptors.* Traffic **10**:552-566.

Mauro C., Pacifico F., Lavorgna A., Mellone S., Iannetti A., Acquaviva R., Formisano S., Vito P. and Leonardi A. (2006). *ABIN-1 binds to NEMO/ IKKgamma and co-operates with A20 in inhibiting NF-kappaB.* J. Biol. Chem. **281**:18482-18488.

Melanie Mikosch and Ulrike Homann. (2009) *How do ER export motifs work on ion channel trafficking?* Current Opinion in Plant Biology, **12**:685-689.

Mellman I. and Nelson W. J. (2008). *Coordinated protein sorting, targeting and distribution in polarized cells.* Nat. Rev. Mol. Cell Biol. **9**:833-845.

Michelsen, K., Yuan, H. and Schwappach, B. (2005) *Hide and run. Arginine based endoplasmic-reticulum-sorting motifs in the assembly of heteromultimeric membrane proteins.* EMBO Rep. **6**:717-722.

Mirza M., Hreinsson J., Strand M. L., Hovatta O., Soder O., Philipson L., Pettersson R. F. and Sollerbrant K. (2006). *Coxsackievirus and adenovirus receptor (CAR) is expressed in male germ cells and forms a complex with the differentiation factor JAM-C in mouse testis.* Exp. Cell Res. **312**:817-830.

Moller S., J. Vilo, M.D. Croning. (2001) *Bioinformatics 17* (Suppl 1) S174.

Mossessova, E., Bickford, L.C. and Goldberg, J. (2003) *SNARE selectivity of the COPII coat.* Cell **114**:483-495.

Mottola G., Jourdan N., Castaldo G., Malagolini N., Lahm A., Serafini-Cessi F., Migliaccio G. and Bonatti S. (2000). *A new determinant of endoplasmic reticulum localization is contained in the juxtamembrane region of the ectodomain of hepatitis C virus glycoprotein E1.* J. Biol. Chem. **275**:24070-24079.

Mrowiec T. and Schwappach B. (2006) *14-3-3 Proteins in membrane protein transport.* Biol. Chem. **387**:1227-1236.

Mukhopadhyay D, Riezman H (2007) *Proteasome independent functions of ubiquitin in endocytosis and signaling.* Science **315**:201-205.

Munro, S. and Pelham, H.R. (1987) *A C-terminal signal prevents secretion of luminal ER proteins.* Cell **48**:899-907.

Nam J.S. et al. (2006) *Mouse cristin/R-spondin family proteins are novel ligands for the Frizzled 8 and LRP6 receptors and activate beta-catenin-dependent gene expression.* J. Biol. Chem. **281**:13247-13257.

Nancy Zaarour, Sylvie Demaretz, Nadia Defontaine, David Mordasini, and Kamel Laghmani. (2009) *A Highly Conserved Motif at the COOH Terminus Dictates Endoplasmic Reticulum Exit and Cell Surface Expression of NKCC2.* J Biol Chem, **284**:21752-21764.

Naramura M., Jang I. K., Kole H., Huang F., Haines D. and Gu H. (2002). *c-Cbl and Cbl-b regulate T cell responsiveness by promoting ligand-induced TCR downmodulation.* Nat. Immunol **3**:1192-1199.

Nichols W.C. et al. (1998) *Mutations in the ER–Golgi intermediate compartment protein ERGIC-53 cause combined deficiency of coagulation factors V and VIII.* Cell **93**:61-70.

Nielsen E., Christoforidis S., Uttenweiler-Joseph S., Miaczynska M., Dewitte F., Wilm M., Hoflack B. and Zerial M. (2000). *Rabenosyn-5, a novel Rab5 effector, is complexed with hVPS45 and recruited to endosomes through a FYVE finger domain.* J. Cell Biol. **151**:601-612.

Nishimura N, Balch WE. (1997) *A di-acidic signal required for selective export from the endoplasmic reticulum.* Science, **277**:556–558.

Nishimura N, Bannykh S, Slabough S, Matteson J, Altschuler Y, Hahn K, Balch WE. (1999) *A di-acidic (DXE) code directs concentration of cargo during export from the endoplasmic reticulum.* J Biol Chem, **274**:15937-15946.

Nufer O, Guldbrandsen S, Degen M, Kappeler F, Paccaud JP, Tani K, Hauri HP (2002) *Role of cytoplasmic C-terminal amino acids of membrane proteins in ER export.* J Cell Sci **115**:619-628.

Nufer O., F. Kappeler, S. Guldbrandsen, H.P. Hauri. (2003) J. Cell. Sci **116**:4429.

Nufer Oliver and Hans-Peter Hauri. (2003) *ER Export Call 14-3-3.* Current Biology **13**:391-393.

O'Kelly I, Butler MH, Zilberberg N & Goldstein SA. (2002) *Forward transport 14-3-3 binding overcomes retention in endoplasmic reticulum by dibasic signals.* Cell **111**:577-588.

Oka, T. and Nakano, A. (1994) Inhibition of GTP hydrolysis by Sar1p causes accumulation of vesicles that are a functional intermediate of the ER-to-Golgi transport in yeast. J. Cell Biol. **124**:425-434.

Orci, L. and Schekman, R. (2003) *Multiple cargo binding sites on the COPII subunit Sec24p ensure capture of diverse membrane proteins into transport vesicles.* Cell **114**:497-509.

Oved S. and Yosef Yarden (2002) *Signal transduction: Molecular ticket to enter cells.* Nature **416**:133-136.

Parton RG., Ayanthi A. Richards (2003) *Lipid Rafts and Caveolae as Portals for Endocytosis: New Insights and Common Mechanisms.* Traffic **11**:724–738.

Pascale M. C., Erra M. C., Malagolini N., Serafini-Cessi F., Leone A. and Bonatti S. (1992). *Post-translational processing of an O-glycosylated protein, the human CD8 glycoprotein, during the intracellular transport to the plasma membrane.* J. Biol. Chem. **267**:25196-25201.

Pelham, H.R. (1988) *Evidence that luminal ER proteins are sorted from secreted proteins in a post-ER compartment.* Embo J. **7**:913-918.

Pickart C. M. and Fushman D. (2004). *Polyubiquitin chains: polymeric protein signals.* Curr. Opin. Chem. Biol. **8**:610-616.

Piper R. C. and Luzio J. P. (2007). *Ubiquitin-dependent sorting of integral membrane proteins for degradation in lysosomes.* Curr. Opin. Cell Biol. **19**:459-465.

Premont RT, Gainetdinov RR (2007) *Physiological roles of G protein-coupled receptor kinases and arrestins.* Annu Rev Physiol **69**:511-534.

Rahel Byland, Patricia J. Vance, James A. Hoxie and Mark Marsh (2007) *A Conserved Dileucine Motif Mediates Clathrin and AP-2–dependent Endocytosis of the HIV-1 Envelope Protein.* MBC **18**:414-425.

Rajan S, Preisig-Muller R, Wischmeyer E, Nehring R, Hanley PJ, Renigunta V, Musset B, Schlichthorl G, Derst C, Karschin A et al. (2002) *Interaction with 14-3-3 proteins promotes functional expression of the potassium channels TASK-1 and TASK-3.* J Physiol **545**:13-26.

Ralf Schulein, Ricardo Hermosilla, Alexander Oksche, Marcel Dehe, Burkhard Wiesner, Gerd Krause and Walter Rosenthal. (1998) *A Dileucine Sequence and an Upstream Glutamate Residue in the Intracellular Carboxyl Terminus of the Vasopressin V2 Receptor Are Essential for Cell Surface Transport in COS.M6 Cells.* Molecular Pharmacology **54**:525-535.

Reddan JR. (1982) *Control of cell division in the ocular lens, retina and vitreous* (1982) Cell Biology of the Eye. New York Academic Press **299**:275.

Renkawek K, Stege G, Bosman G. (1999) *Dementia, gliosis and expression of the small heat shock proteins hsp27 and aBcrystallin in Parkinson's disease.* Neuroreport **10**:2273-2276.

Rice D. S., Northcutt G. M. and Kurschner C. (2001). *The Lnx family proteins function as molecular scaffolds for Numb family proteins.* Mol. Cell Neurosci. **18**:525-540.

Robben J.H., Sze M., Knoers N.V., P.M. Deen. (2006) *Rescue of vasopressin V2 receptor mutants by chemical chaperones: specificity and mechanism*. Mol. Biol. Cell **17**:379-386.

Robert J., E. Clauser, P.X. Petit, M.A. Ventura. (2005) *A novel C-terminal motif is necessary for the export of the vasopressin V1b/V3 receptor to the plasma membrane.* J.Bio.Chem. **280**(3):2300-8.

Robinson, M. S. (2004) *Adaptable adaptors for coated vesicles.* Trends Cell Biol. **14**:167-174.

Rodriguez, J. et al. (2005) *SFRP1 regulates the growth of retinal ganglion cell axons through the Fz2 receptor.* Nat. Neurosci. **8**:1301-1309.

Rohan D. Teasdale and Michael R. Jackson. (1996) *Signal-Mediated Sorting Of Membrane Proteins Between The Endoplasmic Reticulum And The Golgi Apparatus.* Annu. Rev. Cell Dev. Biol. **12**:27-54.

Rosenbluth, J. & Wissig, S. L. (1964) *The distribution of exogenous ferritin in toad spinal ganglia and the mechanism of its uptake by neurons. J. Cell Biol.* **23**:307-325.

Roth, T. F. & Porter, K. R. (1964) *Yolk protein uptake in the oocyte of the mosquito Aedes Aegypti. L. J. Cell Biol.* **20**:313-332.

Saito K, Chen M, Bard F, Chen S, Zhou H, Woodley D, Polischuk R, Schekman R, Wieland FT, Gleason ML, Serafini TA, Rothman JE. (1987) *The rate of bulk flow from the endoplasmic reticulum to the cell surface.* Cell, **50**:289-300.

Salahpour S., Angers S., J.F. Mercier,M. Lagace, S. Marullo,M. Bouvier. (2004) *Homodimerization of the beta2-adrenergic receptor as a prerequisite for cell surface targeting*. J. Biol. Chem. **279**:33390-33397.

Salmond R. J., Filby A., Qureshi I., Caserta S. and Zamoyska R. (2009). *T-cell receptor proximal signaling via the Src-family kinases, Lck and Fyn, influences T-cell activation, differentiation, and tolerance.* Immunol Rev. **228**:9-22.

Samali A, Orrenius S. (1998) *Heat shock proteins: regulators of stress response and apoptosis.* Cell Stress Chaperones **3**:228-236.

Sax CM, Piatigorsky J. (1994) *Expression of the a-crystallin/ small heat shock protein/molecular chaperone gene in the lens and other tissues.* Adv Enzymol Relat Areas Mol Biol **69**:155-201.

Schmidt AA. (2002) *Membrane transport: the making of a vesicle.* Nature **419**:347-9.

Schmitz J. E., Forman M. A., Lifton M. A., Concepcion O., Reimann K. A., Jr. Crumpacker C. S., Daley J. F., Gelman R. S. and Letvin N. L. (1998) *Expression of the CD8alpha beta-heterodimer on CD8(+) T lymphocytes in peripheral blood lymphocytes of human immunodeficiency virus and human immunodeficiency virus individuals.* Blood **92**:198-206.

Schutze M.P., Peterson P.A. and Jackson M.R. (1994) *An N-terminal doublearginine motif maintains type II membrane proteins in the endoplasmic reticulum.* Embo J. **13**:1696-1705.

Seifert, J.R. and Mlodzik, M. (2007) *Frizzled/PCP signalling: a conserved mechanism regulating cell polarity and directed motility.* Nat. Rev. Genet. **8**:126-138.

Shamie Das, Tekla D. Smith, Jayasri Das Sarma, Jeffrey D. Ritzenthaler, Jose Maza, Benjamin E. Kaplan, Leslie A. Cunningham, Laurence Suaud, Michael J. Hubbard, Ronald C. Rubenstein, and Michael Koval. (2009) *ERp29 Restricts Connexin43 Oligomerization in the Endoplasmic Reticulum.* Molecular Biology of the Cell. **20**:2593-2604.

Slusarski, D.C. (1997) *Interaction of Wnt and a Frizzled homologue triggers G-protein-linked phosphatidylinositol signalling.* Nature **390**:410-413.

Soetens O., De Craene J. O. and Andre B. (2001). *Ubiquitin is required for sorting to the vacuole of the yeast general amino acid permease, Gap1*. J. Biol. Chem. **276**:43949-43957.

Sollerbrant K., Raschperger E., Mirza M., Engstrom U., Philipson L., Ljungdahl P. O. and Pettersson R. F. (2003). *The Coxsackievirus and adenovirus receptor (CAR) forms a complex with the PDZ domain-containing protein ligand-ofnumb protein-X (LNX).* J. Biol. Chem. **278**:7439-7444.

Stagg SM, Gurkan C, Fowler DM, LaPointe P, Foss TR, Potter CS, Carragher B, Balch Yan Shan Ong, Bor Luen Tang, Li Shen Loo, and Wanjin Hong (2010) *p125A exists as part of the mammalian Sec13/Sec31 COPII subcomplex to facilitate ER-Golgi transport.* JBC.

Ste´phanie Simon, Magalie Michiel, Fe´riel Skouri-Panet, Jean Pierre Lechaire, Patrick Vicart, and Annette Tardieu (2007) *Residue R120 Is Essential for the Quaternary Structure and Functional Integrity of Human RB-Crystallin.* Biochemistry **4**: 9605-9614.

Stenmark H. (2009). *Rab GTPases as coordinators of vesicle traffic.* Nat. Rev. Mol. Cell Biol. **10**:513-525.

Takahashi S., Iwamoto N., Sasaki H., Ohashi M., Oda Y., Tsukita S. and Furuse M. (2009). *The E3 ubiquitin ligase LNX1p80 promotes the removal of claudins from tight junctions in MDCK cells.* J. Cell Science **122**:985-994.

Tao Y.X., Johnson, N.B., Segaloff, D.L. (2004) *Constitutive and agonist-dependent self-association of the cell surface human lutropin receptor.* J. Biol. Chem. **279**:5904-5914.

Tao Y.X. (2006) *Inactivating mutations of G protein-coupled receptors and diseases: structure–function insights and therapeutic implications.* Pharmacol. Ther. **111**:949-973.

Teasdale RD, Jackson MR (1996) *Signal-mediated sorting of membrane proteins between the endoplasmic reticulum and the Golgi apparatus.* Annu. Rev. Cell Dev. Biol. **12**:27-54.

Thomas, R.M., Nechamen, C.A., Mazurkiewicz, J.E., Muda, M., Palmer, S., Dias, J.A. (2007) *Follice-stimulating hormone receptor forms*

oligomers and shows evidence of carboxyl-terminal proteolytic processing. Endocrinology **148**:1987-1995.

Tsao P, Cao T, von Zastrow M (2001) *Role of endocytosis in mediating downregulation of G protein-coupled receptors.* Trends Pharmacol Science **22**:91-96.

Van Noort JM, van Sechel AC, Bajramovic JJ, el Ouagmiri M, Polman CH, Lassmann H, Ravid R. (1995) *The small heat-shock protein aB-crystallin as candidate auto antigen in multiple sclerosis.* Nature **375**:798-801.

Viard P, Butcher AJ, Halet G, Davies A, Nurnberg B, Heblich F & Dolphin AC. (2004) *PI3K promotes voltage-dependent calcium channel trafficking to the plasma membrane.* Nat Neurosci **7**:939-946.

Vicart P, Caron A, Guicheney P, Li Z, Prevost MC, Faure A, Chateau D, Chapon F, Tome F, Dupret JM, Paulin D, Fardeau M. (1999) *A missense mutation in the aB-crystallin chaperone gene causes a desmin-related myopathy.* Nat Genet **20**:92-93.

Vincent, M.J., Martin, A.S. and Compans, R.W. (1998) *Function of the KKXX motif in endoplasmic reticulum retrieval of a transmembrane protein depends on the length and structure of the cytoplasmic domain.* J. Biol. Chem. **273**:950-956.

Wang Y, Lauffer B, von Zastrow M, Kobilka B, Xiang Y (2007) *NSF regulates β2 –adrenoceptors trafficking and signaling in cardiomyocytes.* Mol Pharmacol **72**:429-439.

Watson P., Anna K. Townley, Pratyusha Koka, Krysten J. Palmer and David J. Stephens. (2006) *Sec16 Defines Endoplasmic Reticulum Exit Sites and is Required for Secretory Cargo Export in Mammalian Cells*. Traffic **7**:1678-1687.

WE (2006) *Structure of the Sec13/31 COPII coat cage.* Nature, **439**:234-238.

Weiss A. and Littman D. R. (1994). *Signal transduction by lymphocyte antigen receptors.* Cell **76**:263-274.

Whistler JL, Enquist J, Marley A (2002) *Modulation of postendocytic sorting of G protein-coupled receptors.* Science **297**:615-620.

Wilson D.W., Lewis M.J. and Pelham H.R. (1993) *pH-dependent binding of KDEL to its receptor in vitro.* J. Biol. Chem. **268**:7465–7468.

Woolf P.J., Linderman J.J. (2004) *An algebra of dimerization and its implications for G-protein coupled receptor signalling.* J. Theor. Biol. **229**:157-168.

Xiaoping Zhang, Chunmin Dong, Qiong J. Wu, William E. Balch and Guangyu Wu. (2011) *Di-acidic Motifs in the Membrane-distal C-termini Modulate the Transport of Angiotensin II Receptors from the Endoplasmic Reticulum to the Cell Surface.* J. Bio. Chem.

Yamamoto, A. et al. (2005) *Shisa promotes head formation through the inhibition of receptor protein maturation for the caudalizing factors, Wnt and FGF.* Cell **120**:223-235.

Yan Shan Ong, Bor Luen Tang, Li Shen Loo, and Wanjin Hong. (2010) *p125A exists as part of the mammalian Sec13/Sec31 COPII subcomplex to facilitate ER-Golgi transport.* JCB.

Yuan, H., Michelsen, K. and Schwappach, B. (2003) *14-3-3 Dimers probe the assembly status of multimeric membrane proteins.* Curr. Biol. **13**:638-646.

Yukari Okamoto and Sojin Shikano. (2010) *Phosphorylation-dependent C-Terminal binding of 14-3-3 proteins promotes cell surface expression of HIV co-receptor GPR15.* J.Bio.Chem. **10**:199-695.

Zheng D., Sun Y., Gu S., Ji C., Zhao W., Xie Y. and Mao Y. (2010). *LNX (Ligand of Numb-protein X) interacts with RhoC, both of which regulate AP-1- mediated transcriptional activation.* Mol. Biol. Rep. **37**:2431-2437.

JCS ePress online publication date 1 November 2011

Ligand of Numb proteins LNX1p80 and LNX2 interact with the human glycoprotein CD8α and promote its ubiquitylation and endocytosis

Massimo D'Agostino[1], Giusy Tornillo[1], Maria Gabriella Caporaso[1], Maria Vittoria Barone[2], Eric Ghigo[3], Stefano Bonatti[1,*] and Giovanna Mottola[1,*]

[1]Dipartimento di Biochimica e Biotecnologie Mediche, University of Naples 'Federico II', Via S. Pansini 5, 80131 Naples, Italy
[2]Dipartimento di Pediatria, European Laboratory For the Investigation of Food Induced Disease, University of Naples 'Federico II', Via S. Pansini 5, 80131 Naples, Italy
[3]URMITE, CNRS UMR6236-IRD 3R198, Université de la Méditerranée, 27 Bd Jean Moulin 13358 Marseille CEDEX 05, France
*Authors for correspondence (mottola@dbbm.unina.it; bonatti@dbbm.unina.it)

Accepted 13 June 2011
Journal of Cell Science 124, 1–12

doi: 10.1242/jcs.081224

Summary

E3 ubiquitin ligases give specificity to the ubiquitylation process by selectively binding substrates. Recently, their function has emerged as a crucial modulator of T-cell tolerance and immunity. However, substrates, partners and mechanism of action for most E3 ligases remain largely unknown. In this study, we identified the human T-cell co-receptor CD8 α-chain as binding partner of the ligand of Numb proteins X1 (LNX1p80 isoform) and X2 (LNX2). Both *LNX* mRNAs were found expressed in T cells purified from human blood, and both proteins interacted with CD8α in human HPB-ALL T cells. By using an in vitro assay and a heterologous expression system we showed that the interaction is mediated by the PDZ (PSD95-DlgA-ZO-1) domains of LNX proteins and the cytosolic C-terminal valine motif of CD8α. Moreover, CD8α redistributed LNX1 or LNX2 from the cytosol to the plasma membrane, whereas, remarkably, LNX1 or LNX2 promoted CD8α ubiquitylation, downregulation from the plasma membrane, transport to the lysosomes, and degradation. Our findings highlight the function of LNX proteins as E3 ligases and suggest a mechanism of regulation for CD8α localization at the plasma membrane by ubiquitylation and endocytosis.

Key words: CD8, E3 ligase, LNX protein, Endocytosis, Ubiquitylation

Introduction

The localization of transmembrane receptors at the plasma membrane (PM) is dynamically controlled by both the rate of delivery via the exocytic pathway and the rate of internalization and transport to the endosomes via endocytosis. Intrinsic protein-sorting signals and cellular machineries able to decode them regulate traffic along the two routes. Alteration in these mechanisms affects proper receptor function at the PM and is often correlated to pathologies (reviewed in Benado et al., 2009; Mellman and Nelson, 2008; Stenmark, 2009).

One of the sorting signals for proteins along the exo- and endocytic pathways is the ubiquitylation, a post-translational modification by which ubiquitin, a polypeptide of 76 amino acid residues, is covalently attached to lysine (Lys) residues of a substrate protein (Hershko and Ciechanover, 1992). Once thought to only mediate proteasomal degradation in the cytosol (Pickart and Fushman, 2004), ubiquitylation might also occur at the PM where it regulates protein internalization, at the trans-Golgi complex where it directs proteins to the late endosomes, and in endosomes to sort proteins to the multivesicular bodies (reviewed in Mukhopadhyay and Riezman, 2007; Piper and Luzio, 2007). In all these cases, it results in protein degradation into the lysosomes. The fate and the transport of the tagged substrate will depend on the Lys residue involved in the formation of ubiquitylation chains, as well as on the number of residues added. Single ubiquitin monomers can be attached to one or several Lys of a protein (mono- or multimonoubiquitylation, respectively). Ubiquitin itself possesses several Lys residues that can be used for the attachment of another ubiquitin molecule, allowing substrates to be modified with different types of ubiquitin chains (polyubiquitylation). Ubiquitylation occurs in a stepwise manner involving three enzymes: an ubiquitin-activating enzyme E1 is responsible for the attachment of free ubiquitin; a second ubiquitin-conjugating enzyme E2 receives it from E1; and a third ubiquitin ligase E3 catalyzes the final transfer of the ubiquitin from the E2 enzyme to the substrate. The specificity of the ubiquitylation process is determined by the E3 ligases, which are suggested to function as an adaptor to bind substrates selectively. More than 600 E3 ligases were found in the human proteome and were classified into two major groups, defined by the presence of either a HECT (homologous to the E6 associated protein C terminus) or a RING (really interesting new gene) domain as catalytic domain.

Recently, it has been emerging that E3 ligases play an important function in regulating T-cell tolerance and immunity (reviewed in Bhoj and Chen, 2009; Deshaies and Joazeiro, 2009; Gomez-Martin et al., 2008). For instance, the E3 ligase c-Cbl regulates T-cell receptor (TCR) activation by both degrading key signalling molecules such as PLCγ-1 (Jeon et al., 2004) and controlling TCR internalization and transport to the lysosomes (Naramura et al., 2002). Interestingly, the defective expression of

some E3 ligases has been related to the development of autoimmune diseases, such as encephalomyelitis, arthritis and autoimmune diabetes (Chiang et al., 2000; Gronski et al., 2004; Jeon et al., 2004). However, to date, our knowledge of the substrates, partners, biological functions and mechanism of action for most E3 ligases remains elusive.

The T-cell co-receptor CD8 is a type I transmembrane protein expressed as αα homodimer on the surface of intestinal T cells, γδ T cells, thymic T-cell precursors and NK cells, and as αβ heterodimer on thymocytes and peripheral T cells (Gangadharan and Cheroutre, 2004; Irie et al., 1995). The surface expression of CD8αβ heterodimer depends on the α-chain (Goldrath et al., 1997). Efficient surface expression of the α-chain requires its cytosolic C-terminal valine motif (C-TVM), a ligand of PDZ domains that modulate its delivery to the PM by sequentially interacting with GRASP65 and GRASP55 proteins (D'Angelo et al., 2009; Iodice et al., 2001). Required for the activation of cytotoxic T lymphocytes, CD8 stabilizes the interaction between the TCR on the surface of the lymphocytes and the class I major histocompatibility complex on antigen-presenting cells. Furthermore, it recruits the $p56^{lck}$ protein tyrosine kinase, bound to the cytosolic tail of its α-chain, to the vicinity of the TCR. As such, CD8 functions as coactivator, because Lck is a major proximal effector of the T cell activation cascade (Salmond et al., 2009; Weiss and Littman, 1994). Development of cytotoxic T lymphocytes was greatly reduced in mice lacking CD8α (Fung-Leung et al., 1991), and defects in CD8α and CD8β expression were shown to correlate with pathological conditions such as immunodeficiencies and Wiskott-Aldrich syndrome (de la Calle-Martin et al., 2001; Kawabata et al., 1996; Schmitz et al., 1998). How CD8 function is regulated at the PM and whether and how its impairment leads to immune diseases is still largely unknown.

In this study, we were looking for proteins that could modulate CD8α localization at the PM by using CD8α cytosolic tail as bait in a two-hybrid assay. We identified and characterized the interactions between CD8α and LNX1p80 and LNX2, which result in CD8α ubiquitylation, internalization in the endocytic pathway and degradation. We also demonstrated that LNX proteins are expressed in the same physiological context as CD8α and interact with it in human HPB-ALL T cells. Thus, our data strongly suggest that the E3 ubiquitin ligase activity of both LNX proteins is involved in the regulation of CD8α localization at the PM.

Results

CD8α binds the LNX proteins LNX2 and LNX1p80

In order to identify novel interacting-proteins involved in the regulation of CD8α intracellular trafficking, we performed a yeast two-hybrid screening using a human liver cDNA library and the CD8α cytosolic C-terminal tail as bait (Fig. 1A). Among

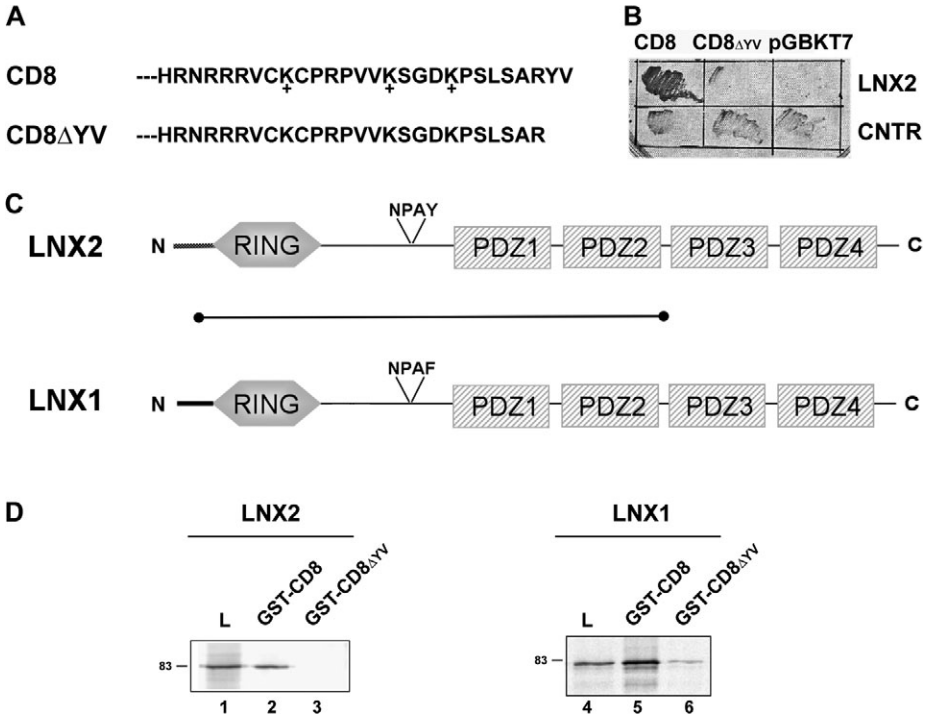

Fig. 1. Identification and characterization of LNX2 and LNX1p80 as interacting partners of CD8α. (**A**) Amino acid sequences of CD8α wild-type and ΔYV mutant cytosolic C-terminal tail used as baits in the two-hybrid assay. The + symbol indicates lysine residues where ubiquitin chains might be attached. (**B**) Identification of the N-terminal fragment of LNX2 by two-hybrid assay: the yeast colony expressing the N-terminal fragment was able to grow on a high-stringency selection plate when co-transformed with plasmid expressing the CD8α wild-type cytosolic tail. No growth was detected when either a control plasmid (pGBKT7, vector with the GAL4 DNA binding domain) or a plasmid expressing the ΔYV-mutated tail was co-transformed. CNTR represents yeast colony transfected with the vector expressing only the GAL4 activation domain, which grew at low extent in all the transformations. (**C**) Representation of LNX2 and LNX1p80. LNX proteins contain a RING finger domain, an NPAY or NPAF motif for interaction with Numb protein and four PDZ domains. The line underneath LNX2 indicates the fragment obtained by two-hybrid assay. (**D**) In vitro interaction between either LNX2 or LNX1p80 and the cytosolic tail of CD8α. Glutathione-Sepharose beads, loaded with GST fused to CD8α wild-type (lanes 2 and 5) or ΔYV mutant cytosolic tail (lanes 3 and 6), were incubated with LNX2 (lanes 2 and 3) or LNX1p80 (lanes 5 and 6) that had been labelled with [^{35}S]methionine and translated in vitro. Bound proteins were eluted from the beads and analyzed together with the loaded samples (L, lanes 1 and 4) by SDS-PAGE and autoradiography. Numbers on the left indicate the molecular mass (kDa).

positive clones, one contained a cDNA fragment encoding amino acids 56–451 of the LNX2 protein (Fig. 1B). LNX2 was initially identified as a ligand of the endocytic protein Numb (ligand of Numb protein X) (Dho et al., 1998; Rice et al., 2001). It was classified as a RING-type E3 ligase because it contains an N-terminal RING finger domain (Fig. 1C). However, it has been poorly characterized and its function as E3 ligase has never been addressed. In addition, it also contains four PDZ domains, presumably mediating protein–protein interactions. The cDNA fragment identified by the two-hybrid assay corresponded to the LNX2 N-terminal region including the RING finger domain, the NPAY motif for the interaction with Numb, and the first two PDZ domains (Fig. 1C). Interestingly, the interaction was disrupted when the PDZ ligand signal was removed from the bait by deletion of the terminal Tyr and Val residues from the C-TVM (CD8-ΔYV) (Fig. 1B), indicating that the binding between CD8α and LNX2 is strongly dependent on this signal.

To confirm the interaction between LNX2 and CD8α, *LNX2* cDNA was transcribed in vitro and translated. The radioactively labelled protein was incubated with either the CD8α cytosolic C-terminal tail or its ΔYV-mutant fused to GST (see Materials and Methods). The bound proteins were separated by SDS-PAGE and revealed by autoradiography. As shown in Fig. 1D, LNX2 associates in vitro with the cytosolic C-terminal tail of CD8α (Fig. 1D, lane 2), but not with its ΔYV mutant (Fig. 1D, lane 3).

LNX2 is closely related to the p80 isoform of LNX1, another member of the LNX protein family (Fig. 1C) (Dho et al., 1998; Rice et al., 2001). However, in contrast to LNX2, the function of LNX1p80 as E3 ligase has been partially explored (Kansaku et al., 2006; Takahashi et al., 2009). For these reasons, we decided to test whether LNX1 is also a CD8α binding protein. On the other hand, we were not surprised that this protein was not found in our two-hybrid assay because LNX1p80 is poorly expressed in human liver cells (Dho et al., 1998). As observed for LNX2, in vitro transcribed and translated LNX1p80 was also able to interact with the CD8α cytosolic C-terminal tail fused to GST (Fig. 1D, lane 5). The removal of the C-TVM from CD8α decreased the interaction (Fig. 1D, lane 6).

CD8α protein is usually present in T and NK cells, but whether LNX1p80 or LNX2 is expressed in the same cell type has never been described. Therefore, we purified a T- and NK-cell-enriched fraction from human blood (see Materials and Methods) and performed RT-PCR by using primers specific for mRNAs encoding LNX1p80 and LNX2. Both genes were efficiently

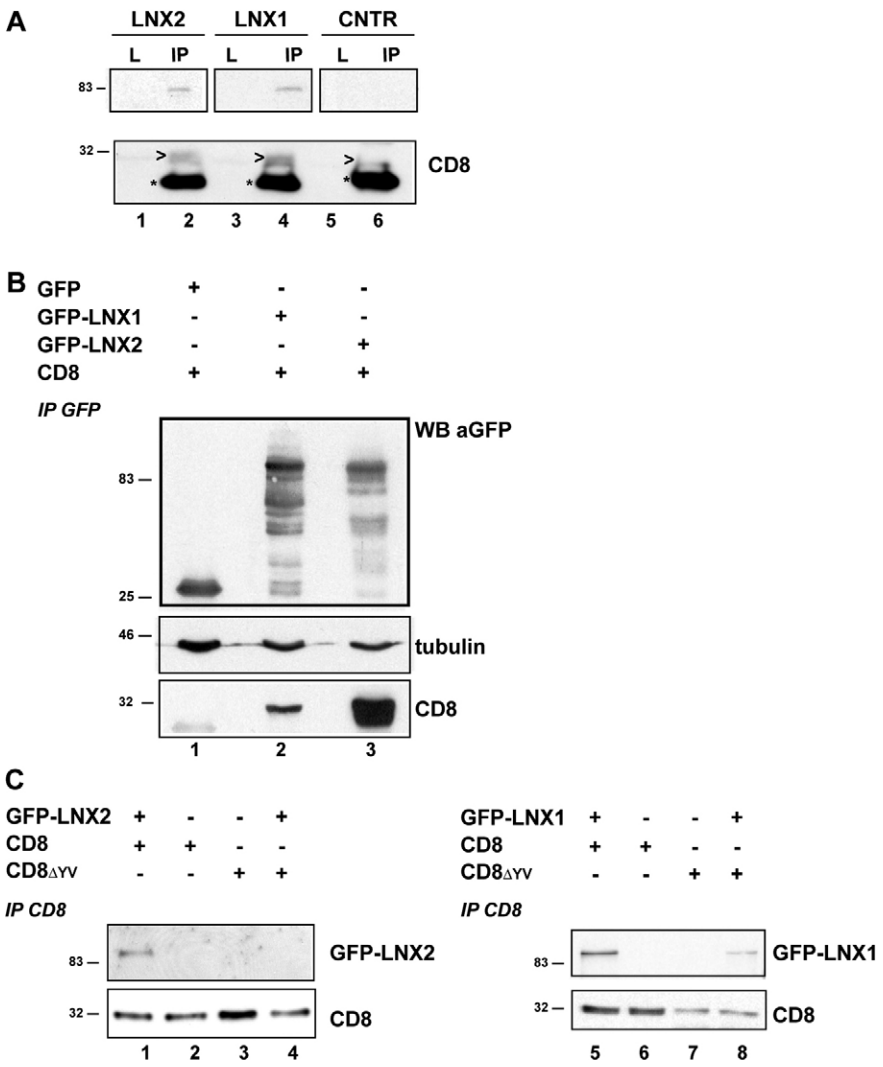

Fig. 2. In vivo interaction between CD8α and either LNX2 or LNX1p80. (**A**) CD8α was immunoprecipitated from human HPB-ALL T cells lysates and visualized by immunoblotting. A control experiment (CNTR) was also performed by using mouse IgGs. Arrowheads point to CD8α, which was immunoprecipitated with the mouse OKT-8 antibody (lanes 2 and 4), but not with mouse IgGs (lane 6). The presence of either LNX1p80 (lane 4) or LNX2 (lane 2) in the immunoprecipitates was revealed with specific antibodies. In the control, immunoblotting was performed by concomitantly using anti-LNX1p80 and anti-LNX2 antibodies (lane 6). Aliquots (100 µg) of total proteins were precipitated and loaded (L). However, CD8α and LNX proteins (lanes 1, 3 and 5) were poorly detectable in these fractions. Asterisks mark the immunoglobulin light chains revealed by immunoblotting. (**B**) CD8α was expressed with GFP (lane 1), GFP–LNX1p80 (lane 2) or GFP–LNX2 (lane 3) in HEK293 cells. After 24 hours of transfection, LNX proteins were immunoprecipitated from cell lysates by an anti-GFP antibody and visualized by immunoblotting. The presence of CD8α in the immunoprecipitates was revealed with anti-CD8α antibody. Lysates were also analysed by immunoblotting with anti-tubulin antibody as loading control. (**C**) CD8α or CD8α-ΔYV was expressed alone (lanes 2, 3, 6 and 7) or together with either GFP–LNX2 (lanes 1 and 4) or GFP–LNX1p80 (lanes 5 and 8) in HEK293 cells. After 24 hours of transfection, CD8α was immunoprecipitated from cell lysates and visualized by immunoblotting. The presence of LNX proteins in the precipitates was revealed with an anti-LNX2 (lanes 1–4) or anti-GFP (lanes 5–8) antibody. Numbers on the left indicate molecular mass (kDa).

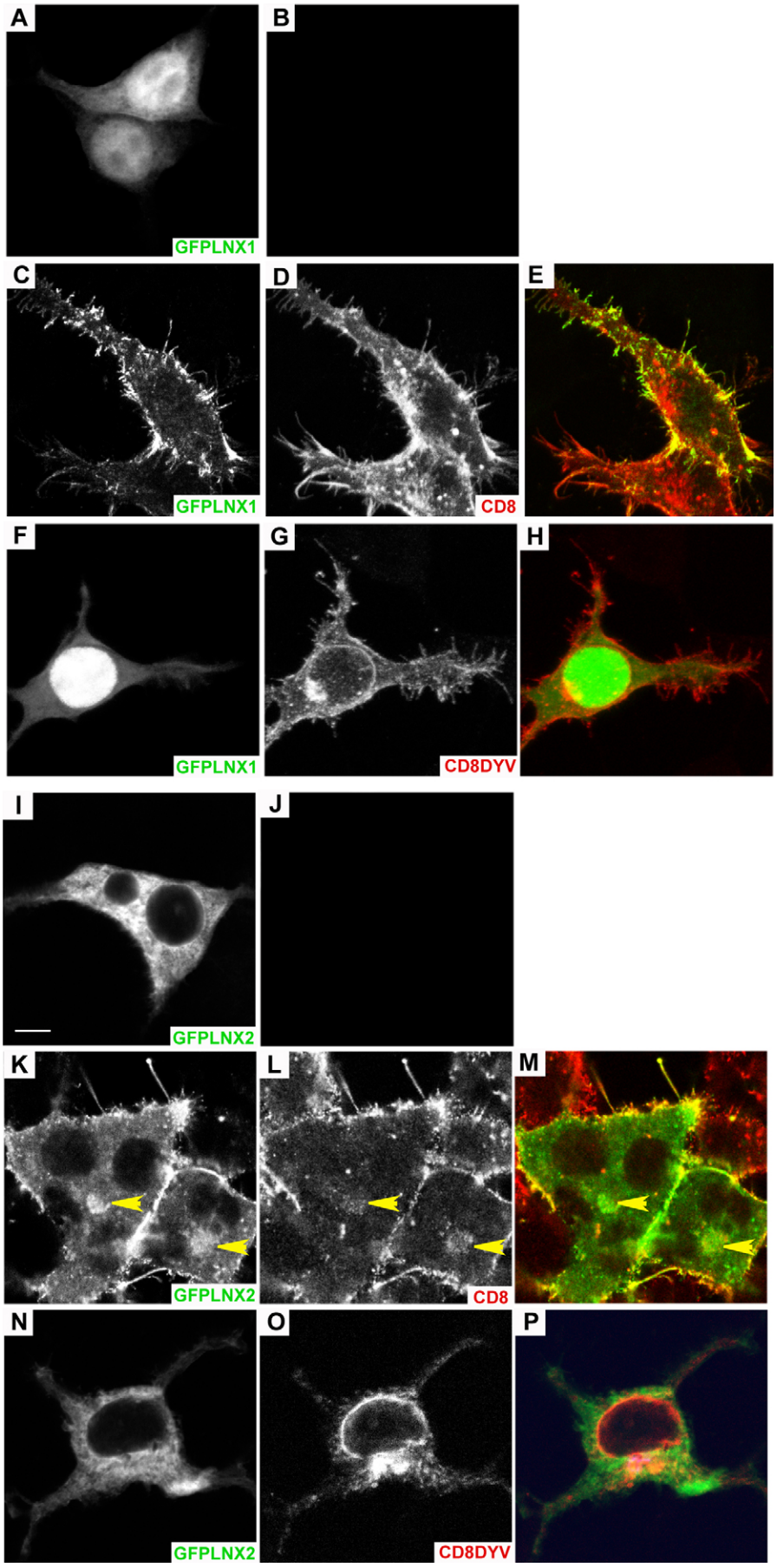

Fig. 3. CD8α expression leads to redistribution of LNX1p80 or LNX2 to the PM. (**A**–**P**) GFP–LNX1p80 (A–H; green,) or GFP–LNX2 (I–P; green,) was expressed in HEK293 cells alone (A–B,I–J) or together with either CD8α (C–E,K–M) or CD8-ΔYV (F–H,N–P). After 24 hours of transfection, cells were fixed and immunostained for CD8α (red). (E,H,M,P) Merged images. Yellow arrowheads in K–M indicate colocalization between CD8α and GFP–LNX2, presumably at the Golgi complex. A single confocal section is shown. Scale bars: 3 μm.

expressed in these cells (supplementary material Fig. S1, lanes 2 and 3). Unfortunately, the low level of endogenous CD8α protein did not allow us to co-immunoprecipitate LNX proteins from this cell fraction. Therefore, we used the human HPB-ALL T-cell line and demonstrated that, in these cells, LNX1p80 and LNX2 were pulled down by CD8α (Fig. 2A, lanes 2 and 4). Therefore, these data suggested that such interactions also occur in the physiological context of the T-cell co-receptor CD8α.

In order to further characterize this interaction, we decided to shift to a heterologous expression system that could be more easily handled and allow higher level of protein expression. Therefore, GFP and GFP-tagged versions of LNX1p80 and LNX2 were generated, transfected with CD8α in HEK293 cells, and then immunoprecipitated from cell lysates by an anti-GFP antibody. The presence of CD8α in the precipitates was tested by immunoblotting. Consistent with the previous data, GFP–LNX1p80 (Fig. 2B, lane 2) and GFP–LNX2 (Fig. 2B, lane 3), but not GFP (Fig. 2B, lane 1), were able to co-immunoprecipitate CD8α. Likewise, CD8α pulled-down GFP–LNX2 (Fig. 2C, lane 1) and GFP–LNX1p80 (Fig. 2C, lane 5). In the absence of CD8α C-TVM, LNX2 interaction was completely lost (Fig. 2C, lane 4), whereas LNX1p80 interaction decreased (Fig. 2C, lane 8). Therefore, CD8α in vitro and in vivo interacts with LNX2 and LNX1p80 and these interactions require its C-TVM.

It has been previously shown that LNX1p80 interacts with the junctional proteins JAM-4 via the second PDZ domain (Kansaku et al., 2006), and that the first two PDZ domains of LNX2 are required for binding to the cell surface coxsackievirus and adenovirus receptor (CAR) (Sollerbrant et al., 2003). To identify regions of LNX1p80 and LNX2 important for CD8α recognition, we generated a series of truncation mutants containing separately the distinct domains, and tested their ability to bind the CD8α cytosolic C-terminal tail or its ΔYV mutant fused to the GST (supplementary material Fig. S2). Consistent with the results of the two-hybrid assay, the N-terminal fragment of LNX2 including the RING domain, NPAY signal and the first two PDZ domains was able, although to a less extent, to interact with the CD8α tail in a YV-dependent manner. However, neither the RING domain nor the NPAY motif alone interacted in the same way as the full-length protein. By contrast, we found that the fragment including all four PDZ domains was indispensable for a proper interaction with CD8α. Indeed, the in vitro binding efficiency of the fragment was comparable to that observed for the full-length protein (supplementary material Fig. S2). Moreover, when expressed in HEK293 cells, it was co-immunoprecipitated by CD8α (supplementary material Fig. S3A, lane 3). Among the four PDZ domains of LNX2, the first two appeared to have a major role because they were sufficient, although to a lesser extent, to bind the CD8α tail in a YV-dependent manner. Similar results were overall observed for the LNX1p80 protein (supplementary material Figs S2 and S3A), thus fully confirming the observation that LNX1p80 and LNX2 interact with CD8α via their four PDZ domains.

CD8α expression leads to redistribution of LNX1p80 or LNX2 to the plasma membrane

To examine the intracellular localization of LNX1p80 and LNX2 in mammalian cells, GFP- or haemagglutinin (HA)-tagged constructs of the two proteins were generated and expressed in HEK293 cells. GFP–LNX1p80 exhibited both a cytosolic and nuclear localization (Fig. 3A), as previously described (Zheng et al., 2010). By contrast, GFP–LNX2 was exclusively cytosolic (Fig. 3I). Remarkably, we found that this localization was changed upon simultaneous expression of wild-type CD8α: both GFP–LNX1p80 (Fig. 3C–E) and GFP–LNX2 (Fig. 3K–M) appeared to redistribute at the PM, where CD8α localized as well. In addition, GFP–LNX2 was also recruited by CD8α at the Golgi complex (Fig. 3K–M, arrowheads). Interestingly, HA-tagged fragments containing the four PDZ domains of either LNX1p80 or LNX2 were also relocated at the PM upon CD8α coexpression (supplementary material Fig. S3Ba–c,Bg–i). Moreover, as expected, expression of the CD8-ΔYV did not have any effect on the intracellular distribution of all these chimeric proteins (Fig. 3F–H,N–P, and supplementary material Fig. S3Bd–f,Bj–l). These results confirmed that CD8α interacts in live cells with LNX1p80 and LNX2, strongly suggesting a functional role of these interactions.

LNX1p80 and LNX2 promote ubiquitylation of CD8α

Next, we examined whether LNX1p80 was able to ubiquitylate CD8α, as previously described for claudin (Takahashi et al., 2009), and whether also LNX2 was endowed of ubiquitylation activity. For this purpose, we coexpressed CD8α, HA-tagged ubiquitin, and GFP, GFP–LNX1p80 or GFP–LNX2 in HEK293 cells (Fig. 4). After 24 hours of transfection, CD8α was

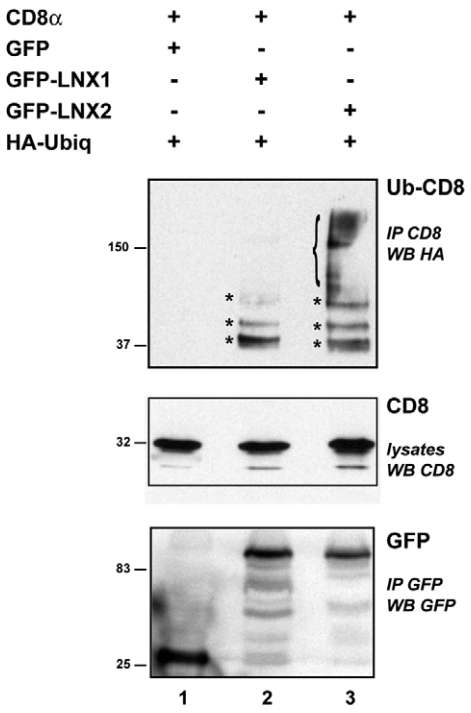

Fig. 4. LNX1p80- and LNX2-dependent ubiquitylation of CD8α. Plasmids expressing CD8α, HA-tagged ubiquitin and GFP, GFP–LNX1p80 or GFP–LNX2 were transiently co-transfected in HEK293 cells. After 24 hours, CD8α was immunoprecipitated from cell lysates and the ubiquitylated CD8α fraction (Ub-CD8) was revealed by immunoblotting with anti-HA antibody. Total lysates were also analyzed by immunoblotting with anti-CD8α antibody. GFP-tagged LNX proteins were immunoprecipitated from cell lysates with a GFP monoclonal antibody followed by immunoblotting with an anti-GFP polyclonal antibody. The asterisks indicate three ubiquitylated CD8α bands, which might correspond to monoubiquitylation of single, double and triple Lys residues. The parenthesis indicates the smear pattern and higher molecular weight ubiquitylated CD8α forms detected only in the presence of LNX2. Numbers on the left indicate molecular mass (kDa).

immunoprecipitated from cell lysates and its level of ubiquitylation was analyzed by immunoblotting with an anti-HA antibody (Fig. 4). In contrast to the control (Fig. 4, lane 1), a pattern of HA signal was found in the presence of the coexpressed GFP–LNX1p80 (Fig. 4, lane 2) or GFP–LNX2 (Fig. 4, lane 3). Because the cytosolic tail of CD8α has three

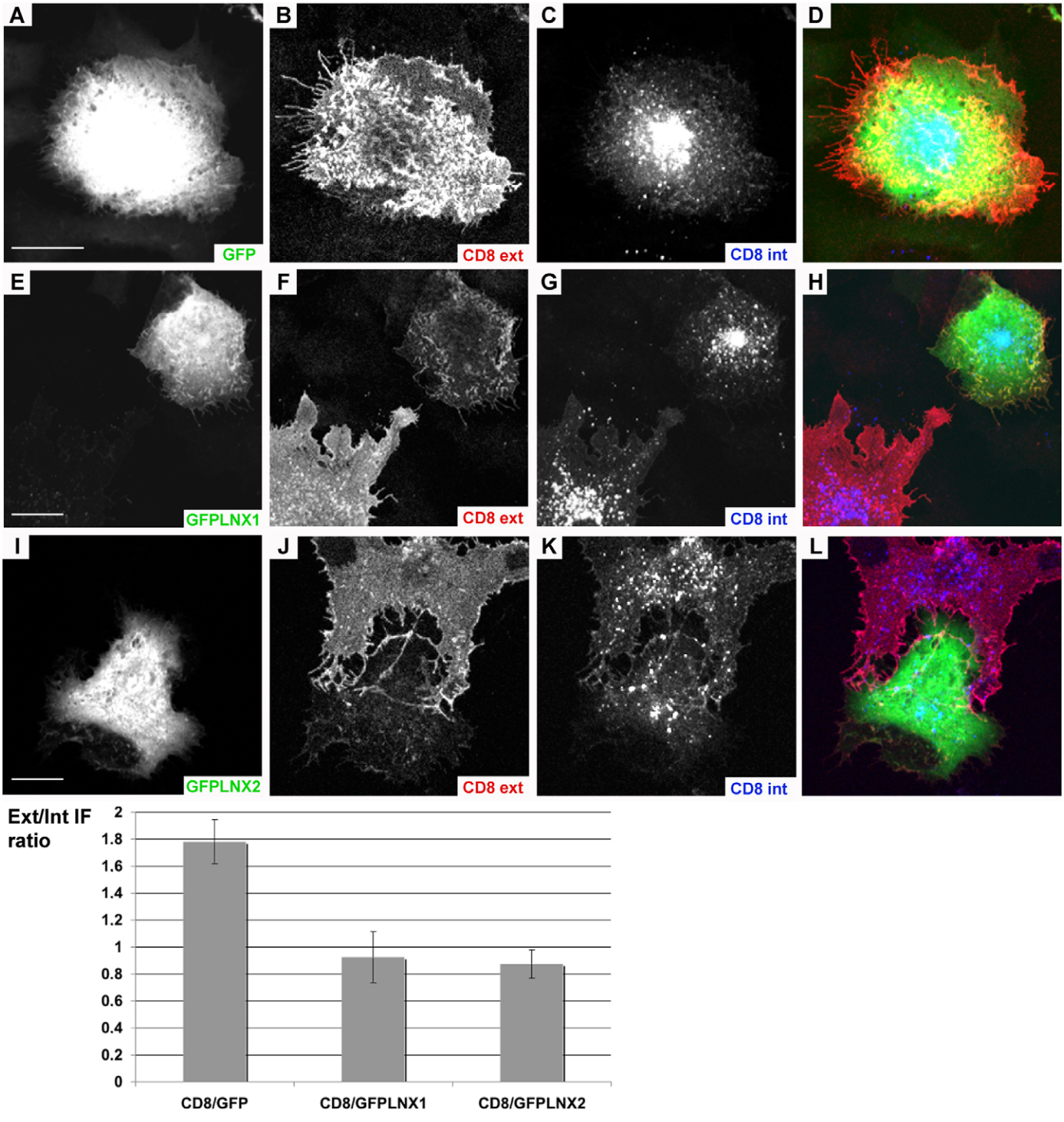

Fig. 5. High expression of GFP–LNX1p80 and GFP–LNX2, but not GFP, induces CD8α downregulation from the PM. (**A**–**L**) Huh-7 cells expressing, by the new transfection procedure, CD8α and a high level of GFP (A–D), GFP–LNX1p80 (E–H) or GFP–LNX2 (I–L) were fixed and analyzed by indirect immunofluorescence. (B,F,J) Cells stained for CD8α before permeabilization in order to label the CD8α fraction localized on the PM (CD8 ext; red). (C,G,K) Cells stained for CD8α after permeabilization to label the CD8α intracellular fraction (CD8 int; blue). (D,H,L) Merged images. Expression of GFP (A; green), GFP–LNX1p80 (E; green) or GFP–LNX2 (I; green) are shown. A single confocal section is shown. Histogram shows the ratio between the external and the internal CD8α fraction quantified for the three distinct co-transfections, as described in Materials and Methods. Scale bars: 3 μm.

potential Lys residues for ubiquitylation (Fig. 1A), the lower three bands visualized by the anti-HA antibody (Fig. 4, asterisks) might correspond to monoubiquitylation of single, double and triple Lys residues. Higher bands, possibly corresponding to polyubiquitylated forms, and a smear pattern were detected exclusively when CD8α was coexpressed with LNX2 (Fig. 4, lane 3). These results clearly indicated that both LNX1p80 and LNX2 induce CD8α ubiquitylation.

LNX1p80 and LNX2 control CD8α localization at the plasma membrane

While performing the immunofluorescence experiments on HEK293 cells, we observed a reduction in CD8α levels at the PM, which correlated with higher levels of LNX protein expression (data not shown). In order to verify and clearly visualize this effect, we decided to shift to the human hepatoma cell line Huh-7, because these cells are bigger and more spread than HEK293 cells, allowing a better visualization of protein localization at the PM. Moreover, we changed our transfection procedure by initially transfecting cells with GFP–LNX1p80, GFP–LNX2 or GFP and, only 24 hours later, with CD8α. This allowed us to accumulate high level of LNX proteins in cells before CD8α expression. Then, after a further 24 hours, cells were fixed and, before detergent permeabilization, directly treated with an anti-CD8 polyclonal antibody to uniquely label the CD8α fraction localized at the PM. Cells were then permeabilized and the CD8α intracellular fraction was revealed by using an anti-CD8 monoclonal antibody. As shown in Fig. 5,

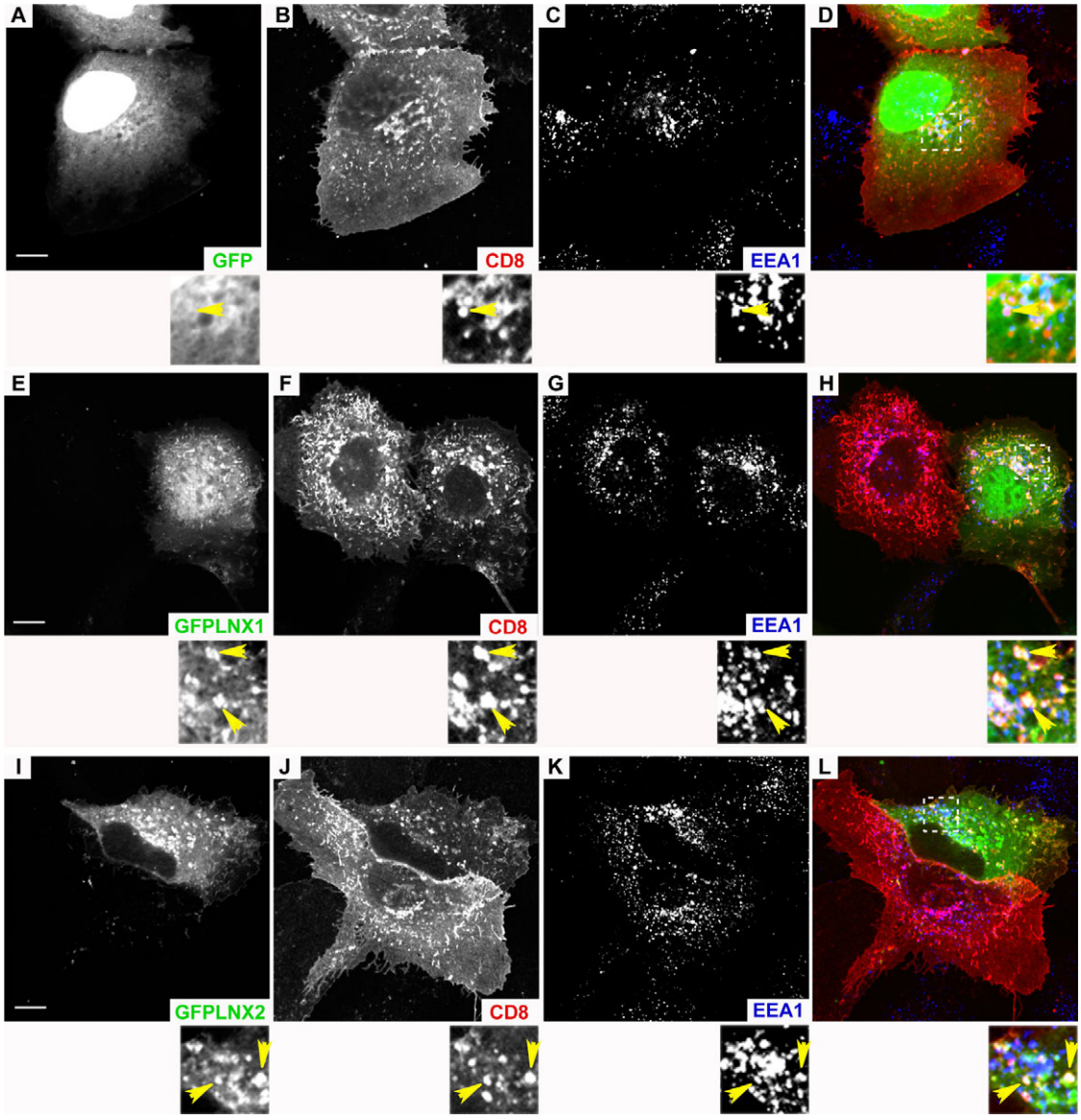

Fig. 6. High expression of GFP–LNX1p80 and GFP–LNX2, but not GFP, promotes CD8α transport to the early endosomes. (**A**–**L**) Huh-7 cells expressing, by the new transfection procedure, CD8α and a high level of GFP (A–D), GFP–LNX1p80 (E–H) or GFP–LNX2 (I–L) were fixed and stained for CD8α (B,F,J; red) and the early endosomes marker EEA1 (C,G,K; blue). (D,H,L) Merge images. Higher magnification of the cell areas marked by yellow lines are shown below. Arrowheads indicate endocytic structures where CD8α colocalizes with GFP–LNX1p80 or GFP–LNX2, but not GFP. Asterisks mark cells expressing only CD8α. A single confocal section is shown. Scale bars: 3 μm.

upon coexpression with either GFP–LNX1p80 (Fig. 5E–H) or GFP–LNX2 (Fig. 5I–L), the amount of CD8α localized at the PM was strongly decreased in comparison with cells expressing CD8α alone (Fig. 5F,J) or together with GFP (Fig. 5A–D). We quantified this decrease by measuring the ratio between the PM and intracellular signal detected by immunofluorescence (for quantification see Materials and Methods). As shown in Fig. 5, with respect to the control coexpression of CD8α and GFP, only ~50% of CD8α at the PM was detected upon GFP–LNX1p80 or GFP–LNX2 coexpression. Therefore, we concluded that LNX1p80 and LNX2 modulate CD8α protein levels at the PM.

LNX1p80 and LNX2 are involved in endocytic trafficking and degradation of CD8α

The monoubiquitylation of CD8α and its downregulation from the PM in the presence of LNX1p80 and LNX2 suggest that the two LNX proteins are involved in CD8α internalization and degradation. To address this hypothesis, Huh-7 cells expressing (by the new transfection procedure) a high level of GFP–LNX1p80, GFP–LNX2 or GFP together with CD8α were examined by immunofluorescence using antibodies specific for an early endosomes marker (EEA1) and a lysosomal marker (LAMP1), aiming to detect accumulation of CD8α into endocytic compartments. We found that in the presence of either GFP–LNX1p80 (Fig. 6E–H; Fig. 7E–H) or GFP–LNX2 (Fig. 6I–L; Fig. 7I–L), concomitantly to its downregulation from the PM, a fraction of CD8α accumulated in EEA1- or LAMP1-positive compartments (Fig. 6E–L; Fig. 7E–L, arrowheads). By contrast, in cells expressing only CD8α (Fig. 6F,J, asterisks) or CD8α together with GFP (Fig. 6A–D; Fig. 7A–D), CD8α was not significantly detected in endocytic structures and was mainly visualized at the PM. Similar results were also observed in HEK293 cells (data not shown).

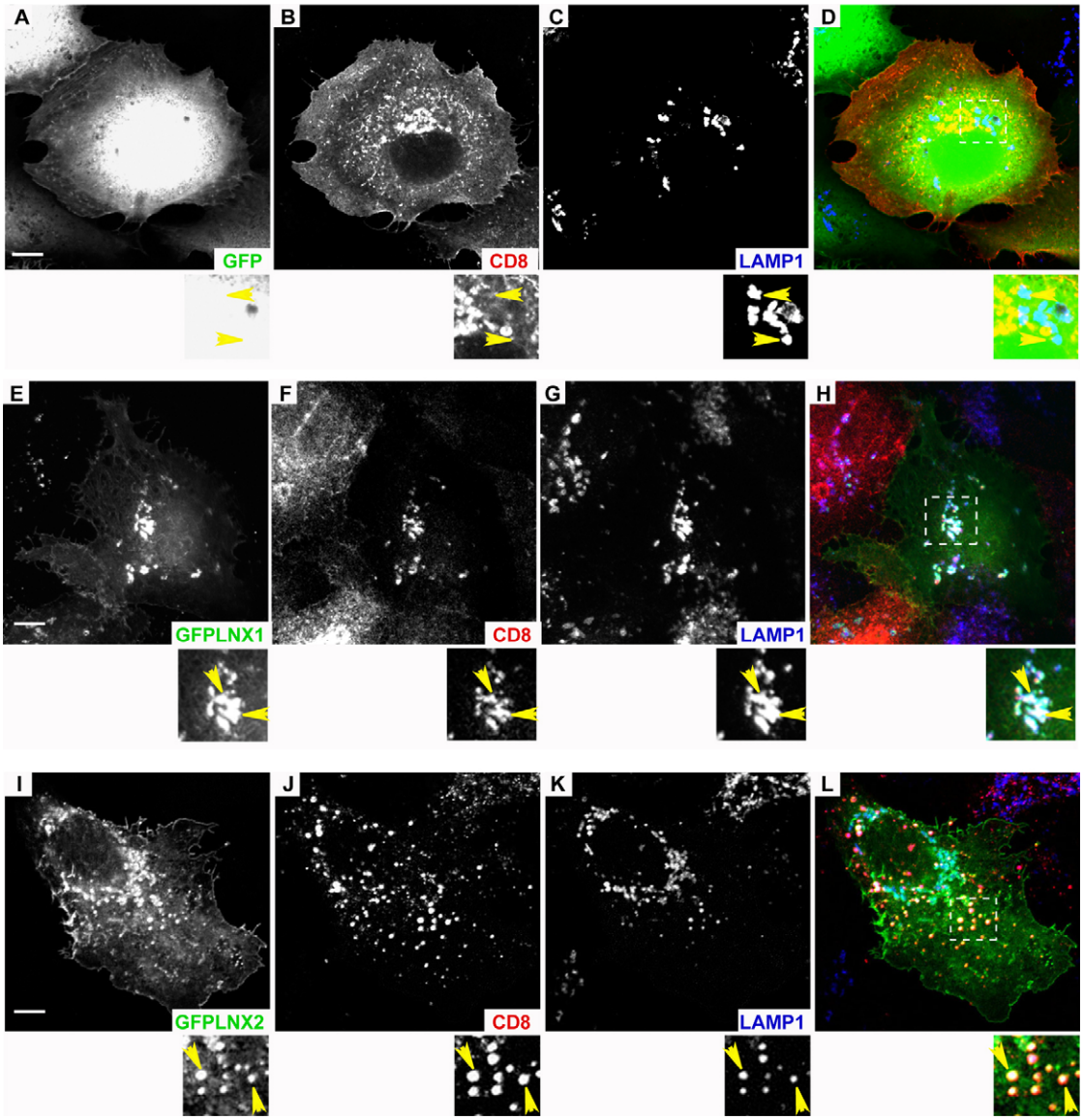

Fig. 7. High expression of GFP–LNX1p80 and GFP–LNX2, but not GFP, promotes CD8α transport to the lysosomes. (**A**–**L**) Huh-7 cells expressing, by the new transfection procedure, CD8α and a high level of GFP (A–D), GFP–LNX1p80 (E–H) or GFP–LNX2 (I–L) were fixed and stained for CD8α (B,F,J; red) and the lysosomal marker LAMP1 (C,G,K; blue). (D,H,L) Merged images. Higher magnification of the cell areas marked by yellow lines are shown below. Arrowheads indicate endocytic structures where CD8α colocalizes with GFP–LNX1p80 or GFP–LNX2, but not GFP. A single confocal section is shown. Scale bars: 3 µm.

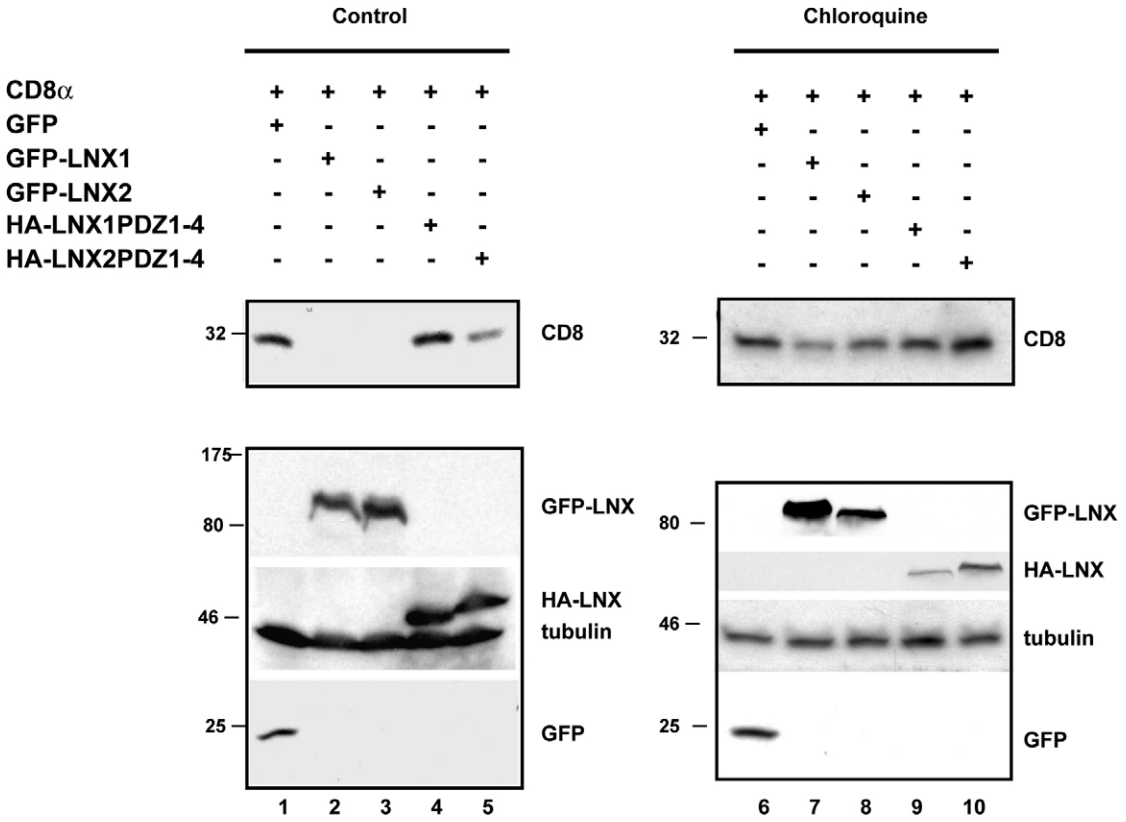

Fig. 8. Lysosomal degradation of CD8α protein in cells highly expressing either GFP–LNX1p80 or GFP–LNX2. HEK293 cells expressing, by the new transfection procedure, CD8α and a high level of GFP (lanes 1 and 6), GFP–LNX1p80 (lanes 2 and 7), GFP–LNX2 (lanes 3 and 8), HA-tagged PDZ1–PDZ4 domains of LNX1p80 (lanes 4 and 9) or LNX2 (lanes 5 and 10), were cultured with or without chloroquine treatment. After cell lysis, CD8α protein was immunoprecipitated from equal cell lysate aliquots and revealed by immunoblotting. In parallel, equal cell lysate aliquots were used to reveal GFP and GFP-tagged LNX proteins with an anti-GFP monoclonal antibody, and HA-tagged PDZ domains of LNX1p80 and LNX2 with an anti-HA monoclonal antibody. Lysates were also analyzed by immunoblotting with anti-tubulin antibody as loading control. Numbers on the left indicate molecular mass (kDa).

Next, we examined whether CD8α downregulation from the PM observed by the new transfection procedure resulted in co-receptor degradation. We have previously observed that simultaneous co-transfection of CD8α and GFP–LNX proteins induced CD8α ubiquitylation but did not decrease the total amount of CD8α in the whole lysate (Fig. 4, lanes 1–3). By contrast, Fig. 8 clearly shows that, on equal conditions of co-transfection efficiency and input protein level (tubulin protein level), when GFP–LNX1p80 (Fig. 8, lane 2) or GFP–LNX2 (Fig. 8, lane 3) are highly expressed, the total amount of CD8α in the whole lysate was smaller than that of GFP-coexpressing cells (Fig. 8, lane 1). Remarkably, such effect on CD8α was not observed when CD8α was coexpressed with the HA-tagged PDZ domains of either LNX1p80 or LNX2 (Fig. 8, lanes 4 and 5), which bind CD8α (supplementary material Figs S2 and S3), but lack the RING domains. To understand whether this degradation takes place in the lysosomes, we treated cells with the lysosome inhibitor chloroquine (Fig. 8, lanes 6–10) and found that the amount of CD8α in the whole lysate was significantly increased by this treatment (Fig. 8, lanes 7 and 8). These data strongly suggest that LNX1p80 and LNX2 induce CD8α transport to the lysosomes and subsequent degradation.

Discussion

In this paper, we identify and characterize the interaction between the human co-receptor CD8α and LNX1p80 and LNX2 proteins. Our data show that this binding occurs in vitro and in vivo and mutually affects the localization of each partner: CD8α recruits LNX1p80 or LNX2 from the cytosol to the PM, whereas, remarkably, LNX1p80 or LNX2 expression leads to CD8α ubiquitylation, downregulation from the PM, endocytosis and degradation.

RING-based E3 ligases confer specificity to ubiquitylation by recognizing target substrates. Accordingly, they have been linked to the control of many cellular processes and to multiple human diseases. However, despite their relevance, the functional characterization of most of them remains at a rudimentary stage (Deshaies and Joazeiro, 2009). The activity of LNX1 as E3 ubiquitin ligase has been recently explored. Two splicing variants of LNX1 exist, p70 and p80. The LNX1p70 binds the junctional protein JAM4, and its overexpression facilitates JAM4 endocytosis (Kansaku et al., 2006). On the other hand, LNX1p80 is an interacting partner of claudin-1 and promotes its ubiquitylation, removal from the tight junctions and transport to the lysosomes (Takahashi et al., 2009). Interestingly, LNX1 downregulation has been associated to gliomas (Chen et al., 2005) and to the cardiovascular Kawasaki infectious disease (Burgner et al., 2009), indicating its indispensable relevance for the proper functionality of distinct tissues and organs. In contrast to LNX1, LNX2 has been poorly studied and the only interacting protein so far identified was the cell surface coxsackievirus and adenovirus receptor (CAR)

(Mirza et al., 2006). No information is available to date on whether LNX2 behaves, similarly to LNX1, as an E3 ubiquitin ligase in mammalian cells. Here, we shed much light on the function of both LNX proteins: we demonstrate that they are expressed in human T lymphocytes and we identify an important novel partner for them, the human TCR co-receptor CD8α. This finding suggests that LNX proteins play a role in the regulation of T-cell tolerance and immunity, similarly to the E3 ligase c-Cbl, which also has a RING finger domain (Jeon et al., 2004; Naramura et al., 2002). Future work will test this interesting hypothesis.

Although the anterograde transport of CD8α and β chains along the exocytic pathway has been described (D'Angelo et al., 2009; Erra et al., 1999; Goldrath et al., 1997; Pascale et al., 1992), whether and how CD8 localization at PM is regulated by endocytic trafficking and which signals and cellular machineries are involved are so far largely unknown. The identification of the LNX ubiquitin ligases as interacting proteins of CD8α, their redistribution at the PM upon CD8α expression, and the effect of LNX protein expression on CD8α localization and expression can help answer these questions and help in understanding how impairment of CD8 function and localization at the PM might lead to immune diseases. It will also be interesting to investigate whether and how LNX proteins regulate the localization of the CD8 αβ heterodimer.

Despite the strong similarity between LNX1p80 and LNX2 structure and function, potentially interesting differences might distinguish them. In contrast to LNX1p80, LNX2 is recruited by CD8α also to the Golgi complex; its interaction is more severely dependent on the C-TVM of CD8α, and LNX2 expression also induces a smear pattern of ubiquitylation, which might correspond to CD8α polyubiquitylated forms. Intriguingly, although mono- or multimonoubiquitylation has been notably involved in endocytosis (Mukhopadhyay and Riezman, 2007), polyubiquitylation has also been associated with direct sorting from the Golgi to the vacuole of the yeast protein Gap1 (Soetens et al., 2001). Therefore, LNX2 might be also involved in the regulation of CD8α transport to, through, or from the Golgi complex, which has already been shown to be strongly dependent on the C-TVM of the co-receptor (D'Angelo et al., 2009). Further work is required to verify this hypothesis.

In conclusion, our results identify two major interacting partners of the human co-receptor CD8α, providing the first link between the possible regulation of the function of CD8α at the PM of lymphocytes and ubiquitylation, endocytosis and lysosomal degradation.

Materials and Methods

Reagents

All of the culture reagents were obtained from Sigma-Aldrich (Milan, Italy). The solid chemical and liquid reagents were obtained from E. Merck (Darmstadt, Germany), Farmitalia Carlo Erba (Milan, Italy), Serva Feinbiochemica (Heidelberg, Germany), Delchimica (Naples, Italy) and BDH (Poole, United Kingdom). The radiochemicals were obtained from Perkin Elmer (Bruxelles, Belgium). Protein A-Sepharose CL-4B and the enhanced chemiluminescence reagents were from Amersham Biosciences (Milan, Italy).

Antibodies

The following antibodies were used: the OKT8 mouse anti-CD8α monoclonal antibody from Ortho (Raritan, NJ); the N1 mouse anti-CD8α monoclonal antibody and rabbit anti-CD8α polyclonal antibody from M. Jackson (Martire et al., 1996); rabbit anti-LNX1 antibody (Kansaku et al., 2006); rabbit and mouse anti-GFP and anti-HA antibodies (Santa Cruz Biotechnology); mouse anti-EEA1 monoclonal antibody (BD Transduction Laboratories, Lexington, KY); mouse anti- CD7107a (LAMP1) monoclonal antibody (Biolegend, San Diego, CA); peroxidase-conjugated anti-mouse and anti-rabbit IgG (Sigma-Aldrich, Milan, Italy); and Texas-Red-conjugated anti-mouse IgG and FITC-conjugated anti-rabbit IgG (Jackson ImmunoResearch Laboratories, West Grove, PA).

Antibody production

A polyclonal antiserum against LNX2 was generated by immunizing rabbits with GST fused to the first 50 amino acids of LNX2, which are specific for LNX2 and not conserved in LNX1p80. The antibody was affinity-purified as described (Nielsen et al., 2000) and its ability to recognize LNX2, but not LNX1p80, was verified by western blot analysis of extracts from cells transfected either with GFP–LNX1p80 or GFP–LNX2.

Yeast two-hybrid assay

In order to construct the bait vector, the cDNA fragment encoding the wild-type or ΔTY mutant C-terminal tail of CD8α was amplified by PCR and subcloned in the vector pGBKT7 (Clontech). The vector expressing the wild-type CD8α C-terminal tail was used to screen a human liver cDNA library made in the pGAD10 vector (Clontech) using the *Saccharomyces cerevisiae* strain AH109. The transformants were plated on synthetic medium lacking histidine, leucine, and tryptophan. His+ colonies were transferred onto nitrocellulose filters and assayed for β-galactosidase activity. His+ and *lacZ*+ colonies were indicative of positive interaction. cDNA from positive clones was extracted, purified and sequenced. The recovered library plasmids were then tested for interaction with CD8α tail by co-transformation with the vectors pGBKT7, pGBKT7-CD8α or pGBKT7-CD8α−ΔTY in *S. cerevisiae* strain AH109. To quantify the interactions, the β-galactosidase assay was again used.

cDNA cloning and plasmid construction

The expression vector FLTRβT8 for wild-type CD8α and CD8α-ΔYV (Iodice et al., 2001; Mottola et al., 2000) and HA-ubiquitin (Mauro et al., 2006) have been previously described. cDNAs encoding LNX1p80 (ID 4995278) and LNX2 (ID 5541168) were obtained from I.M.A.G.E. Consortium. GFP–LNX1p80 and GFP–LNX2 expression vectors were generated by PCR and subcloning of *LNX1p80* and *LNX2* cDNAs in the pEGFP-N1 vector (Clontech).

For in vitro binding assays, GST fused to wild-type or ΔYV-mutant CD8α were expressed using pGEX-6P-1 (Pharmacia Biotech.). LNX1p80, LNX2 and all their truncated forms were subcloned in the expression vector pcDNA3 (Clontech). The following *LNX1p80* cDNA fragments were expressed for the in vitro binding assay shown in supplementary material Fig. S1: RING-NPAF (1–760 bp); RING (1–309 bp); NPAF (309–760 bp); PDZ(1–4) (760–2187 bp); PDZ(1–2) (760–1415 bp); PDZ(3–4) (1480–2187 bp); PDZ(1) (760–1074 bp), PDZ(2) (1114–1415 bp).

The following *LNX2* cDNA fragments were expressed for the in vitro binding assay shown in supplementary material Fig. S1: RING-NPAY (1–666 bp); RING (1–340 bp); NPAY (510–666 bp); PDZ(1–4) (637–2073 bp); PDZ(1–2) (682–1386 bp); PDZ(3–4) (1378–2073 bp); PDZ(1) (682–983 bp), PDZ(2) (961–1386 bp).

In vitro binding assay

LNX1p80 or LNX2 proteins were translated in vitro and labelled with ^{35}S-methionine using the TnT^{R} coupled reticulocyte lysate system (Promega). 10 µl of the full-length LNX proteins or fragments were incubated with 30 µl of glutathione-Sepharose beads loaded with GST or GST fused to wild-type or ΔYV-mutant CD8α. Bound proteins were eluted from the beads and analysed by SDS-PAGE and autoradiography. In all the GST-pull down experiments, the loading control (L) represents 20% of the whole amount of in vitro translated proteins used for incubation.

Cell culture, transfection and immunofluorescence

Human embryonal kidney HEK293 and human hepatoma Huh-7 cells were routinely grown at 37℃ in Dulbecco's modified essential medium (DMEM), containing 10% foetal bovine serum (FBS). HPB-ALL T cells were cultured in RPMI 1640, containing 15% FBS.

HEK293 and Huh-7 cells were transfected by using FuGene 6.0 (Roche) according to the manufacturer's instructions. The effect of CD8α expression on LNX protein localization was obtained by simultaneous co-transfection of CD8α and LNX protein expression vectors and, 24 hours later, cell fixation or lysis. To observe the effect of LNX protein expression on CD8α localization and protein level, cells were initially transfected with LNX protein expression vectors in order to allow accumulation of LNX proteins and, 24 hours later, transfected a second time with CD8α expression vectors. Then, after a further 24 hours, they were either lysed or fixed.

Indirect immunofluorescence was performed as previously described (Mottola et al., 2000). Single confocal images were acquired at 63× and 100× magnification on a Meta Zeiss Confocal Microscope (Carl Zeiss, Jena, Germany).

To separately stain CD8α protein on either cell surface or intracellular membranes, cells were incubated after fixation with the rabbit anti-CD8α polyclonal antibody, then permeabilized and incubated with the mouse anti-CD8α

monoclonal antibody (Mottola et al., 2000). Two distinct secondary antibodies allow separately visualizing the two fractions. Then, in order to measure the ratio between levels of PM and intracellular CD8α, the immunofluorescence intensity in the two channels was measured by using Adobe Photoshop and NIH ImageJ Biophotonic programs. For each co-transfection, 15 cells were considered for quantification. The results are given as mean ± s.d.

Preparation of cell extracts, immunoprecipitation SDS-PAGE and western immunoblotting

Cells were lysed with 10 mM Tris-HCl pH 7.4, 150 mM NaCl, 1 mM EDTA pH 8.0, and 1% Triton X-100. For all the experiments on transfected HEK293, 6×10^6 cells were lysed and used for each co-immunoprecipitation. For the experiment on HPB-ALL cells, 100×10^6 cells were used for each co-immunoprecipitation. Immunoprecipitation was performed by overnight incubation with OKT-8, a conformation-sensitive antibody anti-CD8α, followed by addition of Protein A-Sepharose beads (Pharmacia). The immunoprecipitated pellets were washed, treated for SDS-PAGE and resolved on a 10% polyacrylamide gel. For each experiment, aliquots of the lysate (100 µg total protein per aliquot) were also precipitated with acetone and treated for SDS-PAGE. Next, proteins were transferred to nitrocellulose filters, which were then incubated with primary antibodies diluted in blocking buffer (5% non-fat dry milk, 0.1% Tween-20 in PBS), followed by peroxidase-conjugated secondary antibodies. For anti-LNX1p80 and anti-LNX2 antibodies, western blot was performed in PBS containing 1% BSA. After washing, bound antibodies were detected by enhanced chemiluminescence (Amersham Biosciences).

CD8α degradation was detected by previously treating cells with or without 90 µM chloroquine for 16 hours.

Preparation of human T cells

Peripheral blood mononuclear cells were isolated from leukopacks (Etablissement Français du Sang) by Ficoll gradient (MSL, Eurobio). T and NK cells were then isolated by removing monocytes with $CD14^+$ columns as recommended by the manufacturer (Miltenyi Biotec).

Real time RT-PCR

Real time reverse-transcription PCR was performed as previously described (Ben Amara et al., 2010). Total RNA was extracted from the T-cell-enriched fraction and reverse transcribed using the MMLV-RT kit according to the manufacturer's protocol (Invitrogen). Forward and reverse primers were designed with the free web software Primer3.

The following primers were used: For human LNX1: forward 5′-GGAATTACCACGGTGCTTGTAT-3′, reverse 5′-TGTATGCTGGTGTTCCTTCAAC-3′; expected PCR fragment length, 154 bp. For human LNX2: forward 5′-TCTTCATAAACGGGACTCTGGT-3′, reverse 5′-GCTGCTATGATTTCCTGCTTCT-3′; expected PCR fragment length 291 bp. For human β-actin: forward 5′-GGAAATCGTGCGTGACATTA-3′, reverse 5′-AGGAAGGAAGGCTGGAAGAG-3′; expected PCR fragment length: 309 bp.

Real time PCR was performed using the Applied Biosystem 7900HT Fast real-time PCR system according to the manufacturer's recommendations. The experiments were performed in triplicate.

Acknowledgements

We thank Giuliana De Luca, Luisa Iodice and Alessandro Sorrentino for participating in the initial steps of the work; Cecilia Bucci for helping to set up the two-hybrid assay and critical reading of the manuscript; A. Leonardi for generously providing the HA-ubiquitin construct; André Le Bivic for temporary hospitality in his laboratory; the group of Eric Ghigo and Jean-Louis Mege for technical support; and Massimo Mallardo for helpful discussion and critical reading of the manuscript. We hereby declare that none of the authors have a financial interest related to this work.

Funding

This work was supported by grants from Ministero Università Ricerca Scientifica e Tecnologica to S.B.; and from Telethon Italia [grant number GGP09029].

Supplementary material available online at
http://jcs.biologists.org/lookup/suppl/doi:10.1242/jcs.081224/-/DC1

References

Ben Amara, A., Ghigo, E., Le Priol, Y., Lepolard, C., Salcedo, S. P., Lemichez, E., Bretelle, F., Capo, C. and Mege, J. L. (2010). Coxiella burnetii, the agent of Q fever, replicates within trophoblasts and induces a unique transcriptional response. *PLoS One* **5**, e15315.

Benado, A., Nasagi-Atiya, Y. and Sagi-Eisenberg, R. (2009). Protein trafficking in immune cells. *Immunobiology* **214**, 403-421.

Bhoj, V. G. and Chen, Z. J. (2009). Ubiquitylation in innate and adaptive immunity. *Nature* **458**, 430-437.

Burgner, D., Davila, S., Breunis, W. B., Ng, S. B., Li, Y., Bonnard, C., Ling, L., Wright, V. J., Thalamuthu, A., Odam, M. et al. (2009). A genome-wide association study identifies novel and functionally related susceptibility Loci for Kawasaki disease. *PLoS Genet* **5**, e1000319.

Chen, J., Xu, J., Zhao, W., Hu, G., Cheng, H., Kang, Y., Xie, Y. and Lu, Y. (2005). Characterization of human LNX, a novel ligand of Numb protein X that is downregulated in human gliomas. *Int. J. Biochem Cell Biol.* **37**, 2273-2283.

Chiang, Y. J., Kole, H. K., Brown, K., Naramura, M., Fukuhara, S., Hu, R. J., Jang, I. K., Gutkind, J. S., Shevach, E. and Gu, H. (2000). Cbl-b regulates the CD28 dependence of T-cell activation. *Nature* **403**, 216-220.

D'Angelo, G., Prencipe, L., Iodice, L., Beznoussenko, G., Savarese, M., Marra, P., Di Tullio, G., Martire, G., De Matteis, M. A. and Bonatti, S. (2009). GRASP65 and GRASP55 sequentially promote the transport of C-terminal valine-bearing cargos to and through the Golgi complex. *J. Biol. Chem.* **284**, 34849-34860.

de la Calle-Martin, O., Hernandez, M., Ordi, J., Casamitjana, N., Arostegui, J. I., Caragol, I., Ferrando, M., Labrador, M., Rodriguez-Sanchez, J. L. and Espanol, T. (2001). Familial CD8 deficiency due to a mutation in the CD8 alpha gene. *J. Clin. Invest.* **108**, 117-123.

Deshaies, R. J. and Joazeiro, C. A. (2009). RING domain E3 ubiquitin ligases. *Annu. Rev. Biochem* **78**, 399-434.

Dho, S. E., Jacob, S., Wolting, C. D., French, M. B., Rohrschneider, L. R. and McGlade, C. J. (1998). The mammalian numb phosphotyrosine-binding domain. Characterization of binding specificity and identification of a novel PDZ domain-containing numb binding protein, LNX. *J. Biol. Chem.* **273**, 9179-9187.

Erra, M. C., Iodice, L., Lotti, L. V. and Bonatti, S. (1999). Cell fractionation analysis of human CD8 glycoprotein transport between endoplasmic reticulum, intermediate compartment and Golgi complex in tissue cultured cells. *Cell Biol. Int.* **23**, 571-577.

Fung-Leung, W. P., Schilham, M. W., Rahemtulla, A., Kundig, T. M., Vollenweider, M., Potter, J., van Ewijk, W. and Mak, T. W. (1991). CD8 is needed for development of cytotoxic T cells but not helper T cells. *Cell* **65**, 443-449.

Gangadharan, D. and Cheroutre, H. (2004). The CD8 isoform CD8alphaalpha is not a functional homologue of the TCR co-receptor CD8alphabeta. *Curr. Opin. Immunol* **16**, 264-270.

Goldrath, A. W., Hogquist, K. A. and Bevan, M. J. (1997). CD8 lineage commitment in the absence of CD8. *Immunity* **6**, 633-642.

Gomez-Martin, D., Diaz-Zamudio, M. and Alcocer-Varela, J. (2008). Ubiquitination system and autoimmunity: the bridge towards the modulation of the immune response. *Autoimmun Rev.* **7**, 284-290.

Gronski, M. A., Boulter, J. M., Moskophidis, D., Nguyen, L. T., Holmberg, K., Elford, A. R., Deenick, E. K., Kim, H. O., Penninger, J. M., Odermatt, B. et al. (2004). TCR affinity and negative regulation limit autoimmunity. *Nat. Med.* **10**, 1234-1239.

Hershko, A. and Ciechanover, A. (1992). The ubiquitin system for protein degradation. *Annu. Rev. Biochem.* **61**, 761-807.

Iodice, L., Sarnataro, S. and Bonatti, S. (2001). The carboxyl-terminal valine is required for transport of glycoprotein CD8 alpha from the endoplasmic reticulum to the intermediate compartment. *J. Biol. Chem.* **276**, 28920-28926.

Irie, H. Y., Ravichandran, K. S. and Burakoff, S. J. (1995). CD8 beta chain influences CD8 alpha chain-associated Lck kinase activity. *J. Exp. Med.* **181**, 1267-1273.

Jeon, M. S., Atfield, A., Venuprasad, K., Krawczyk, C., Sarao, R., Elly, C., Yang, C., Arya, S., Bachmaier, K., Su, L. et al. (2004). Essential role of the E3 ubiquitin ligase Cbl-b in T cell anergy induction. *Immunity* **21**, 167-177.

Kansaku, A., Hirabayashi, S., Mori, H., Fujiwara, N., Kawata, A., Ikeda, M., Rokukawa, C., Kurihara, H. and Hata, Y. (2006). Ligand-of-Numb protein X is an endocytic scaffold for junctional adhesion molecule 4. *Oncogene* **25**, 5071-5084.

Kawabata, K., Nagasawa, M., Morio, T., Okawa, H. and Yata, J. (1996). Decreased alpha/beta heterodimer among CD8 molecules of peripheral blood T cells in Wiskott-Aldrich syndrome. *Clin. Immunol Immunopathol* **81**, 129-135.

Martire, G., Mottola, G., Pascale, M. C., Malagolini, N., Turrini, I., Serafini-Cessi, F., Jackson, M. R. and Bonatti, S. (1996). Different fate of a single reporter protein containing KDEL or KKXX targeting signals stably expressed in mammalian cells. *J. Biol. Chem.* **271**, 3541-3547.

Mauro, C., Pacifico, F., Lavorgna, A., Mellone, S., Iannetti, A., Acquaviva, R., Formisano, S., Vito, P. and Leonardi, A. (2006). ABIN-1 binds to NEMO/IKKgamma and co-operates with A20 in inhibiting NF-kappaB. *J. Biol. Chem.* **281**, 18482-18488.

Mellman, I. and Nelson, W. J. (2008). Coordinated protein sorting, targeting and distribution in polarized cells. *Nat. Rev. Mol. Cell Biol.* **9**, 833-845.

Mirza, M., Hreinsson, J., Strand, M. L., Hovatta, O., Soder, O., Philipson, L., Pettersson, R. F. and Sollerbrant, K. (2006). Coxsackievirus and adenovirus receptor (CAR) is expressed in male germ cells and forms a complex with the differentiation factor JAM-C in mouse testis. *Exp. Cell Res.* **312**, 817-830.

Mottola, G., Jourdan, N., Castaldo, G., Malagolini, N., Lahm, A., Serafini-Cessi, F., Migliaccio, G. and Bonatti, S. (2000). A new determinant of endoplasmic reticulum localization is contained in the juxtamembrane region of the ectodomain of hepatitis C virus glycoprotein E1. *J. Biol. Chem.* **275**, 24070-24079.

Mukhopadhyay, D. and Riezman, H. (2007). Proteasome-independent functions of ubiquitin in endocytosis and signaling. *Science* **315**, 201-205.

Naramura, M., Jang, I. K., Kole, H., Huang, F., Haines, D. and Gu, H. (2002). c-Cbl and Cbl-b regulate T cell responsiveness by promoting ligand-induced TCR down-modulation. *Nat. Immunol* **3**, 1192-1199.

Nielsen, E., Christoforidis, S., Uttenweiler-Joseph, S., Miaczynska, M., Dewitte, F., Wilm, M., Hoflack, B. and Zerial, M. (2000). Rabenosyn-5, a novel Rab5 effector, is complexed with hVPS45 and recruited to endosomes through a FYVE finger domain. *J. Cell Biol.* **151**, 601-612.

Pascale, M. C., Erra, M. C., Malagolini, N., Serafini-Cessi, F., Leone, A. and Bonatti, S. (1992). Post-translational processing of an O-glycosylated protein, the human CD8 glycoprotein, during the intracellular transport to the plasma membrane. *J. Biol. Chem.* **267**, 25196-25201.

Pickart, C. M. and Fushman, D. (2004). Polyubiquitin chains: polymeric protein signals. *Curr. Opin. Chem. Biol.* **8**, 610-616.

Piper, R. C. and Luzio, J. P. (2007). Ubiquitin-dependent sorting of integral membrane proteins for degradation in lysosomes. *Curr. Opin. Cell Biol.* **19**, 459-465.

Rice, D. S., Northcutt, G. M. and Kurschner, C. (2001). The Lnx family proteins function as molecular scaffolds for Numb family proteins. *Mol. Cell Neurosci.* **18**, 525-540.

Salmond, R. J., Filby, A., Qureshi, I., Caserta, S. and Zamoyska, R. (2009). T-cell receptor proximal signaling via the Src-family kinases, Lck and Fyn, influences T-cell activation, differentiation, and tolerance. *Immunol Rev.* **228**, 9-22.

Schmitz, J. E., Forman, M. A., Lifton, M. A., Concepcion, O., Reimann, K. A., Jr., Crumpacker, C. S., Daley, J. F., Gelman, R. S. and Letvin, N. L. (1998). Expression of the CD8alpha beta-heterodimer on CD8(+) T lymphocytes in peripheral blood lymphocytes of human immunodeficiency virus- and human immunodeficiency virus+ individuals. *Blood* **92**, 198-206.

Soetens, O., De Craene, J. O. and Andre, B. (2001). Ubiquitin is required for sorting to the vacuole of the yeast general amino acid permease, Gap1. *J. Biol. Chem.* **276**, 43949-43957.

Sollerbrant, K., Raschperger, E., Mirza, M., Engstrom, U., Philipson, L., Ljungdahl, P. O. and Pettersson, R. F. (2003). The Coxsackievirus and adenovirus receptor (CAR) forms a complex with the PDZ domain-containing protein ligand-of-numb protein-X (LNX). *J. Biol. Chem.* **278**, 7439-7444.

Stenmark, H. (2009). Rab GTPases as coordinators of vesicle traffic. *Nat. Rev. Mol. Cell Biol.* **10**, 513-525.

Takahashi, S., Iwamoto, N., Sasaki, H., Ohashi, M., Oda, Y., Tsukita, S. and Furuse, M. (2009). The E3 ubiquitin ligase LNX1p80 promotes the removal of claudins from tight junctions in MDCK cells. *J. Cell Sci.* **122**, 985-994.

Weiss, A. and Littman, D. R. (1994). Signal transduction by lymphocyte antigen receptors. *Cell* **76**, 263-274.

Zheng, D., Sun, Y., Gu, S., Ji, C., Zhao, W., Xie, Y. and Mao, Y. (2010). LNX (Ligand of Numb-protein X) interacts with RhoC, both of which regulate AP-1-mediated transcriptional activation. *Mol. Biol. Rep.* **37**, 2431-2437.